

Exploration of Virtual Reality Applications for the Purpose of Medical
Device Design/Atrial Septal Defect Anatomical Model Creation

A THESIS
SUBMITTED TO THE FACULTY OF THE GRADUATE SCHOOL
OF THE UNIVERSITY OF MINNESOTA
BY

Eric P. Jerke

IN PARTIAL FULFILLMENT OF THE REQUIREMENTS
FOR THE DEGREE OF
MASTER OF SCIENCE

Professor Arthur Erdman

June 2012

© Eric P. Jerke 2012

Acknowledgements

I would like to thank Dr. Arthur Erdman who first had the vision for this thesis work as well as the foresight to pursue the partnerships which enriched the project, the University of Minnesota, and also my experience as an engineer. Dr. Erdman believed in me and our team and his encouragement and wisdom extended well beyond the confines of this document.

I would also like to thank St. Jude Medical who sponsored the specific research related to atrial septal defects. Specifically, I would like to thank Peter Ness, Ted Dale, Mike Brenzel, and Paul Hindrichs. Their guidance and assistance was crucial for my projects success. My gratitude extends beyond these four to the rest of the CTG team.

The virtual reality portion of the thesis would not have been possible without the help of Nancy Rowe and the Minnesota Super Computing Institute. Nancy was excited by this project and her motivation was a blessing. She provided many hours of her time to be able to help us with our first look at virtual reality models. Without her help we would not have been able to take the first steps toward the goal of using virtual reality to aid in the development of medical devices.

I would like to specifically thank Nathan Handel. We were joined together by our work on this thesis and class. He helped me realize a completely different side to things and I appreciate his help and guidance throughout the entire process.

Lastly, I would like to acknowledge all the support that I received from my family and friends who believed in me and pushed me to persevere. The road to writing a thesis can be a long one especially when you start your career before finishing. This thesis was only possible with the help of my parents and Lindsey Hoehn.

Dedication

This thesis is dedicated to my parents. Their help and encouragement all of my life has made me the person I am today.

Table of Contents

Acknowledgements.....	i
Dedication.....	iii
List of Tables	vi
List of Figures.....	vii
List of Abbreviations	x
1. Introduction.....	1
2. Understanding Virtual Reality Technology	4
2.1 VR History	4
2.2 VR Categories	5
2.2.1 Information Viewing.....	6
2.2.2 Virtual Prototyping	8
2.2.3 Surgical Simulation.....	10
2.3 VR and the Medical Device Industry.....	11
2.3.1 Overview of Medical Device Industry.....	11
2.3.2 Introduction to VR Medical Device Design Environment	15
2.3.3 Prior Art	16
3. Virtual Reality Based Medical Device Design Environment	21
3.1 Design Requirements	22
3.2 System Architecture	24
3.2.1 Merging Technologies	25
3.2.2 Exporting Changes.....	26
3.2.3 Visualization System and Haptic Tools.....	28
3.3 VR Anatomic Model Creation	29
3.4 Design Challenges and Limitations.....	32
3.4.1 CAD to VR Challenges.....	32
3.4.2 CT Issues.....	34
4. Atrial Septal Defect Anatomical Model Creation.....	36
4.1 Motivation	36
4.2 Objective	39
4.2.1 Description of Pumper Station.....	40
4.3 PFO Anatomy.....	41

4.3.1	Embryology.....	42
4.3.2	PFO Prevalence.....	44
4.3.3	Risk Factors	45
4.3.4	Treatment	46
4.4	Anatomically Important Features for Device Deployment	47
4.4.1	Location	48
4.4.2	Size.....	50
4.4.3	Rim Dimensions.....	53
4.4.4	Tissue Properties	54
4.5	3D Anatomical Model Creation	56
4.5.1	CT Data Acquisition	57
4.5.2	Image Processing	64
4.5.3	3D Reconstruction	76
4.5.4	Comparing 3D Object to Cadaver.....	77
4.6	Anatomical CAD and Bench Top Model Creation	79
4.6.1	Converting the 3D Object into a 3D CAD Model	80
4.6.2	3D CAD Model Development	89
4.6.3	Mold Creation	94
4.6.4	2 nd Generation 3D CAD Model Development.....	98
4.6.5	2 nd Generation Mold Creation.....	100
4.7	Mold Validation and Verification	104
4.7.1	The Pumper Station.....	104
4.7.2	ICE Background.....	106
4.7.3	Mold Validation and Verification using ICE.....	107
5.	Conclusion	112
5.1	Future Work	117
	Works Cited	118

List of Tables

Table 1 – PFO sizing from literature	53
--	----

List of Figures

Figure 1 – Virtual Reality Component Categories	6
Figure 2 – (Left) Normal development cycle w/ majority of prototypes occurring in the late stage of project. (Right) Using virtual prototyping the majority of designs are eliminated before the first prototype is built.....	9
Figure 3 – Total Product Life Cycle [37].....	13
Figure 4 – Basic Development Cycle	14
Figure 5 – CAVE at the University of Minnesota Supercomputing Institute.....	18
Figure 6 – (Left) ImmersaDesk (Right) ImmersaDesk M1	18
Figure 7 – Visualization of complex structure using a PowerWall	19
Figure 8 – ImmersiveTouch combines collocation and haptic feedback to provide a realistic surgical simulation of procedures	19
Figure 9 – Virtual reality medical device design system schematic	22
Figure 10 – Result feedback loop. Results from virtual environment are inputted back into CAD model and analysis.	27
Figure 11 – Desktop VR design studio that links design, analysis, VR, and user interfaces	28
Figure 12 – CT scans are used to define and segment desired anatomic region	30
Figure 13 – Volumetric models are created from CT scans using Mimics software by Materialise™	30
Figure 14 – Anatomic models from Mimics are imported and viewed in virtual environment. (Right) Eric Jerke and Nathan Handel viewing virtual reality skeleton model created from CT scans.	31
Figure 15 - Flat 2D Puck [17].....	37
Figure 16 - 3D Heart Anatomy [1]	37
Figure 17 - Premere Device Implantation [17].....	38
Figure 18 – Bench Top Model Creation Process	39
Figure 19 – Center block of pumper station	41
Figure 20 – PFO embryology; Right sagittal and coronal views. LA = left atrium; RA = right atrium [41].....	43
Figure 21 – Cadaver specimens. (Left) Right atrial PFO opening (Right) Left atrial PFO opening.....	44
Figure 22 – Representation of the heart structures including the PFO passageway from the right to left atriums. [25]	44
Figure 23 – Presence of a PFO in 965 cadavers of all cause of deaths at various ages [61]	45
Figure 24 – PFO closure devices [61].....	47
Figure 25 – PFO anatomical locations (Left) Right atrial view. CS: coronary sinus; CT: crista terminalis; FO: fossa ovalis; IVC, SVS: inferior and superior vena cavae; mevs: membranous ventricular septum; PA: pulmonary artery; RPVs: right pulmonary veins; TV: tricuspid valve; W _{AI} , W _{PI} , W _{FO} : width of anterior and posterior isthmi, fossa ovalis. (Right) Left atrial view. Ch: persistent channel of foramen ovale; MV: mitral valve [82]	49

Figure 26 – Anatomic locations in a cadaver. (Left) Right atrium view (Right) Left atrium view [Pictures taken by Eric Jerke and Nathan Handel at the University of Minnesota’s Anatomy Laboratory].....	50
Figure 27 – Images of PFO sizing techniques (Image courtesy of SJM) [17].....	51
Figure 28 – Balloon sizing of a PFO [25].....	51
Figure 29 - Tunnel diameter and direction [42].....	52
Figure 30 – PFO tunnel length. (1) Septum secundum thickness (2) tunnel length (3) collapsed tunnel (4) offset after device placement [60].....	54
Figure 31 – Septum primum compliance. (Left) Arrows represent the tunnel length prior to balloon sizing. (Right) Arrows represent the tunnel length after balloon sizing [60] ..	55
Figure 32 – Hypermobile Septum [67]	55
Figure 33 – Cadaver hypermobile specimen (picture taken by Eric Jerke and Nathan Handel at the University of Minnesota Anatomy Lab).....	55
Figure 34 – CT Scanner [65]	57
Figure 35 – Hounsfield Units Gray Scale Correlation to Air, Water, etc. [9]	57
Figure 36 – CT scanning evolution. (Top) Sequential, (Middle) Spiral, (Bottom) Multislice CT [65].....	58
Figure 37 – Timing bolus image acquisition. Images are taken every 2 secs to determine when the contrast media will reach the desired anatomical region. This delay is then used to determine when to initiate the CT scan [47].....	59
Figure 38 – Bolus tracking of contrast media. Contrast media is injected at 5ml/s and an axial image is taken every 2 secs. When the contrast reaches its peak level determines the scan delay that is needed [65].	59
Figure 39 – Voxel [65].....	60
Figure 40 – Voxel size comparison (Image courtesy of SJM) [17].....	60
Figure 41 – Temporal resolution [65].....	61
Figure 42 – CT scan motion artifact [47].....	62
Figure 43 – Retrospective ECG [65]	63
Figure 44 – Mimics Automatic Import Wizard	67
Figure 45 – Mimics orienting DICOM data	67
Figure 46 – Mimics CT scan with image distortion	68
Figure 47 – Mimics windowing of imported CT scan. (Left) Standard window. (Right) Adjusted window	69
Figure 48 – Mimics profile line	71
Figure 49 – Mimics effect of region growing will eliminate floating pixels.....	72
Figure 50 – Mimics image cropping.....	73
Figure 51 – Mimics local segmentation use of profile line	75
Figure 52 – Mimics slicing of the 3D reconstructed object.....	77
Figure 53 – Mimics right atrium comparison to cadaver.....	78
Figure 54 – Mimics left atrium comparison to cadaver	78
Figure 55 – Bench Top Model Creation Process	79
Figure 56 – Mimics direct import	82
Figure 57 – Mimics MedCAD surface model reconstruction [81].....	84
Figure 58 – Conversion process from CT to CAD [64].....	85
Figure 59 – Conversion process from Mimics to CAD using GeoMagics [81]	86
Figure 60 – Mimics 3D reconstructed Model	87

Figure 61 – Anatomical model converted to IGES.....	89
Figure 62 – SolidWorks PFO creation.....	90
Figure 63 – SolidWorks PFO.....	90
Figure 64 – SolidWorks right atrium view of anatomical features.....	91
Figure 65 – CAD to functional bench top prototype	92
Figure 66 – SolidWorks offset convert entity sketch.....	92
Figure 67 – Brackets added to provide support and pressure seal.....	93
Figure 68 – SolidWorks 1 st generation CAD bench top model	94
Figure 69 – SolidWorks 1 st generation bench top mold pieces	95
Figure 70 – SolidWorks 1 st generation bench top mold keying feature	96
Figure 71 – SolidWorks alignment of ¾ bracket in 1 st generation mold.....	96
Figure 72 – 1 st generation mold with SJM Premere device deployed	98
Figure 73 – SolidWorks ASA defect creation	99
Figure 74 – SolidWorks 2 nd generation CAD bench top model	100
Figure 75 – SolidWorks 2 nd generation CAD bench top mold.....	101
Figure 76 – SolidWorks 2 nd generation bench top mold removal	103
Figure 77 – 2 nd generation mold with SJM Premere device deployed	104
Figure 78 – SJM pumper station [17]	105
Figure 79 – Representative fluoroscopic view [55].....	107
Figure 80 – Relative ICE position [54].....	107
Figure 81 – Representative ICE view [54]	107
Figure 82 – Introducing Contrast.....	108
Figure 83 – PFO Detection	108
Figure 84 – Device Placement	108
Figure 85 – Representative echocardiograms. (Left) TEE (Right) ICE [17].....	108
Figure 86 – ICE probe in Pumper station	109
Figure 87 – ASA left mobility verification of 2 nd generation bench top mold versus patient data. (Left) Patient TEE image of the ASA. (Right) 2 nd generation bench top mold ICE image of the ASA. [17]	110
Figure 88 – ASA right mobility verification of 2 nd gen bench top mold versus patient data. (Left) Patient TEE image of the ASA. (Right) 2 nd gen bench top mold ICE image of the ASA. [17].....	110
Figure 89 – Modeling techniques	114

List of Abbreviations

2D	Two Dimensional
3D	Three Dimensional
ASA	Atrial Septal Aneurysm
ASD	Atrial Septal Defect
CAD	Computed Assisted Drafting
CAVE	Cave Automatic Virtual Environment
CD	Compact Disc
CREST	Center for Research in Education and Simulation Technologies
CT	Computed Tomography
DAT	Digital Audio Tape
DICOM	Digital Imaging and Communications in Medicine
ECG	Electrocardiography
FEA	Finite Element Analysis
HMD	Head Mounted Display
ICE	Intracardiac Echocardiography
IGES	Initial Graphics Exchange Specification
IVC	Inferior Vena Cava
NURBS	Non-Uniform Rational B-Spline
PFO	Patent Foramen Ovale
SJM	St. Jude Medical
SLA	Stereolithography
STEP	Standard for the Exchange of Product model data

STL	Standard Tessellation Language
SVC	Superior Vena Cava
TEE	Transesophageal Echocardiography
TTE	Transthoracic echocardiogram
VE	Virtual Environment
VR	Virtual Reality
VRAC	Virtual Reality Applications Center
VRML	Virtual Reality Modeling Language

1. Introduction

The concept of virtual reality (VR), once seen to be science fiction, is now becoming an actuality. The development of medical devices can be challenging as the human body is complex. Thus, the use of VR was envisioned to increase the knowledge and understanding of anatomy, by providing an engineer an enhanced window into the human body. This led to the question – how can medical device companies use virtual reality to develop medical devices? This author, with a team at the University of Minnesota, had the opportunity to use VR in the setting of medical device design for a patent foramen ovale heart defect. VR proved to be a valuable tool to enhance visualization of the anatomy as well as understand how a device may interact with the anatomy, allowing engineers to modify devices in a radical new way. However, further technology is required for VR to be used for medical device model creation.

The first step to developing a medical device using VR is to understand current VR technology. This included reviewing VR history, classifying VR components into categories, and understanding the application of VR in the medical device industry as well as the hardware and software products available. Specifically, research was focused on becoming familiar with technology that relates to visualization of anatomy and use in the design of medical devices.

It was the intention to use this understanding and knowledge base to integrate existing virtual reality products into the creation of a design environment for medical device development. Thus, the design requirements for the ideal system were outlined along with the basic system

architecture. In order for the VR based medical device design environment to work as intended it required multiple technologies to be merged together along with the ability to export changes to the device, back to the CAD model. Also, the visualization system needed to be small and either portable or take up no more room than a current desktop environment. In an attempt to test the ability to merge technologies, a VR anatomical model was created. The creation of this model allowed the research team to better understand some of the challenges and limitations that currently exist.

As a result of the initial work in VR applications, a collaborative effort with St. Jude Medical (SJM) resulted in the creation of virtual heart models that were used to develop physical models for bench top testing. Work was concentrated on the anatomy that affected the design and performance of patent foramen ovale (PFO) closure devices. Research focused on understanding the variations in anatomy that affected device deployment and efficacy in order to develop anatomically accurate bench top models. Also, computed tomography (CT) heart models were used to create virtual models that could be visualized in a VR environment and manipulated in a computer aided design (CAD) environment. The bench top models were then combined with a beating heart simulator created by SJM for the testing of PFO closure devices.

This thesis will seek to sufficiently describe the research in order to provide an understanding of all that is involved with the development of a VR based medical device design environment. Information presented on the field of VR will include the capabilities, obstacles, and limitations of using VR. Also, the thesis will provide a description of the development of anatomic models and the challenges that existed with

trying to accurately model the variability of a heart defect. The use of models and research to understand a defect is essential to designing a medical device that is able to treat the defect safely and effectively. This thesis will show how the integration of VR components, classification of anatomical structures, and the creation of virtual and bench top models will improve medical device development.

The exploration into the VR medical device design environment was made possible by the Digital Technology Initiative of the University of Minnesota's Digital Technology Center and the portion of this thesis associated with the creation of a more anatomically accurate bench top model was sponsored by St. Jude Medical's Cardiac Technology Group. Partnerships with the Minnesota Supercomputing Institute (MSI) and St. Jude Medical were formed. The collaboration with MSI focused on importing anatomic models into a VR environment. St. Jude Medical provided access to CT scans, as well as Mimics by Materialise [9], a computer program used to create anatomic models from CT scans. The initial work in the exploration of VR was performed in conjunction with Nathan Handel, a fellow graduate student in the Medical Device Laboratory at the University of Minnesota.

2. Understanding Virtual Reality Technology

The research into virtual reality technology was not meant to be comprehensive or a complete investigation of all virtual reality (VR) areas, but to provide an understanding of the VR products and their uses as related to the end user. Specifically, the research was focused on becoming familiar with technology that relates to visualization of anatomy and its use in the design of medical devices. An explanation of technical challenges will be addressed only when it directly relates to the implementation of VR technology into a virtual design environment.

Research in the area for VR medical device design environment was made possible by The Digital Technology Center's 'Digital Technology Initiative' at the University of Minnesota along with patient computed tomography (CT) data provided by St. Jude Medical, Inc. Nathan Handel and I conducted the research that follows.

2.1 VR History

In its most basic definition, VR is any experience where the user is immersed in a virtual environment [26]. The definition of VR is broad and can be applied to a wide variety of technologies. During a lecture in 1965, Ivan Sutherland explained that his vision for VR would allow the user to utilize a computer screen as a window into a virtual world. Furthermore, a computer would maintain a model environment in real time so the user could directly manipulate virtual objects [26]. The designer would be able to interact with the anatomical world by manipulating a design to function in its intended manner and

adequately address the design criteria and purpose. VR for the purpose of medical device design would allow the user a window into the human body.

The field of VR has grown from Sutherland's vision into a multi-faceted industry. In 1999, Dr. Frederick Brooks, Kenan Professor of Computer Science at the University of North Carolina at Chapel Hill, did an overall assessment of the field of VR. He found that the verifiable production applications included vehicle simulation, vehicle design, entertainment, architectural design and spatial arrangement, training, medicine, and probe microscopy [26]. Over the past 10 years since Brooks' assessment was conducted, the field has continued to develop as obstacles have been overcome. Far beyond the realm of science fiction, VR has now become a subject of research at most major universities across the world.

2.2 VR Categories

The field of VR can be divided into various classification systems. In his book *Metaphysics of Virtual Reality*, Michael Helm defined VR in seven different categories: simulation, interaction, artificiality, immersion, telepresence, full-body immersion, and network communication [44]. However, Dr. Brooks took a different approach and separated VR by the four technologies that are crucial to virtual reality: visual displays, graphics rendering systems, tracking systems, and database construction. He further defined four less critical auxiliary technologies such as synthesized sound, display of forces using haptic (sense of touch) feedback, devices such as gloves and joysticks, and interaction techniques [26].

Both classification systems help convey the range of topics VR can cover. In order to focus the research to only those products and technologies that relate to the development of a medical device design environment, three main categories of VR products were defined as information viewing, virtual prototyping, and surgical simulation.

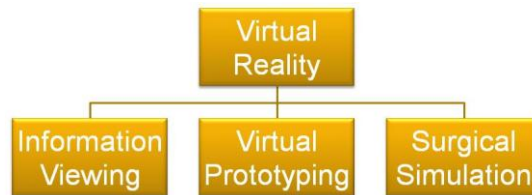


Figure 1 – Virtual Reality Component Categories

2.2.1 Information Viewing

One of the main benefits of VR, whether it is fully immersive or simple three dimensional (3D) stereo, is the enhanced visualization of information. The goal of any VR application, gaming or scientific, is to enhance access to information through interaction and perception of displayed reality. Instead of representing 3D objects using two dimensional (2D) projection (television, computers, paper), VR seeks to display the processed information in a 3D environment that simulates the world around us. In a sense, it is displaying data in a way that models and simulates the physical object from which it was taken.

Using information viewing, the researcher can distinguish products and technologies that are solely designed to enhance the display of data. VR products in the information viewing category are distinguished from one another based on the level of immersion that

the system provides to the user. For example, a 3D movie or television program is a VR experience; however, the user is still aware of their surroundings and the level of immersion into the virtual environment is low. Whereas using a head-mounted display (HMD), the user is completely immersed within the viewing environment. One researcher noted that it is important to distinguish when and how to use these sophisticated levels of immersive VR for certain applications. In many ways, VR can be beneficial, but sometimes it can impair or be distracting. Striking a balance is a key component when selecting what product to use for a particular application [8].

With information viewing products, the level of immersion extends from basic systems that use a projector to display a 3D image to six-sided rooms that use multiple projectors to immerse the user in a virtual environment [12]. Multiple projectors are used to produce stereoscopic images as the user wears either active or passive stereo glasses to view the image.

One example of a basic information viewing system is the GeoWall, which was developed by University of Illinois in Chicago (UIC) and the University of Minnesota. The system was developed as a turn-key system that could fit in a trunk and uses a back projected (2 projectors) screen to present virtual geological models on the screen. The GeoWall is used as a classroom tool to enhance the visualization of geological and topographical information. Using GeoWall, students have been better able to understand topological relationships and geological features compared to using pictures and maps alone [7].

The use of VR for information viewing continues to change and develop as the desire to enhance the visualization of data increases. A case could be made that all VR products and technologies fit into the information viewing category. With improved computing power, development of more complex models, increased technology in gaming and television, and a desire to simulate the world around us, information viewing will continue to be a main focus of VR development.

2.2.2 Virtual Prototyping

The second VR category, virtual prototyping, is the method of designing and testing prototypes using advanced analysis with a computational based system. The results can be displayed on a desktop computer, but advanced systems integrate a virtual environment. While attending a Virtual Engineering Workshop, Dr. Mark Bryden, from the Virtual Reality Applications Center (VRAC) at Iowa State University said, “The goal of virtual prototyping is engineering not visualization”. Though the output may be displayed using an information viewing system as described previously, it is not required.

The majority of companies current design process is to create a design, build, test, revise, build, and test again until the design is completed. Though the final design may work, there is no way to know if it is the optimal design solution. Also, as shown in Figure 2, the majority of prototypes built and tested occur during the latter stages of the development process. At this point, if a design fails a company must delay production

and increase development time. Defects not caught, often lead to device recalls which cost millions of dollars in product cost and can hurt market reputation.

Using virtual prototyping, the development process includes iterations done on a virtual model. This allows an engineer to not only optimize one design, but it can also be used to evaluate multiple designs. The second graph in Figure 2 shows the ideal design situation which reduces the number of physical prototypes built. A company is able to reduce the amount of time and money necessary to develop the product.

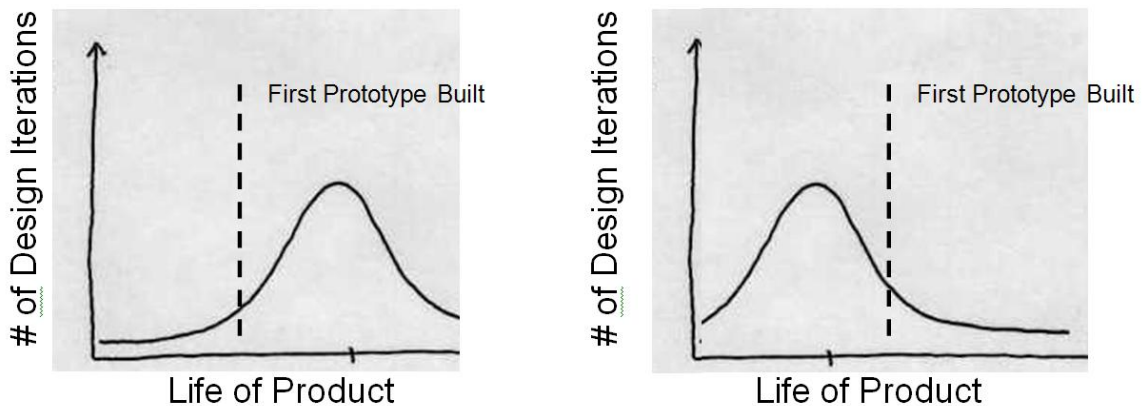


Figure 2 – (Left) Normal development cycle w/ majority of prototypes occurring in the late stage of project. (Right) Using virtual prototyping the majority of designs are eliminated before the first prototype is built

Dr. Bryden and his research team have been developing a sophisticated virtual prototyping program called VE Suite with the support of industrial partners. VE Suite integrates results and displays the results with visualization hardware. VE Suite allows the engineer to design from a systems approach and move back to component level, as opposed to design on a component level and integrate into a systems approach. By linking analysis tools such as Matlab or ANSYS, VE Suite provides the user with information to make sound engineering decisions. The overall goal of Dr. Bryden and his

team is to build tools that help enable users to create their own virtual environments to determine an optimal design and perform the analysis specific to their projects.

A closing comment that Dr. Bryden made during the Virtual Engineering Workshop highlights the importance of virtual prototyping for the growth and development of the engineering field. Dr Bryden stated, “Virtual prototyping will be trivial in twenty years. It will be an industry standard and if companies aren’t doing it, they will disappear.” Even if Dr. Bryden is off in his prediction by a few years, it is likely that the design process will be altered by the development of virtual prototyping, the integration of analysis with advanced visualization, and the continued technological development of VR products.

2.2.3 Surgical Simulation

The final VR category, surgical simulation, has been a main focus for the application of VR due to its ability to allow the surgeon or the student to train in a realistic setting. Surgical simulation software and products seek to mimic real-world medical situations in order to better train the physician to perform a surgery or diagnose a patient. Surgical simulation emphasizes skill development for improved surgical performance; therefore, several systems have been developed commercially in the area of endoscopic surgery (urology), suturing, and laparoscopic surgery [76]. Furthermore, virtual surgery simulators are being developed for advanced robotic assisted surgery.

Seymour outlined, in *Surgical Endoscopy* in 2006, five challenges (summarized below) for the field of surgical simulation [79]:

1. Coupling of surgical instruments with simulated tissue.
2. Simulation of object/geometric instruments and physical modeling. Limitations due to computer program interface and model development create barriers for combining a design environment with simulated dynamic properties of devices.
3. Simulation of interaction between objects (collision).
4. Display of operative field and the simulated operating room [79].
5. Signal processing for visualization and graphic rendering. This includes realistic lighting and texture effects.

Though a lot of challenges still exist, it is clear that the development of advanced analysis software will continue to benefit the field of surgical simulation. Likewise, as progress continues in realism and modeling of tissue in the field of surgical simulation, the door will begin to open for advanced modeling of the human body for design.

2.3 VR and the Medical Device Industry

Before the proposed system is described, this section will explain current design practices; as well as introduce the use of VR in the Medical Device Industry and current virtual reality systems that are available.

2.3.1 Overview of Medical Device Industry

The medical device field is expanding; every advance brings new challenges and hurdles. Now more than ever, large companies are becoming more risk adverse in the face of

more stringent FDA regulations and the increased risk of liability for device failure. Each year, there are examples of device recalls that damage company reputation, market share, and stock value. With the medical device giants trying to appease investors and the FDA, the smaller start-up companies are positioning themselves to be dynamic and efficient to fill voids and win market share. Start-up companies must rely on investors to fund their development of new technology. The turnaround time must be accelerated as start-up companies are judged on progress and potential. Where large companies are cautious to make smart business decisions and limit risk of device failures, small companies are pushed to show fast growth.

Though large and small medical device companies face different challenges, they all must address the challenges that exist with bringing a successful and safe device to market. Large companies need tools to ensure patient safety and bolster device performance where as small companies need tools that will enable them to arrive at design decisions in an expedient manner. To be successful, both large and small companies would benefit from a VR based medical device design system that would provide these tools.

The development of a VR medical device design system that allows the company to virtually test devices would improve device safety and help companies foresee potential design risks. Also, the system may allow the development of technology which specifically addresses patient needs and medical conditions. By using a system to iterate through design options quickly, effective designs would be produced in a shorter amount

of time. Furthermore, a VR medical device design system would help engineers become familiar with anatomic challenges that affect successful device function.

2.3.1.1 The Development Cycle

Medical device development includes both mechanical design and regulatory control. For all companies, whether in established markets or new market exploration, time to market is a critical factor in the successful adoption of a new device. Figure 3 shows the total product life cycle defined by the Center for Devices and Radiological Health [37].

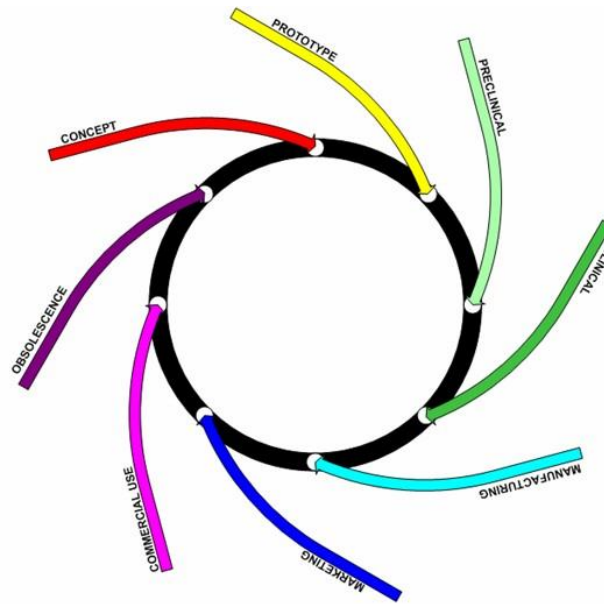


Figure 3 – Total Product Life Cycle [37]

The purpose of developing a VR medical device design system is to improve the overall quality and time to market for new medical products. A normal design cycle consists of initial device/market research which identifies areas of need. Concept development begins through a process of concept generation and concept selection. At this point, prototypes are developed and tested for feasibility and performance. During testing,

several factors are analyzed including fatigue, manufacturability, ability to adhere to product specifications, and analysis of component interaction and strength. Testing will lead to additional prototypes and the cycle will continue until an eventual “final” design is reached. As shown in Figure 4 the design cycle is highly iterative and can be costly.

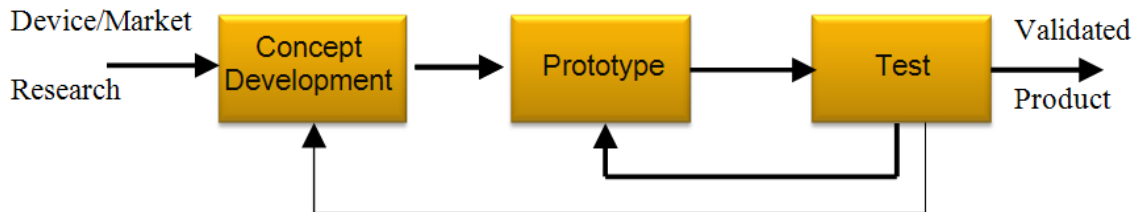


Figure 4 – Basic Development Cycle

During the development of a device, companies seek to test out designs using adequate bench top models. After ample testing has been performed on the bench, or if additional testing is desired for a particular feature that cannot be tested, human or animal models may be used for further development. However, using these models is expensive and their use is limited.

As previously mentioned, the goal of prototyping is to catch design flaws early on. The later in the development cycle that a change is made, the more expensive it is to the company. Considering that a large barrier to medical device development is the overall cost [36], reducing the number of design iterations reduces the development costs and increases the successfulness of the project. Though engineers use a variety of tools at their disposal, new analysis techniques and design aids for prototypes are necessary to continue to develop and advance the field of medical devices. Using a VR based design

platform that incorporates virtual prototyping and advanced design aides will help companies accomplish this goal.

2.3.2 Introduction to VR Medical Device Design Environment

When research began in the area of development of a VR based medical device design environment, the understanding of the varied and fast progressing field of VR was limited. Today, many engineers are using a computer aided drafting (CAD) system to increase productivity, shorten product design lifecycles, and to optimize their designs. CAD software is primarily used to create mathematically precise models in three dimensions of real-world physical objects [4]. Popular CAD software, like Pro/Engineer (PTC[®]) and SolidWorks (SolidWorks Corporation), provide accurate models that are of great use for designing parts and assemblies for use in numerous fields. One drawback, however, is the lack of detailed material and texture information associated with these models [28]. Even though many CAD packages allow the user to input this information, it is not required for the current CAD designing process. Due to this missing information, it is harder for the users to feel “immersed” when viewing CAD models.

Another drawback is CAD’s passive design environment for the user. The use of VR in the design process has emerged to overcome the shortcomings of CAD’s computer-human interfaces [48]. In VR environments, the user is an active part of the simulation loop [74]. Besides the actual physical environment, VR systems provide the most realistic experience when viewing computer-generated models compared to other viewing modalities [4]. Communication between the environment and user is important when

using VR; therefore, inputs such as haptic devices are often integrated as well. EnSight (CEI) and other VR software will allow engineers to import their CAD models and link engineering analyses. VR models can be visualized in real-time which is beneficial for interaction, but somewhat inaccurate as finite detail is traded for faster information processing speeds.

Along with viewing CAD models in a VR environment, the ability to overlay analyses and adding patient specific anatomy will fully immerse the user in the medical device design environment. Most VR software will allow the user to overlay their 3D vector analysis on top of the computer generated model to visualize the effect of the simulation in an immersed 3D environment. Finite element analysis (FEA) and computational fluid dynamics (CFD) are two analysis types often used with CAD models to simulate static or dynamic loading of the parts. In general, users of the VR community interested in real-time deformation of their models develop their own FEA code to allow for faster processing time by decreasing the complexity of the analysis. Secondly, patient specific anatomy can be converted from stacked medical images such as CT into a 3D model by using commercial software such as Mimics (Materialise). These 3D models can be converted as needed for simulation, FEA and CFD analysis, and design validation.

2.3.3 Prior Art

The original idea for the development of a VR design environment was to combine the benefits of advanced VR systems already developed. The CAVE [14], ImmersaDesk™ [30], PowerWall [11], and ImmersiveTouch® [59] systems were the four systems

identified and researched. The characteristic of each and those that could be utilized for a design system is summarized below.

1. CAVE™ – A rear-projected multiple screens, up to 6 sides, featuring a large field of view (allowing up to 10 people to view).
 - Advanced visualization and user interaction through tracking devices [14]
2. ImmersaDesk™ – A rear-projected drawing table with either HMD or stereo glasses and glove or wand based tracking systems.
 - Immersive desktop design environment [30]
3. PowerWall – A rear projected large single high resolution screen for small group collaborations.
 - Conference room presentation and collaborative design review [11]
4. ImmersiveTouch® – Combines 3D stereo visualization, haptic feedback, tracking systems, and 3D audio.
 - Haptic desktop with collocated immersive objects [59]

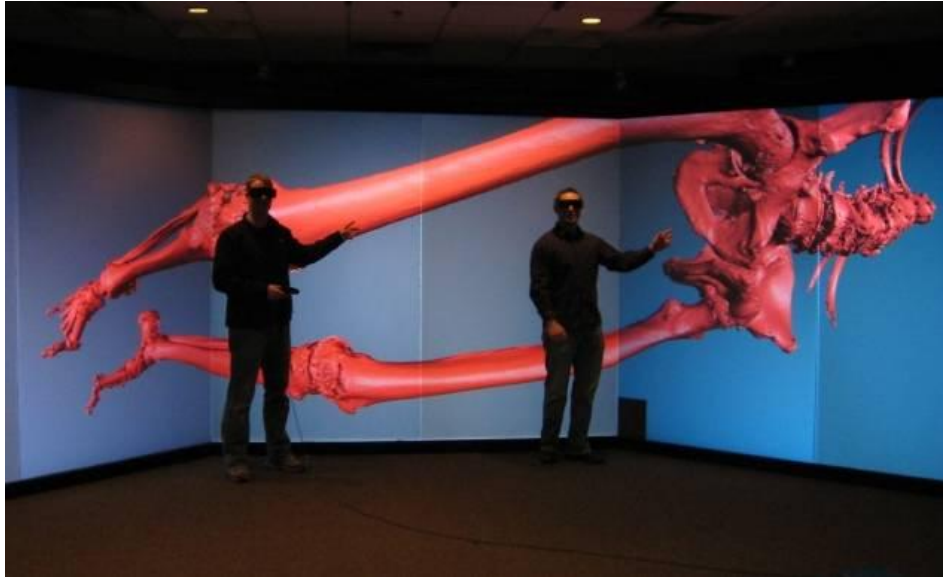


Figure 5 – CAVE at the University of Minnesota Supercomputing Institute

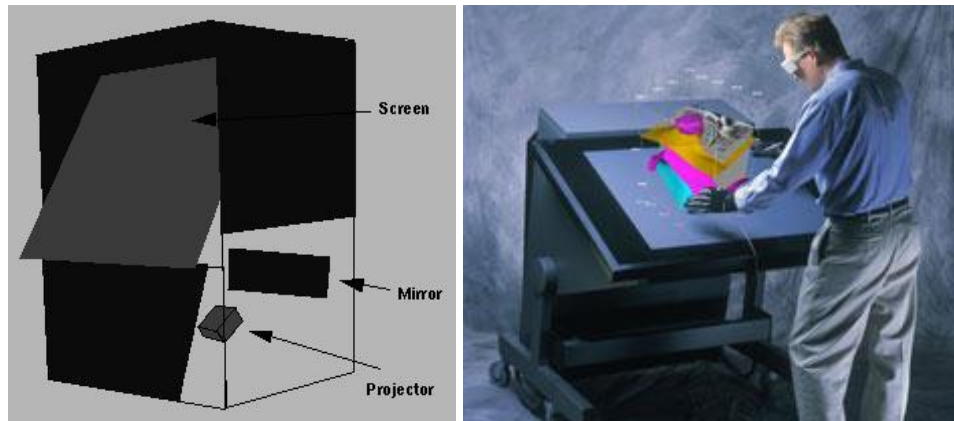


Figure 6 – (Left) ImmersaDesk (Right) ImmersaDesk M1

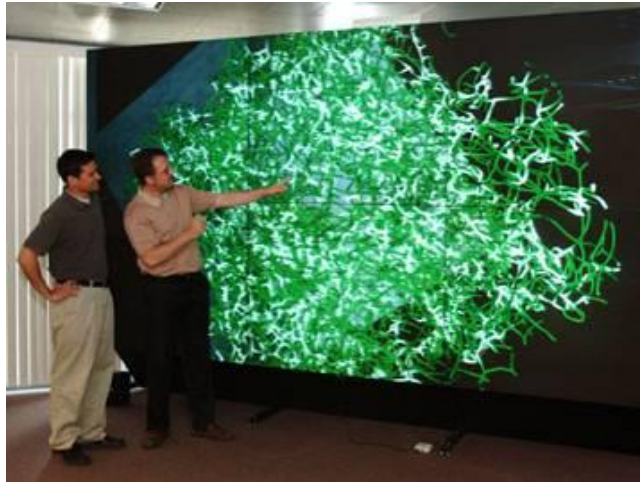


Figure 7 – Visualization of complex structure using a PowerWall

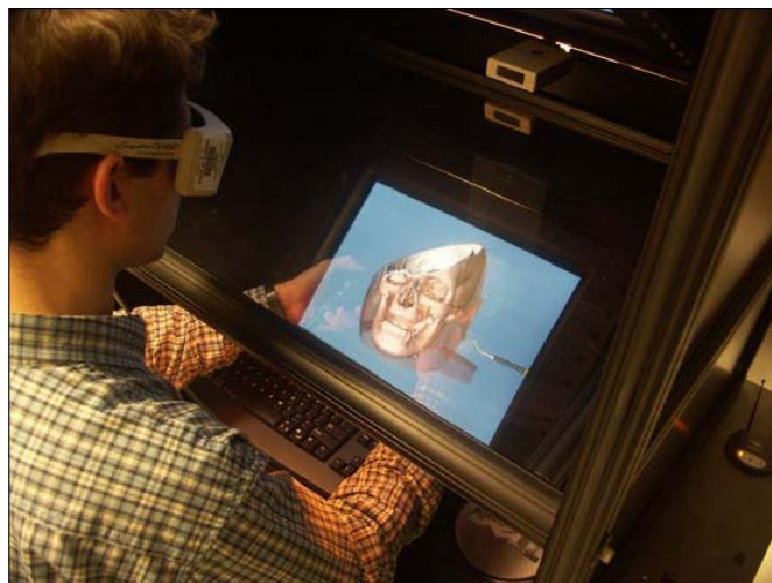


Figure 8 – ImmersiveTouch combines collocation and haptic feedback to provide a realistic surgical simulation of procedures

Though each system is impressive and is advanced in its abilities, each system has a drawback that does not make it adequate to use for the development of a medical device design system. The major drawback for each system is the overall cost. The ImmersiveTouch costs in excess of \$100,000 [59] and CAVE-like systems can be even more expensive. Furthermore, the goal of the CAVE and PowerWall is for large-scale

visualization. It would be taxing and unnecessary to design on these systems each day. The ImmersiveTouch provides interaction with anatomic models, but the primary purpose and function is surgical skill development. Furthermore, the Immersive Touch does not have the ability to allow the user to design or test devices and equipment.

Understanding the benefits and drawbacks of haptic feedback is critical when determining whether to incorporate it into a design system. With the ImmersiveTouch, it is beneficial to have haptic feedback for surgical simulation and training or to replicate bench top testing, but in a design setting, the haptic response would become tiring and not benefit the user. Furthermore, rear projected systems suffer from occlusion of the image by the user's hand or interaction device, which confuses the brain and breaks the stereoscopic illusion [59]. Thus, the addition of haptic feedback needs to collocate the 3D image with the user's hands without rear projection.

Out of the four systems described above, the ImmersaDesk was the closest system to the desired design environment. The drawback of the ImmersaDesk was that it mainly allowed for the design and visualization of devices in an immersive environment, but did not provide the ability to view anatomic environments or incorporate detailed analysis. It may be the case that for the first generation system an ImmersaDesk like system is incorporated into the design, but only as a single piece of a larger design system.

3. Virtual Reality Based Medical Device Design Environment

The primary objective of the system is a novel integration of CAD software with 3D anatomical and surgical modeling programs into a single software VR environment. The CAD model would interact directly with computer simulated anatomical environment allowing the user to select the optimal design(s) for a given medical application. Designers could test the performance of the device and make specific adjustments to the device characteristics (i.e. geometry and material properties) based on the reaction of the device with this environment. Overall, a wider set of device parameters would be evaluated more quickly and at less cost prior to manufacturing and testing prototypes on biological systems.

Furthermore, the visualization component of the VR system would allow users to do research, gain information, and view anatomical structures while designing the medical device in the CAD system. The user would be able to walk-through the anatomy in a VR environment to define the design constraints associated with the anatomy specific to the device.

The team developed the diagram shown below in Figure 9, in an attempt to create a schematic that would help depict how all the individual components integrated into a single system.

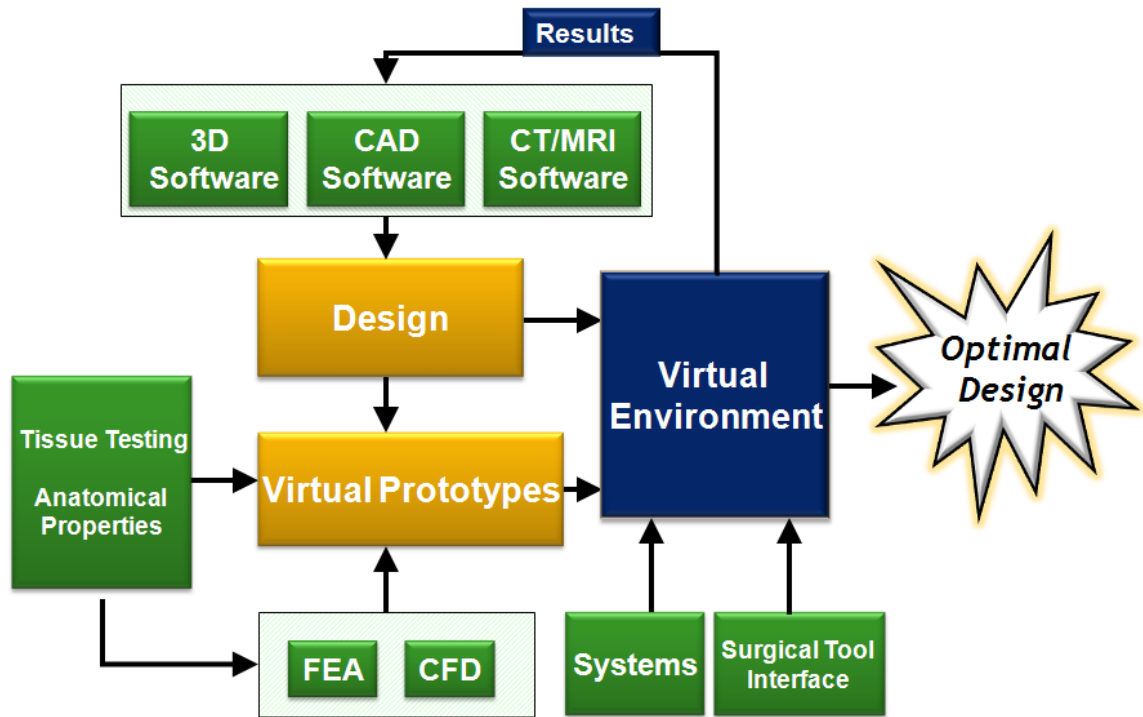


Figure 9 – Virtual reality medical device design system schematic

In order to accomplish the primary objective, the team developed a list of design requirements and attempted to explain how the system would accomplish the design requirements.

3.1 Design Requirements

The University of Minnesota team developed a list of characteristics and requirements that the virtual design environment would need in order to be successfully adopted by the medical device community. It was not the intention that the system would compete with previously designed systems, but would be a unique and novel entity to fill a void that was present within the medical device community. The requirements and considerations are described in brief below:

1. Analysis: The system must include advanced analysis software that is efficiently linked to the CAD design to allow the engineer to optimize the design. The level of complexity must be sufficient to produce accurate results, but not so advanced to make analysis time lengthy and inefficient.
2. Change CAD: The design environment would need to allow the user to change the CAD model based on the results derived from the analysis. Any changes made in the analysis software to optimize the medical device design should be directly transferred back to the CAD model.
3. Portable: The system must be portable. If not, then it must be able to be integrated into an office setting without requiring additional work space or its own room.
4. Toggle: The system must have the ability to toggle between an immersive environment for use with simulation and anatomic exploration or interaction, and a basic design desktop.
5. User-Friendly: The system must be user-friendly so the user does not have to be an expert in FEA or modeling to use the analysis tools effectively.
6. Effective: The system must provide the user with the ability to display information and analytical results in a meaningful manner. The display must be simple so as not to be cluttered or confusing to the user, but complex enough to adequately represent the level of detail necessary to fully display the data.
7. Haptics: Haptics should only be used when absolutely necessary to enhance the design experience. There is a potential for haptics to not provide adequate feedback and be more distracting than beneficial.

8. Intuitive: Current CAD software is easy to learn and engineers are able to efficiently design models. If the design environment is less intuitive than the CAD environment, the adoption will be slow.
9. Cost: The cost must not outweigh the benefits. One of the largest barriers to VR adoption is the high cost for the systems.
10. Comfortable: Engineers often design at desktop computers for several hours at a time. The user interface and input devices must allow for this without user fatigue.
11. Immersive: The level of immersion must be adequate to allow the engineer the ability to visualize analytic results and interaction between the device and the anatomy.

Using the list of design requirements and the system architecture previously described, the system architecture will be described below.

3.2 System Architecture

There are three components to the system. First, is to merge CAD, anatomic modeling, and analytical software into a single virtual environment that will allow for the technologies to interact. Next, based on the interaction, the user is able to make changes in one or more design features and export them directly back to the CAD software. Finally, a visualization system and other haptic tools are used to enhance the user's design ability in the virtual environment.

By merging the technologies and allowing for direct export, there will be a transformative effect to the field of minimally invasive device technologies. The benefits will include a better understanding of the interaction between anatomic structures and medical devices as well as a more efficient design and redesign environment.

3.2.1 Merging Technologies

The goal is to merge CAD, anatomic modeling, and analytical software into a single virtual environment that will allow for the technologies to interact. Currently, both anatomic modeling and CAD programs allow the user to export the final product. The goal is to export both the device and the anatomic region into a single virtual environment. Though CAD is a great tool to create 3D models of devices, it does not handle large data sets that are often associated with 3D anatomic models. Likewise, anatomical modeling programs are great at creating complex 3D models from native CT or MRI, but it is limited in its ability to import even simple CAD parts and have the two interact together. By merging the technologies in a virtual environment, ideally there would be an interaction between the CAD model and the anatomic environment by having an efficient link to analysis software and allow for virtual testing of the prototype.

Instead of being a simple geometric interaction, defining the anatomical and device material properties will allow the interaction to be a more realistic simulation and effective use of analysis programs such as FEA and CFD. Medical device companies continue to use advanced materials to minimize size while maximizing performance. Materials such as nitinol and complex composites are difficult to model accurately.

Furthermore, modeling tissue, which is often anisotropic (properties are directionally dependant), is also difficult [62].

The virtual environment must be able to display the device and anatomic data in a VR environment, which allows for better visualization of complex data sets. If the virtual environment is just a simulation environment, the desire to make changes and manipulate the device or anatomic model will not be possible. The virtual environment must also allow the user the ability to make changes based on the interaction between the device and the anatomy. This will ensure the device will function properly under a variety of anatomic models and not cause damage to the anatomy. Furthermore, the user needs to be able to explore the anatomic region by zooming, rotating, or performing a fly-through of the anatomy. Without a user-interface aspect of the environment, none of this is possible.

3.2.2 Exporting Changes

Based on the interaction between the device and the anatomical structure, the user may desire to make changes to the device; a device component may need to be lengthened or the mechanical properties of a certain component may need to be altered. For this reason, the virtual environment must preserve the individual features of the device and allow user to interface and edit these features. The goal of this project was not to recreate a CAD system in the virtual environment; therefore, the ability to create new models within the virtual environment is not a requirement. However, the ability to manipulate or edit the design is a requirement for the virtual environment.

By exporting the changes back to the CAD software, the user does not have to try and duplicate any desired changes that were made within the virtual environment. For example, the user would be able to customize the device to fit the anatomy and those specifications will be updated on the original model. As shown below, in Figure 10, the results feedback loop would save time, create a smooth design process, and keep the user from losing the precise, customized nature of the changes that may have been made.

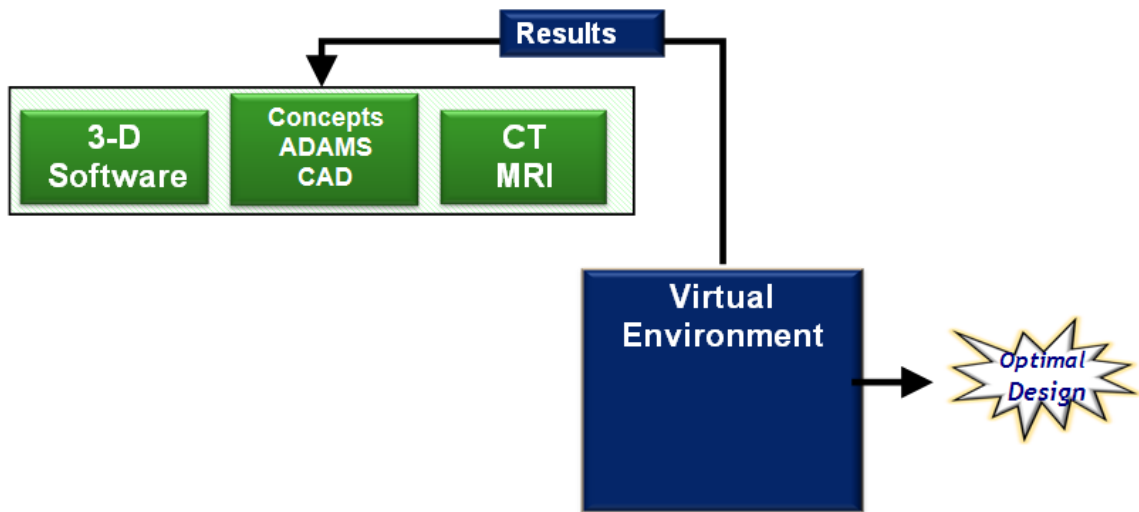


Figure 10 – Result feedback loop. Results from virtual environment are inputted back into CAD model and analysis.

Many research groups are working with CAD and VR, but very few are uniting them; those that are, use them for virtual prototyping, surgical simulation, and other fields such as geography, architecture, and construction. Geometries are generated in CAD software, and then imported to VR software for visualization. To the best of our knowledge, no system exists that will allow the user to make changes in the VR environment to the CAD model and move freely back and forth between the CAD and VR environment [28].

3.2.3 Visualization System and Haptic Tools

The visualization system's design will incorporate an immersive or VR mode and a normal desktop design mode that the user will be able to switch between. A few examples of this that incorporate a comfortable design environment and are still portable or integrated into a standard office environment are:

- A multi-tiled high resolution screen could be used to allow for the switching between stereo applications and 2D high resolution lay-outs. On occasion it may be desirable to have the 2D screen be side-by-side with an immersive anatomical environment. During design of a device, the engineer could switch between the two screens to increase efficiency.
- The set-up could be designed as a 2-panel CAVE-like desktop system. By reducing the CAVE to a desktop platform, the design system can be integrated easily into an office environment, as shown in Figure 11.



Figure 11 – Desktop VR design studio that links design, analysis, VR, and user interfaces

Both of these designs are very similar to normal desktop design's where the user would be seated using a mouse for extended hours. This is important because as Dr. Jason Leigh at UIC described, one large drawback of the CAVE is that the user interface is often a wand. After 8-10 minutes, the user will experience "gorilla arm" and fatigue will set in [58].

When designing a medical device, one important aspect is simulated use testing. One method of doing this with the proposed virtual environment would be to integrate medical instruments or tools and haptic feedback. An example of this would be to create an interchangeable box that would replicate catheter loading, scissors or other medical device accessories. Haptic feedback could be designed for the box to give the designer a realistic feel to the procedure. However, as mentioned earlier, the use of haptics in a design setting would tire the user and become not beneficial. Therefore, the incorporation of haptics should only be used when deemed necessary to validate the design.

3.3 VR Anatomic Model Creation

Through the partnership with St. Jude Medical, patient CT data sets were imported into Mimics software [9] to create 3D volume models that were exported to a VR environment. CT scans allow for the creation of desired anatomic structures. CT heart scans were processed for creation of a 3D volume heart model.

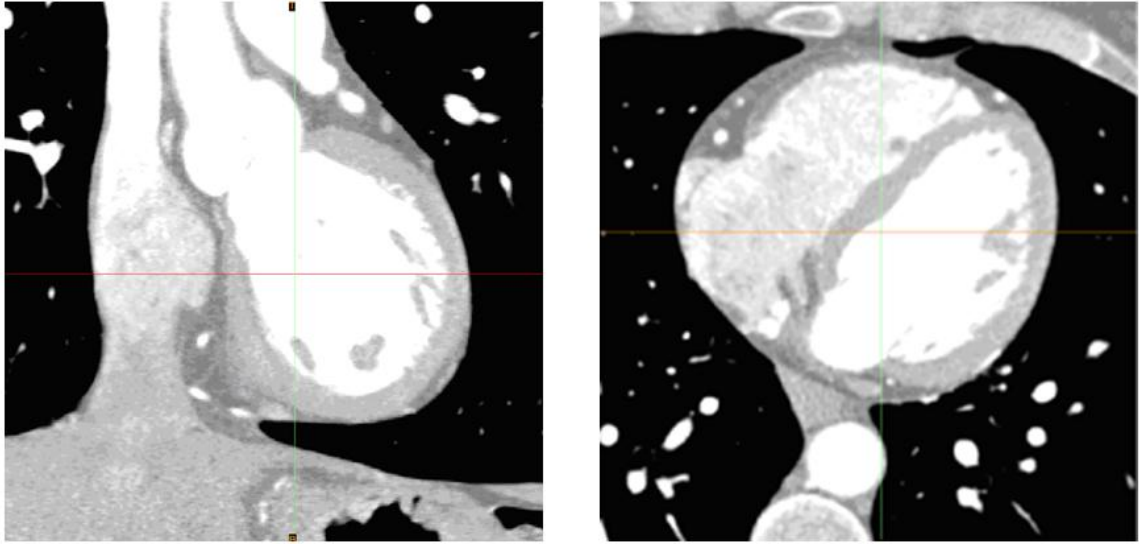


Figure 12 – CT scans are used to define and segment desired anatomic region

The CT data was compiled and formatted using Mimics software [9]. Once the data is segmented, Mimics creates 3D models that can be exported and analyzed using VR or an FEA analysis module. Once the 3D anatomic models were created, the goal was to use VR and bench top models to enhance visualization for the purpose of medical device design. The process of creating these anatomic models in Mimics will be described in more depth in section 4.5.2.

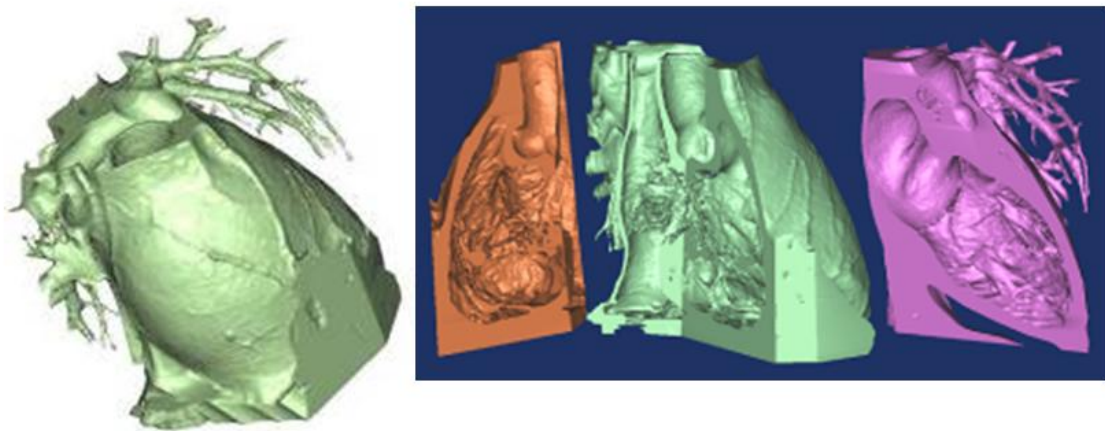


Figure 13 – Volumetric models are created from CT scans using Mimics software by Materialise™

A virtual 3D model and a fly-through of the VR model was created using EnSight software [6]. Through the partnership with the University of Minnesota Supercomputing Institute (MSI), the group has access to all of the MSI software programs, lab space, and 3D visualization equipment. MSI has a visualization facility that provides a cutting edge 3D visualization system connected to a super computer. The system is a three screen fully immersive environment for the interaction and enhancement of the visualization of complex objects and images. The team worked with Nancy Rowe of MSI, to import the anatomic models into the MSI visualization laboratory.

Viewing anatomy in an immersive environment helped to improve the understanding of anatomic structures in the heart. Informally, groups were shown the cardiac fly-through model in VR or a 2D rendering. The feedback was that the fly-through using VR helped to distinguish cardiac structures as well as give a sense of relationships between structures based on depth and orientation.

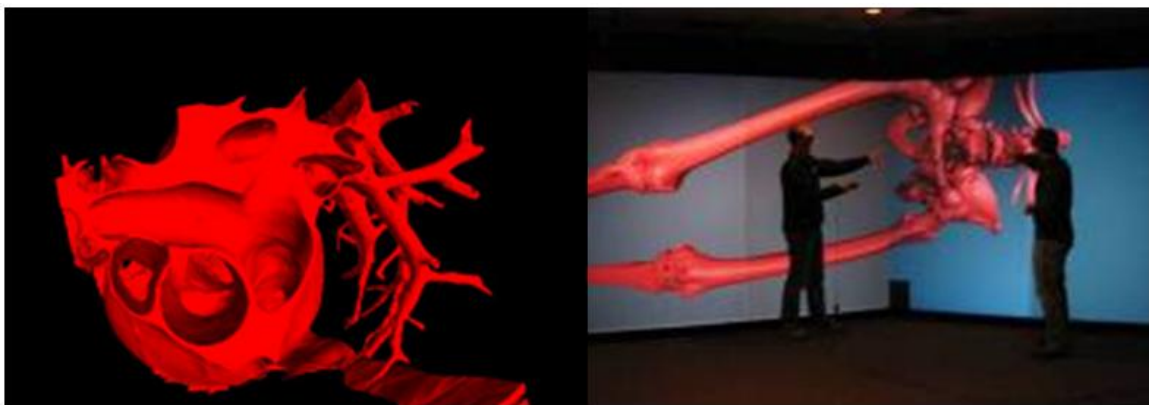


Figure 14 – Anatomic models from Mimics are imported and viewed in virtual environment. (Right) Eric Jerke and Nathan Handel viewing virtual reality skeleton model created from CT scans.

3.4 Design Challenges and Limitations

During this research into the VR based medical device design environment, two main challenges arose. The first was the integration of a CAD model with VR and the second was the creation of reconstructed cardiac models due to the quality of a patient's CT scan. In the future, the critical partnerships formed may help overcome some of the challenges described below.

3.4.1 CAD to VR Challenges

Currently, various difficulties exist when converting CAD models to VR models including: inadequate treatment of geometry, low performance for complex models, lack of realism, and one-way conversion [75]. Thus, extensive manual steps are required to adequately convert their CAD model into a VR model.

3.4.1.1 Inadequate Treatment of Geometry

CAD companies define their 3D solids by using a variety of proprietary geometric mathematical representations, where boundary surface forms include planes, Non-uniform rational B-spline (NURBS) surfaces, Bezier surfaces, Coons-type patches, and conics [21]. Typically, there is a geometry manipulation routine within the CAD software that will blend, trim, or interpolate. However, VR software companies typically only support one mathematical surface representation. These surfaces are approximated by triangular meshes because a triangular surface element is the simplest and lowest

common denominator of all the surface elements. This is similar to the output found from rapid prototyping files such as standard tessellation language (STL).

The translation process from a CAD file into the VR environment can be done by exporting files such as STL, VRML, IGES, STEP, etc. Then these forms are imported into the VR software where they ultimately switch to the lowest denominator prior to rendering. One VR software package, Ensight (CEI), has created CAD readers that will allow one to import the files directly, but unfortunately it still converts to the triangular mesh prior to rendering.

Tessellating the CAD solid model into polygonal meshes can result in hundreds or even thousands of polygons per original solid model. Often errors occur during tessellation because a curved surface is now represented by overlapping triangulated surfaces.

3.4.1.2 Low Performance and Lack of Realism

When very complex models are brought into the VR environment, the frame rates achieved can be unsatisfactory. As previously mentioned, the tessellating process usually adds unneeded model complexity by representing a single solid model as hundreds or thousands of polygonal meshes.

As already mentioned, it is not necessary to add material or texture information in the CAD process. This information is, however, significant to develop a realistic VR visualization.

3.4.1.3 One Way Conversion

One of the requirements of the virtual environment was the ability to manipulate or edit the design. Currently, the ability to modify geometric models in VR is now limited to polygonal objects. Also, certain parameter controls inside the CAD program are restricted. Our team was not able to solve the one-way conversion problem.

During an earlier trip to the Electronic Visualization Laboratory (EVL), considered to be a leader in scientific development, the professors commented that CAD packages have always been difficult to work with for use in the field of VR. They felt that the best way to overcome the barrier from VR to CAD was a specific partnership with a CAD company. Thus, a grant was written in partnership with MSC software, the creator of the ADAMS CAD package, to address the one-way conversion problem. For future work, this partnership will provide unique access to resources and parameter controls thus improving the speed at which the combined 3D virtual environment will react to the users need for a new model to be generated. The transfer from VR to CAD is the subject of ongoing research and is outside the scope of this thesis.

3.4.2 CT Issues

Another challenge occurs when creating a model of the anatomical region. At the time of this research, there were three known issues when creating CT scans that affect model

quality: lack of contrast, large voxel size, and motion artifact. Soft tissues such as cardiac anatomy present difficulties when imaging because it is critical that the contrast solution be injected at a precise time so that enough contrast is seen to distinguish between blood and tissue [47]. Just like resolution on a screen, the CT scan's pixel resolution times slice thickness creates a 3D voxel size. A large voxel size will produce a rougher anatomical model [65]. Finally, motion artifact, very similar to taking a picture of a fast moving object, occurs when the patient moves while the CT scan is being taken [47]. All of these will be discussed in more detail in section 4.5.1. The important thing to note is the better the quality of the CT scan, the better the quality of the anatomical model.

4. Atrial Septal Defect Anatomical Model Creation

A partnership was formed with St. Jude Medical's Cardiac Technology Group. The exploration of virtual reality (VR) and the creation of virtual anatomical models using CT data provided by St. Jude Medical, Inc. (SJM) motivated further research into the development of a classification system and more anatomically correct bench top models for patent foramen ovals (PFOs).

Research into the development of atrial septal defect anatomical model creation was made possible through funding provided by SJM's Cardiac Technology Group. The project that was sponsored by SJM was broken into two parts: a PFO classification system and atrial septal defect anatomical model creation. The PFO classification system portion was worked on by Nathan Handel where as this section provided by this author will describe the research for atrial septal defect anatomical model creation.

4.1 Motivation

Previous work performed by SJM yielded flat 2D pucks as shown in Figure 15. These flat pucks included various different anatomical defects that they believed affected device deployment. This initial work was very important to their understanding of how their PFO closure device would work, but these flat 2D pucks weren't an accurate representation of the anatomical PFO region. The PFO region, just like the rest of the heart, is 3D as shown in Figure 16.

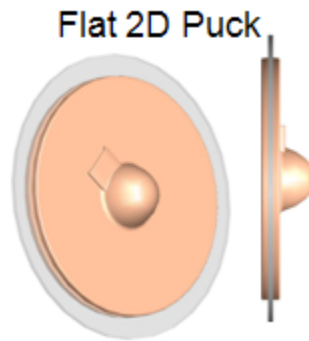


Figure 15 - Flat 2D Puck [17]

3D Heart Anatomy

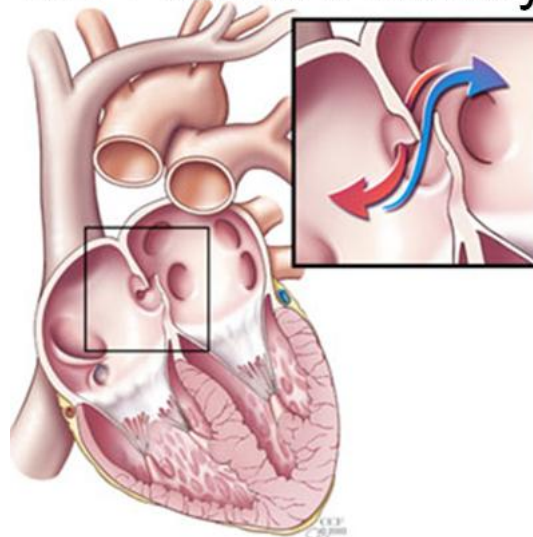


Figure 16 - 3D Heart Anatomy [1]

At the time of this research, SJM desired to visually understand variants in PFO geometric morphology. SJM had a PFO closure device, “Premere PFO Closure System,” see Figure 17, which is intended to correct a PFO. The SJM PFO team had a strong foundation in the implant and delivery technology development, but more information was needed to assist physicians and engineers in the evaluation and treatment of PFOs.

A powerful form of evaluation is to visualize complex geometry and provide a link between anatomy and device using 3D virtual models. Further, SJM and physicians would benefit from a classification system for the entire range of PFO anatomy that may exist. This classification system would allow physicians to classify PFOs uniformly based upon anatomical features to aid in the diagnosis and treatment of a PFO. Current detection of PFOs is almost exclusively done using echocardiograms (ICE & TEE) [31]; therefore, all anatomical features that define the classification system must be able to be measured using this imaging modality. Once complete, the classification system could be added to virtual models for the creation of bench top models and testing of the PFO closure device.

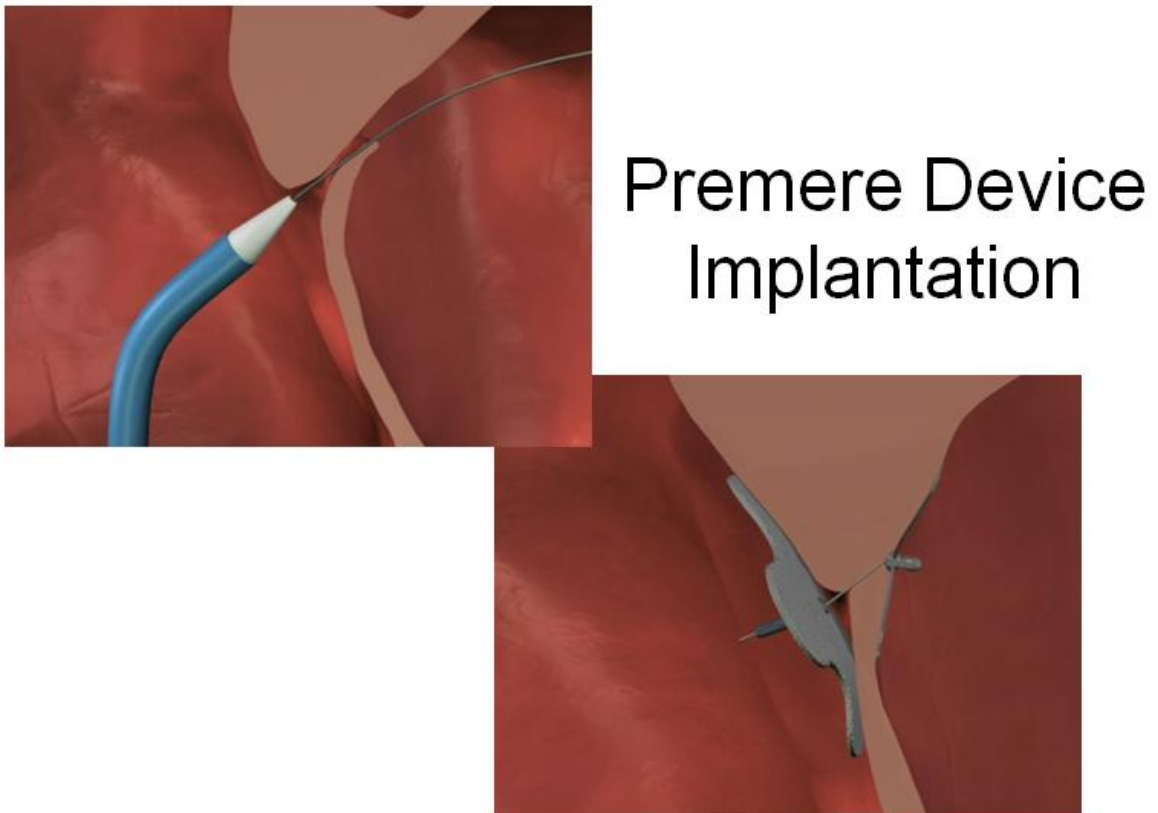


Figure 17 - Premere Device Implantation [17]

4.2 Objective

As described above, SJM desired to better understand the geometric morphology of a PFO as well as the ability to test their devices on a more anatomically correct bench top model. Thus, the objective of this section is to describe the research and efforts it took to create anatomically accurate bench top models for device deployment and testing. Figure 18, below, shows the overall process that will be described in depth in the remaining parts of section 4.

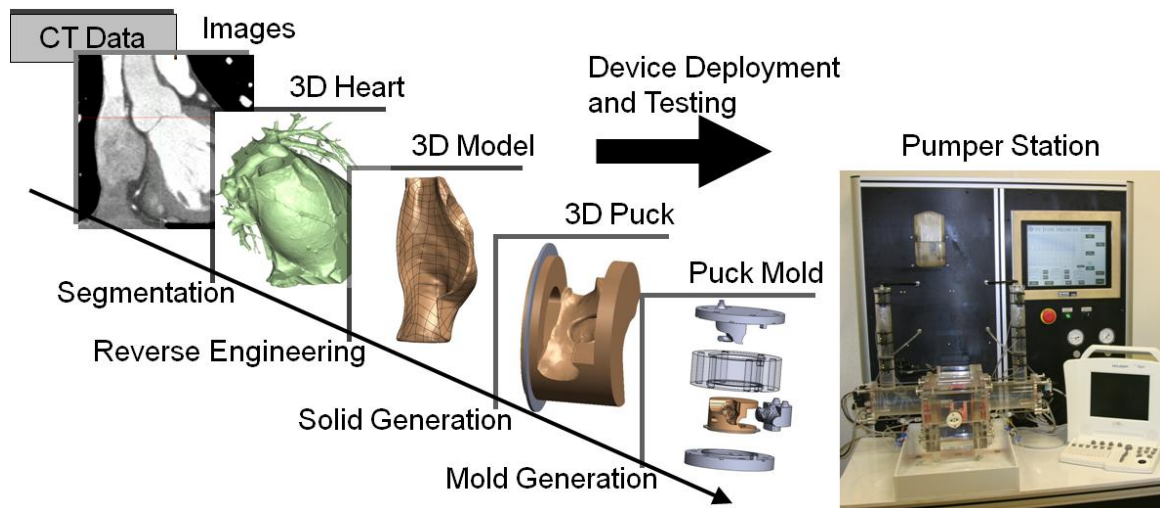


Figure 18 – Bench Top Model Creation Process

To achieve this objective of an anatomically accurate model, first research of the PFO anatomy and anatomically important features that affect device deployment needed to be understood. Once the various features were known, the next step was to create a 3D model of the anatomy. This step proved to be quite difficult as a lot of factors affect the quality of a CT scan. After a 3D reconstructed heart model was created, it was not functional unless defined features could be added. Thus, the difficult task of getting this 3D model into a CAD system existed. Once in a CAD system, features were added that

helped interface with the pumper station (briefly described below in section 4.2.1). After adding these features and the CAD representation of the bench top model was complete (3D Puck), the mold device was created to allow for physical molding to be done. Lastly, the bench top model created was validated using echocardiography. Following this process allowed for successful creation of a bench top model that replicated specific patient anatomy.

4.2.1 Description of Pumper Station

SJM's goal was to create 3D physical models that were anatomically correct to perform device testing. To be able to perform this bench top testing, a device needed to be created that would be able to replicate a beating heart. This device or pumper station needed to control both pressure and pulse individually for each chamber (left and right atriums of the heart). Also, the timing that each chamber cycled needed to be controlled to create a pulse and pressure trace similar to what was found in human patients that undergo device placement for a PFO.

At the time this project was beginning, the pumper station had not been created and was being defined. What was understood was that a center block (Figure 19) of the pumper station would be able to be removed for placement of the bench top model for device deployment and testing. The center block would feature a large and small bore. The small bore would house the bench top model and thus defined the dimensional constraints of the model to 3" in diameter and 2.2" in length.

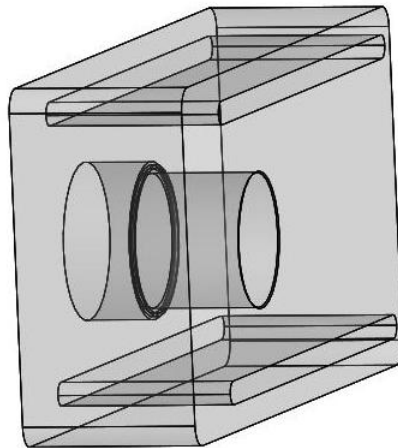


Figure 19 – Center block of pumper station

After creation of the anatomical bench top model, a portal would be drilled that represented typical direction of the device deployment. This portal would serve as the gateway for device delivery and testing similar to clinical practice under echocardiography.

4.3 PFO Anatomy

The heart's atrial septum wall serves as the structural division between the left and right atriums. Anatomical defects that occur in this region are generally circular or oval-shaped and are referred to as atrial septal defects (ASDs) [60]. One ASD known as a PFO resembles a tunnel or slit-shaped opening [25]. The embryology of the foramen ovale and PFO are described below.

4.3.1 Embryology

As a fetus's heart begins to grow and form all of the necessary structures, a hole is created between the left and right atriums called the foramen ovale. The foramen ovale, a crescent shaped cavity, is formed with the opening at the base of the inferior vena cava (IVC). Prior to birth, the oxygenated blood from the mother flows up the IVC into the right atrium and crosses the foramen ovale carrying oxygenated blood throughout the fetus. Figure 20 E-H shows the formation of the septum secundum, septum primum, and foramen ovale. The septum primum normally overlaps the septum secundum, which forms the flap-like valve. Blood flowing across the foramen ovale continues until birth, when the child takes their first breath. The flap-like valve then closes due to a pressure difference that is created as the pressure in the right side of the heart drops. Normally, over the next two years the septum primum flap fuses to the septum secundum [41].

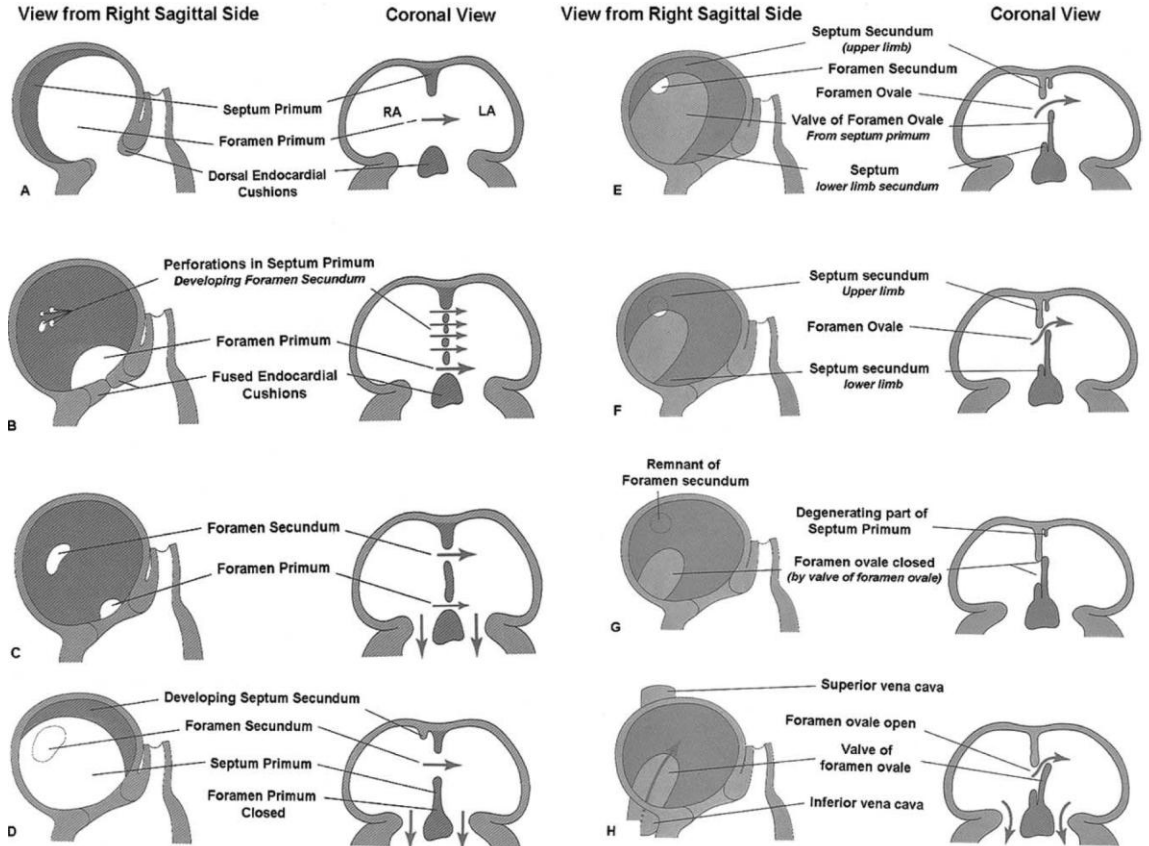


Figure 20 – PFO embryology; Right sagittal and coronal views. LA = left atrium; RA = right atrium [41]

If fusion doesn't occur, a PFO is formed by the overlap of the thick and muscular septum secundum and the thin and compliant septum primum (Figure 21) [60]. The remnant of the foramen ovale is called the fossa ovalis. The location of the fossa ovalis and PFO are in-line with the IVC so the blood flowing from the IVC during fetal development would be directed across the foramen ovale [82]. The left atrium opening of the PFO is superior to the right atrium opening as shown in Figure 22 [25]. Additionally, the tunnel formed is not a straight line, as the left and right atrium openings lie in different planes [27].

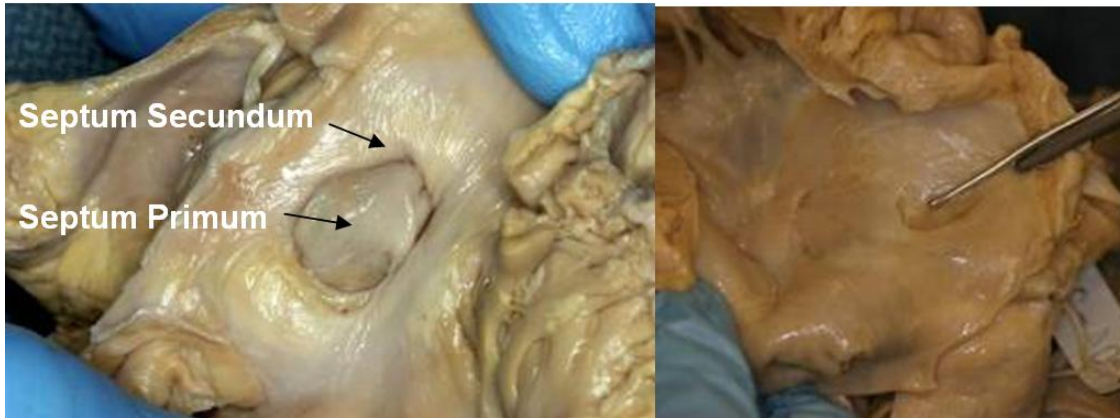


Figure 21 – Cadaver specimens. (Left) Right atrial PFO opening (Right) Left atrial PFO opening

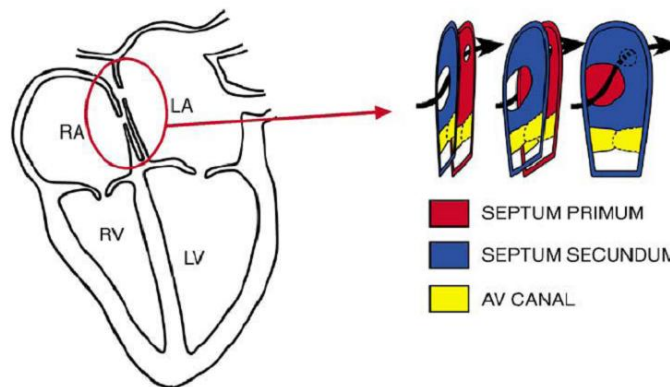


Figure 22 – Representation of the heart structures including the PFO passageway from the right to left atriums. [25]

4.3.2 PFO Prevalence

In 1974, the first ASDs were closed percutaneously by pediatric interventionalists, who typically treat children for complex congenital heart defects, but began to treat adults for PFOs [25] & [61]. At this time, the PFO was considered as a manifestation of an ASD to be closed [61]. However, it was soon realized that the most common of these ASDs is a PFO, which Boucek reports up to 33% of all children retain some communication between the right and left atriums through the PFO [25]. This was then correlated by Hagen in a study that examined 965 human autopsy hearts as reported by Meier et al in

Figure 23 [40]. Similarly, Drighil reported that in approximately 25% of the adult population fusion doesn't occur leaving a slit-shaped defect resembling a tunnel, known as a PFO [34].

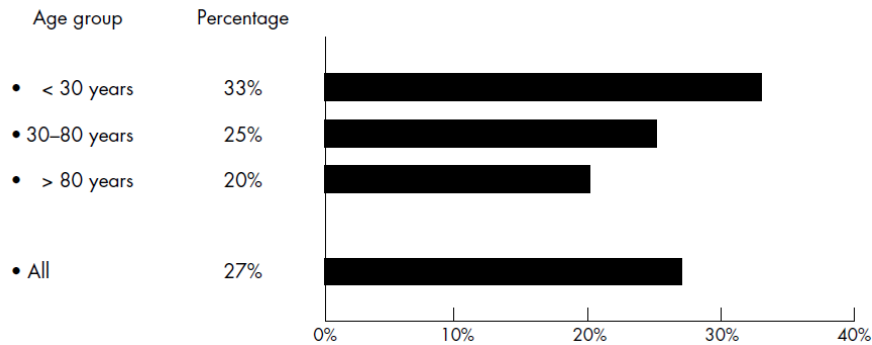


Figure 23 – Presence of a PFO in 965 cadavers of all cause of deaths at various ages [61]

4.3.3 Risk Factors

There are a number of clinical risk factors that have been linked with the presence of a PFO, including: cryptogenic stroke (stroke of unknown origin), decompression illness, migraine headaches with aura, orthodeoxia playpnea (not enough oxygen to the brain), and paradoxical embolism [34] & [51]. In cases of cryptogenic stroke, the prevalence of a PFO increases the risk of recurrent stroke nearly 5 times [51]. For those that suffer from decompression illness, PFO has been linked to an increase in brain lesions for scuba divers [34]. This occurs during scuba diving as the ambient pressure decreases, an increase in bubble formation is created in the body.

At the time this research was conducted, a recent link was revealed between migraine headaches with aura and PFOs. PFO patients were 3.5 times more likely to suffer from

migraine headaches [34]. Patients treated for PFO that suffered from either cryptogenic stroke or decompression illness reported a significant reduction in the number of migraine headaches [51].

PFO has also been linked to orthodeoxia plapnea syndrome. This is theoretically easy to understand as a PFO represents a passageway between un-oxygenated blood and oxygenated blood; however, the actual amount of shunting needed to create the syndrome is not very well understood [34] & [51]. Lastly, if a PFO does exist, it will likely grow in size as a patient gets older [42]. As the size of the PFO grows, an increase in the risk of paradoxical embolism (stroke caused by debris lodging) occurs [41].

4.3.4 Treatment

When designing transcatheter closure devices, one must consider the device placement and anatomic structures for the ultimate goal of closing the defect. When patients undergo treatment for an ASD, their hope is to stop the direct flow from the left atrium to the right atrium by closing the defect. In contrast, the treatment for a PFO is usually done to prevent the associated risk factors [60].

When a PFO was first described by Leonardi Botali in 1564, the clinical importance was poorly understood and was not really studied until the introduction of noninvasive detection using saline-contrast echocardiography within the last 20 years [34]. When a PFO is detected and the patient suffers from one of the risk factors above, an interventional cardiologist will use a variety of devices for transcatheter closure of PFO

in patients (Figure 24). All of the devices share a common theme featuring two anchor sides and a central tether or canal. The opposing anchors help hold the septum primum against the septum secundum eliminating the passageway or shunting until endothelialization (coating of device with tissue) can occur. The design of an intracardiac device needs to consider the anatomic features it will be placed on as well as the delivery techniques [60].

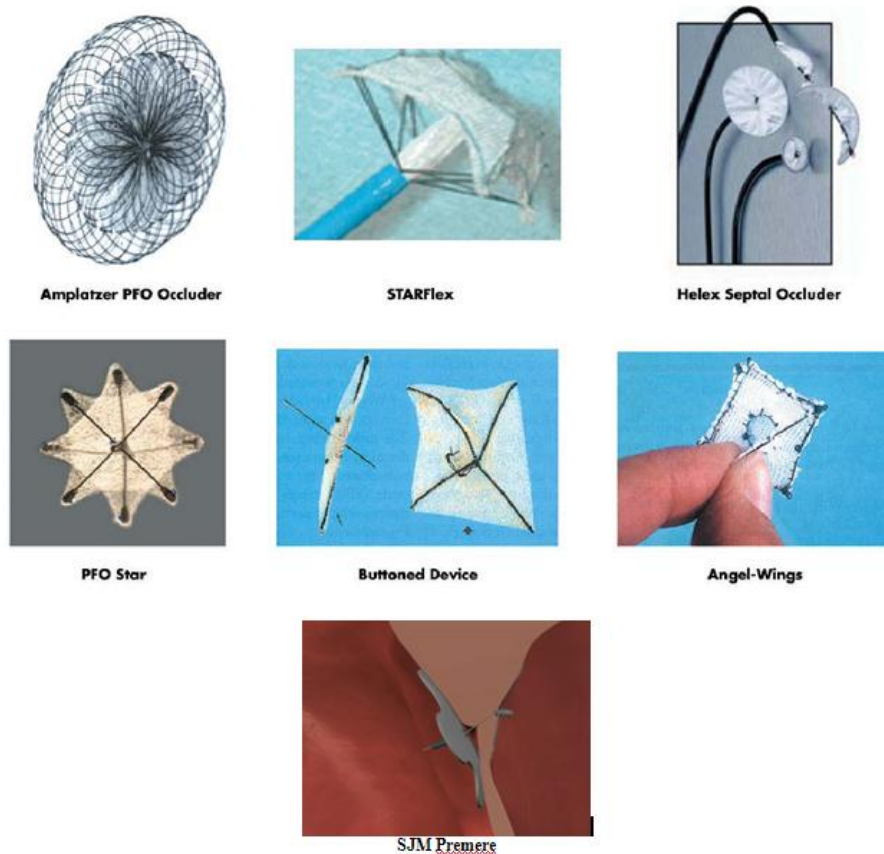


Figure 24 – PFO closure devices [61]

4.4 Anatomically Important Features for Device Deployment

In order for the device to function as intended, it is critical for the device to be designed knowing the anatomic structures that will interact and affect the device. In general, for device design, the engineer must consider the average anatomy that will affect the device,

but almost more importantly, they must consider variations to the norm. Some of the variations that need to be considered for device deployment are the location, size, rim dimensions, and tissue quality of a PFO [51]. Each of these topics will be described below.

4.4.1 Location

When viewing the atrial septal wall from the right atrium, Sweeney describes the atrial septum as a blade-shaped structure as shown below in left side of Figure 25 near the portion labeled FO. The blade tip extends into the superior vena cava (SVC) and is bordered by the aortic root on the anterior margin. The inferior margin is bordered by the Triangle of Koch, which is formed by the coronary sinus, the tricuspid annulus, and the Tendon of Tदारo [82]. The location of the PFO in the right atrium is directly adjacent to the Triangle of Koch [19]. The posterior margin is formed by the fossa ovalis and the entrance of the IVC. The PFO location is in-line with the IVC, as blood flowing from the IVC during fetal development would be directed across the PFO. The fossa ovalis was located halfway between the Triangle of Koch and anterior margin of the SVC. Additionally, the fossa ovalis was separated from the aortic root by only a narrow septal musculature averaging only 5mm in adults [82].

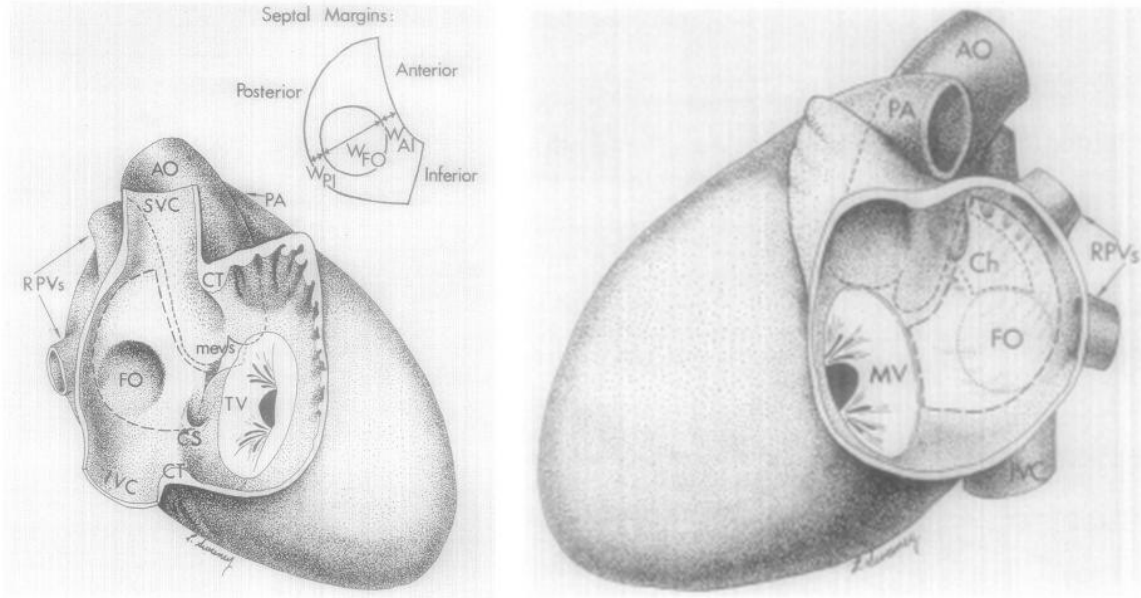


Figure 25 – PFO anatomical locations (Left) Right atrial view. CS: coronary sinus; CT: crista terminalis; FO: fossa ovalis; IVC, SVC: inferior and superior vena caeve; mevs: membraneous ventricular septum; PA: pulmonary artery; RPVs: right pulmonary veins; TV: tricuspid valve; W_{AI}, W_{PI}, W_{FO}: width of anterior and posterior isthmi, fossa ovalis. (Right) Left atrial view. Ch: persistent channel of foramen ovale; MV: mitral valve [82]

Sweeney continues to describe the atrial septal wall, but from the left atrium's perspective. The anterior margin follows the aortic root just like the right atrium. The posterior margin was bordered by the right pulmonary veins with the tip of the blade very close to where the superior pulmonary vein entered. The ridge of the mitral valve formed the inferior margin. The opening of the PFO in the left atrium is superior to the opening of the PFO in the right atrium and lies adjacent to the aortic cusps. The shape of the tunnel was noted to form a crescent arch along the anterior margin [82].

These anatomical positions were verified when examining cadaver specimens at the University of Minnesota's anatomy laboratory, see Figure 26.

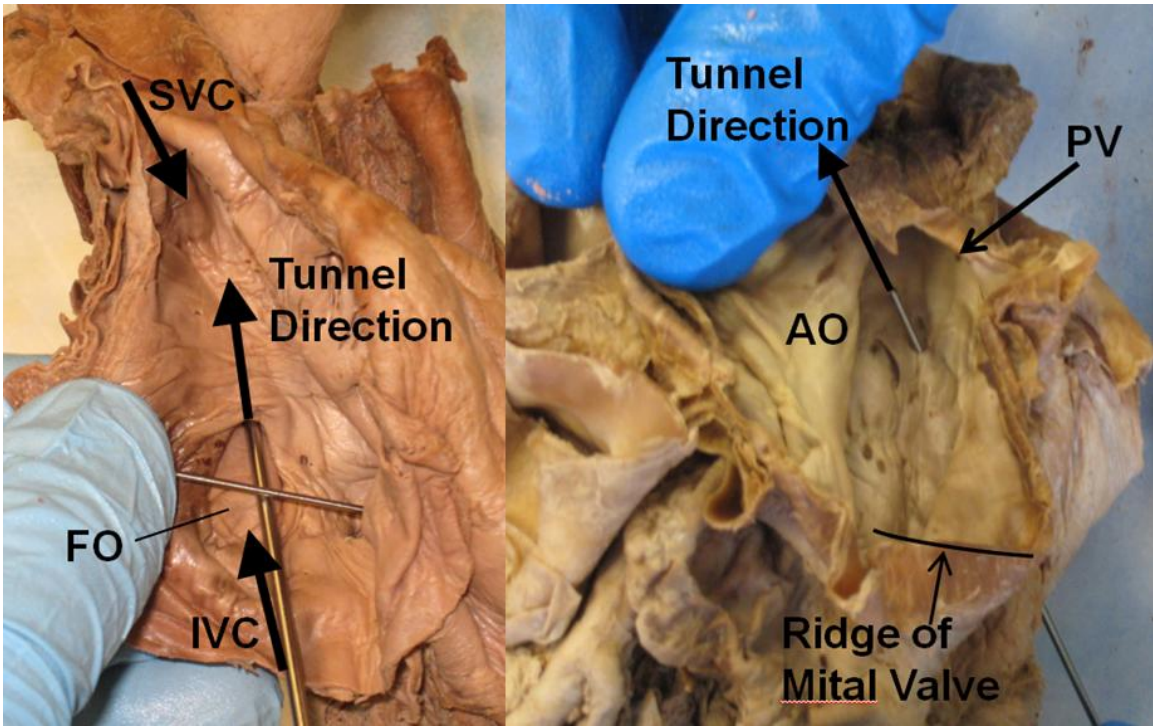


Figure 26 – Anatomic locations in a cadaver. (Left) Right atrium view (Right) Left atrium view [Pictures taken by Eric Jerke and Nathan Handel at the University of Minnesota’s Anatomy Laboratory].

4.4.2 Size

Proper sizing of the PFO can lead to more effective placement and efficacy of the closure device as well as a reduction in clinical complications [51]. At the time of this research, PFOs were almost exclusively sized using either balloon or echocardiography. Another imaging modality that will be explained in greater detail in section 4.5 is the use of multidetector CT for preprocedural evaluation and planning. This imaging modality can be very useful in understanding the spatial orientation and relation of the defect to the surrounding anatomical structures [51]. These three imaging modalities are shown below in Figure 27. Other imaging modalities exist, but were not explored by this researcher.

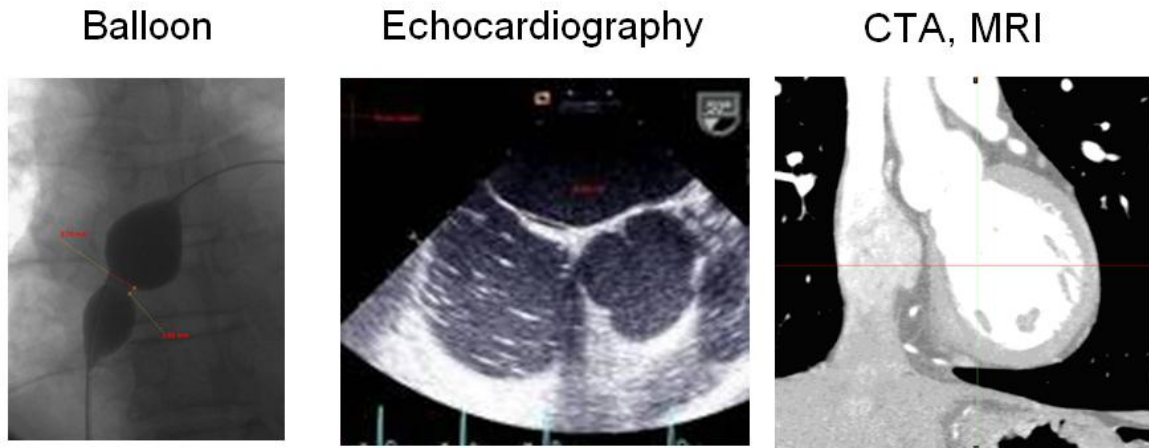


Figure 27 – Images of PFO sizing techniques (Image courtesy of SJM) [17]

Traditionally, balloon sizing has been the primary tool to size ASDs [51]. Fluoroscopy is used to visualize the PFO anatomy when sizing using a balloon. Using a balloon is preferred due to easily identified diameter measurement and understanding of tunnel compliance (Figure 28). The tunnel, initially thought to be a round shape, was later discovered to be an oval as shown in Figure 29 [42]. Since the opening of the PFO is not circular, the use of a balloon will stretch and distort the PFO opening [27].

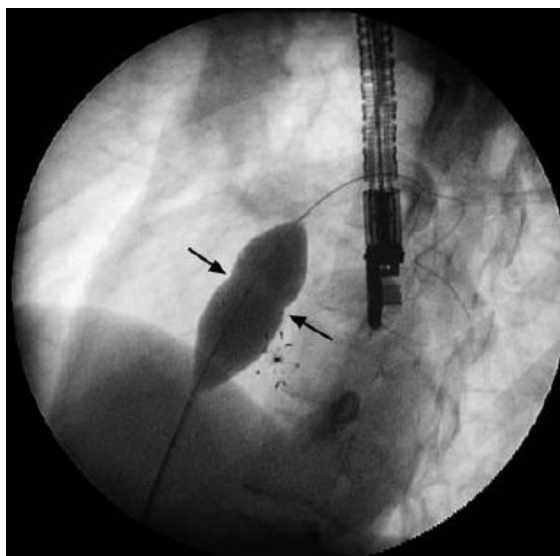


Figure 28 – Balloon sizing of a PFO [25]

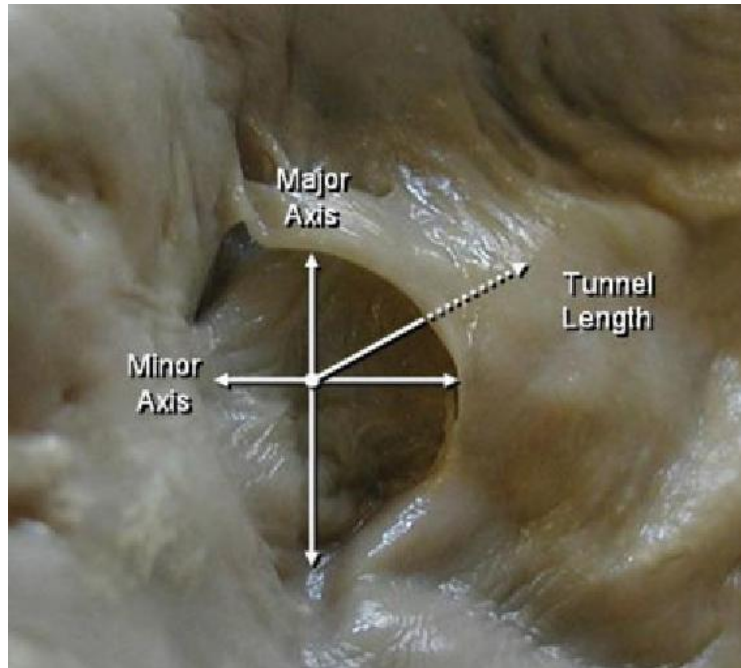


Figure 29 - Tunnel diameter and direction [42]

Transesophageal echocardiography (TEE) is also used to size PFOs as it is one of the main diagnostic tools used to identify a PFO. The main issue with using TEE is the ability to record out of plane measurements that distort the true dimensions. However, there are some disadvantages of TEE when compared to intracardiac echocardiography (ICE). The use of ICE has continued to gain support and might exceed 50% in the United States [51].

The PFO morphology has been well documented in literature. The fossa ovalis represents ~28 percent of the total area of the atrial septal wall [82]. A compiled list of various different size measurements made for PFO anatomy is presented below in Table 1.

Table 1 – PFO sizing from literature

Author	Fossa Ovalis Diameter (mm)	PFO Diameter (mm)	Tunnel Length (mm)	Ballooned Tunnel Length (mm)
Marshall [60]		9.2 ± 2.6	9.1 ± 4.7	.5 ± 1.6
Harms [43]	19.9±5.3	13.0 ±3.5	11.3±3.2	
Hara [42]		7.3 ± 1.7	7.1 ± 3.1	
De Castro [31]	17.9±3.3			
Sweeney [82]	17.5			

4.4.3 Rim Dimensions

The aortic root lies on the roof between the left and right atrium and the portion that is near the septum secundum forms the aortic rim. If the septum secundum is thin, the PFO is closer to the aortic root. The opening of the PFO is along the anterior wall of the aortic root in the left atrium. In some cases, Ho reported that the thickness of this anterior wall of the aortic root was only 1mm thick [46]. The close proximity of aortic root and PFO cannot be overemphasized and complications resulting from the erosion by the device have led to patient deaths [25] & [46]. Closure devices need to be designed to keep the PFO closed, however, those with stiff spokes or arms are at risk for perforating the aortic wall. Due to this catastrophic potential, device companies are trying to develop closure devices to match the PFO anatomy [25]. Also, a deficient aortic rim does not allow the right-sided disc to fully seat and it has the potential to migrate.

4.4.4 Tissue Properties

Tissue properties play a drastic role in the successfulness of device placement. Due to the thin and mobile nature of the septum primum, it can be displaced by balloon sizing or device placement. The length of the tunnel is determined by the overlap of the septum primum and septum secundum. The more hypermobile the septum primum, the more the results will change for tunnel length (Figure 30) [60]. In some cases, opening of the overlap can occur with placement of the closure device. One of the benefits of balloon sizing is the ability to observe the compliance of the septum primum [60]. In cases where a compliant primum is present, the waist of the device will push the septum primum posterior-inferiorly, while being supported by the muscular septum secundum [46].

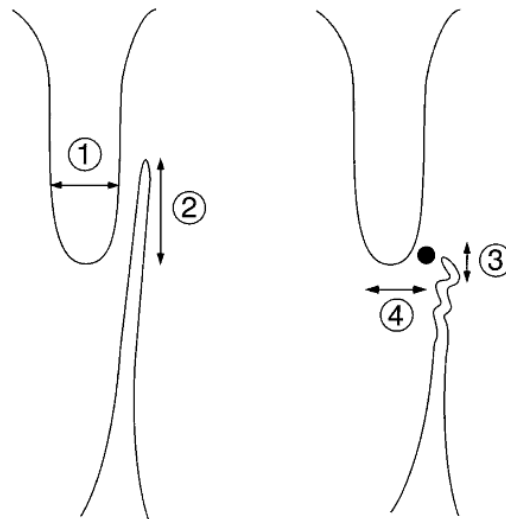


Figure 30 – PFO tunnel length. (1) Septum secundum thickness (2) tunnel length (3) collapsed tunnel (4) offset after device placement [60]

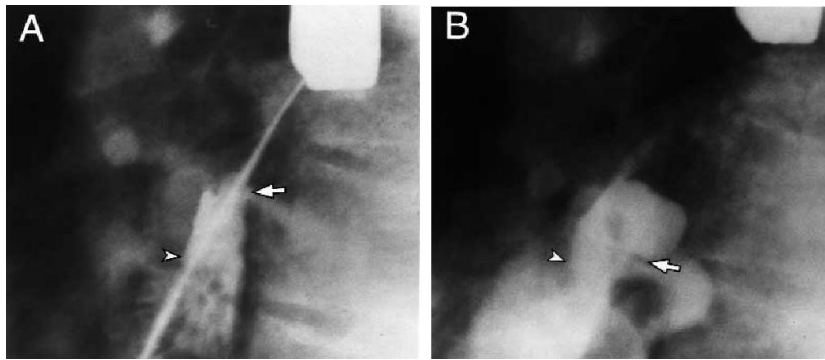


Figure 31 – Septum primum compliance. (Left) Arrows represent the tunnel length prior to balloon sizing. (Right) Arrows represent the tunnel length after balloon sizing [60]

Excessive excursion of the septum primum into either the right or left atrium, during a heart cycle, is referred to as hypermobile and is designated as an atrial septal aneurysm (ASA) [67]. An example of a hypermobile septum is shown below in Figure 32 and Figure 33. Harms defined an ASA with a fossa ovalis diameter of $\geq 15\text{mm}$ and an excursion of $\geq 10\text{mm}$ [43]. With this definition, Harms found 32% of all PFO patients have an ASA [43]. The presence of an ASA has been identified to further increase the risk of paradoxical embolism [61]. Though, in general, it has been shown that the presence of an ASA does not increase the risk of device complications, an ASA does need to be considered when selecting the appropriate device. The device size must be increased to accommodate the hypermobility of the septum primum [67].

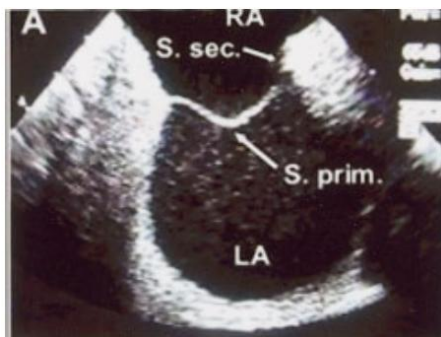


Figure 32 – Hypermobile Septum [67]



Figure 33 – Cadaver hypermobile specimen (picture taken by Eric Jerke and Nathan Handel at the University of Minnesota Anatomy Lab)

4.5 3D Anatomical Model Creation

There are three basic steps to create a 3D anatomical model: CT data acquisition, image processing, and 3D reconstruction [81]. In this section, the basics of how to acquire a good CT scan for the purpose of 3D anatomical model creation will be described as well as the work performed to process and reconstruct the 3D anatomical models from CT scans. After the 3D anatomical models are created, they are verified against cadaver specimens for the location of various heart structures.

At the time of this research, contrast enhanced TEE was the gold standard for diagnosis of a PFO with ICE becoming more widely available, however, both of these techniques are invasive procedures [85]. One of the critical tasks in structural heart disease requires the interventionalist to make a diagnosis of a 3D heart defect using a 2D imaging modality [18]. In recent years, advances in non-invasive diagnostic technology have improved temporal and spatial resolution such that it is now possible image the heart. In this case, two technologies have emerged as non-invasive cardiac imaging modalities: magnetic resonance imaging (MRI) and multislice CT [78]. However, multislice CT has a significant advantage with higher overall accuracy when trying to detect cardiac defects [78]. It is now possible for physicians to create 3D reconstructive models from 2D slices from a CT scan [18]. The improvement of this technology makes it a viable option as a non-invasive diagnostic technique for PFOs [85].

4.5.1 CT Data Acquisition

A CT scanner consists of an X-ray tube that emits an X-ray beam that a row of detectors will pick up. The detectors will read the attenuation (loss of signal) of the X-ray beam as it passes through the body. Higher anatomical density results in higher attenuation (Figure 34) [65].

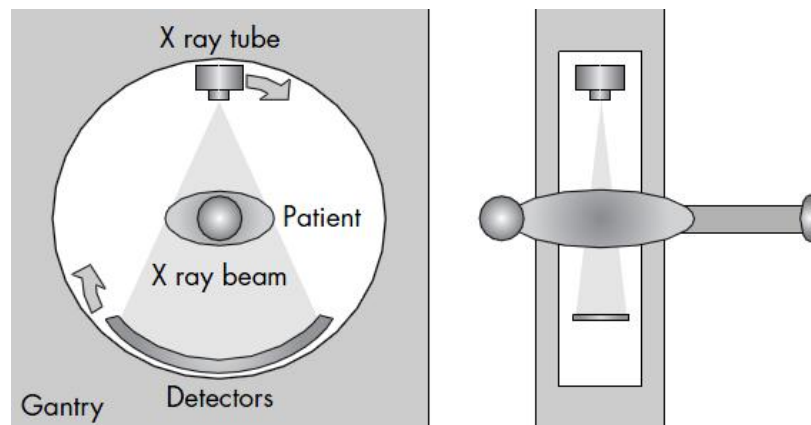


Figure 34 – CT Scanner [65]

The different anatomical densities are read by the detectors using an absolute measuring scale called Hounsfield units (HU) [65]. This scale is shown below in Figure 35.

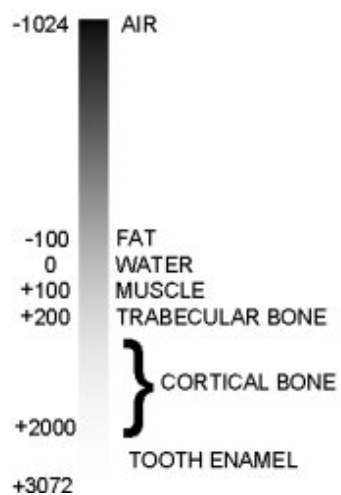


Figure 35 – Hounsfield Units Gray Scale Correlation to Air, Water, etc. [9]

When CT was first introduced, they used a sequential acquisition method referred to as step and shoot. This first generation scanner required the table to be moved for each sequential image to be taken. This process was time consuming and extremely sensitive to motion. Thus, it was not a viable option for cardiac imaging [65]. The introduction of spiral CT allowed for faster scan rates as well as the possibility to reconstruct the axial slices creating a volume model. However, the use of CT for imaging of the heart was not made possible until the addition of multislice spiral CT. These scanners were able to scan much larger volumes in less time [65]. The evolution is pictorially shown below in Figure 36.

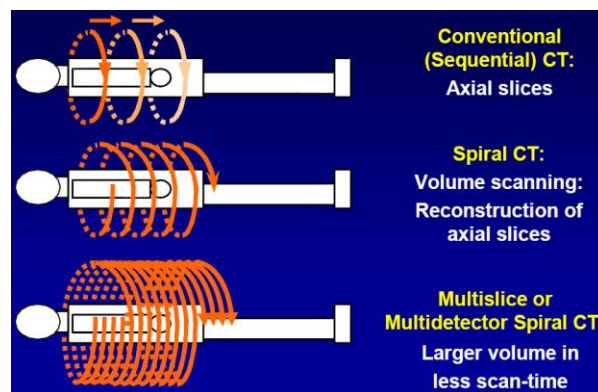


Figure 36 – CT scanning evolution. (Top) Sequential, (Middle) Spiral, (Bottom) Multislice CT [65]

Hoffman et al described the image acquisition process as 3 steps: perform a topogram, determine an adequate image initiation to ensure correct contrast enhancement, and lastly, obtain the CT scan. The first step is to perform a topogram, a low energy scan; helps ensure the patient's anatomy is in the correct position [47].

The second step is to determine how much of a time delay is needed to allow the iodinated contrast media to reach the desired anatomical region. Two techniques are

used: timing bolus (Figure 37) and bolus tracking (Figure 38). A timing bolus utilizes a small amount of contrast media followed by saline solution. Images are taken every two seconds to determine when the contrast media will reach the desired anatomical region. Similarly, bolus tracking requires a contrast media to be injected at 5ml/s and an axial image is taken every two seconds until the contrast reaches its peak level in the desired anatomical region. The time delay is then used to determine when to initiate the CT scan. Both of these techniques produce the same results if used correctly [47].

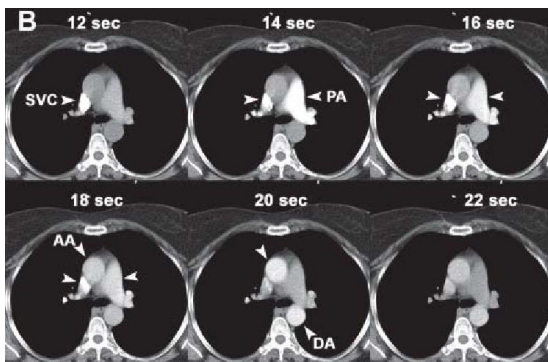


Figure 37 – Timing bolus image acquisition. Images are taken every 2 secs to determine when the contrast media will reach the desired anatomical region. This delay is then used to determine when to initiate the CT scan [47].

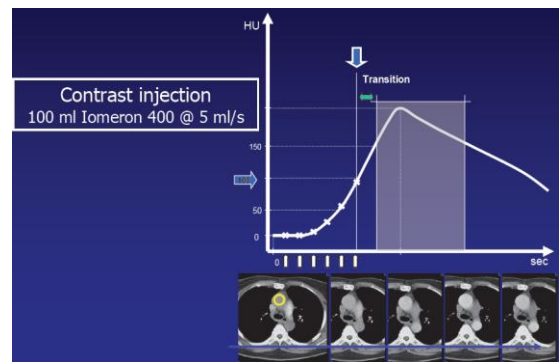


Figure 38 – Bolus tracking of contrast media. Contrast media is injected at 5ml/s and an axial image is taken every 2 secs. When the contrast reaches its peak level determines the scan delay that is needed [65].

The last step is to acquire the CT volume dataset. The CT scan requires a delayed start using the calculated delay obtained in the second step allowing the contrast media to reach the desired anatomical region [47].

The quality of the image acquired affects every processing step downstream when trying to create a more anatomically accurate 3D model. Quite a few things can affect the

quality of the CT scan obtained. These are spatial resolution, temporal resolution, scan time, synchronization with cardiac cycle, and proper contrast media gating [65].

4.5.1.1 Spatial Resolution

Spatial resolution refers to the resolution of the image. Similar to new high definition televisions that feature increased picture pixel resolution, spatial resolution for 3D volume models refers to a voxel (Figure 39) or a pixel multiplied by the slice thickness. A pixel is calculated by the field of view divided by the CT screen resolution. According to Mollet et al a voxel should be less than 0.4 mm^3 [65]. It is this author's experience that a scan size should be closer to $.04 \text{ mm}^3$ as can be seen in Figure 40. Scans can be overlapped to decrease the voxel size, but this will increase the scan time to cover the same area and thus a balance needs to be struck when trying to increase resolution or decrease motion artifacts.

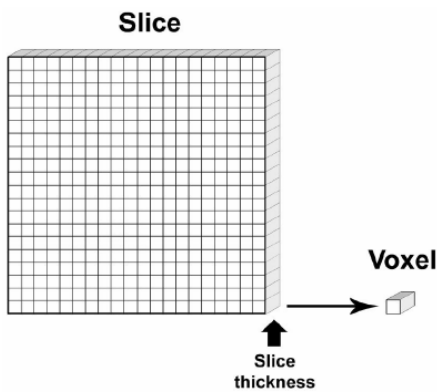


Figure 39 – Voxel [65]

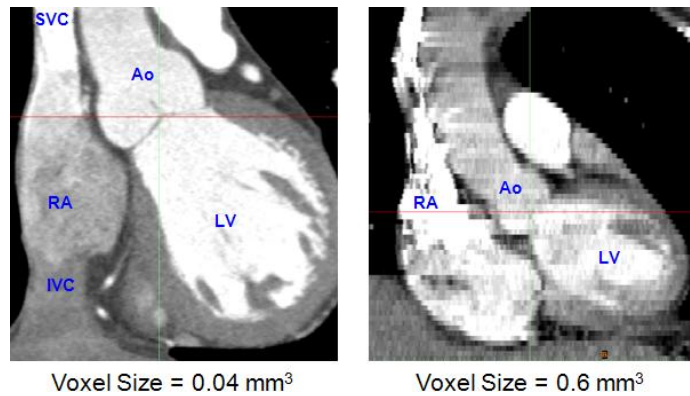


Figure 40 – Voxel size comparison (Image courtesy of SJM) [17]

4.5.1.2 Temporal Resolution

Temporal resolution refers to the precision of a measurement with respect to time. In the case of collecting data using a CT scan, temporal resolution shows up in the form of how fast the heart is beating and the rotation speed and detection time of the CT scanner's X ray tube [65]. According to Hoffman et al, the heart rate should be less than 65 beats per minute and if the heart rate is higher than this an inspirational breath hold technique along with intravenous or oral β -blocker should be applied. Combining these can lead to an average reduction of 11 beats per minute [47]. The rotation speed and detection time is significantly affected by the high heart rate as can be seen below in Figure 41. A single reconstruction requires a larger time frame and this time is not always available for high heart rates. However, the combination of a low heart rate and single segment image reconstruction can lead to the best quality CT scans [65].



Figure 41 – Temporal resolution [65]

4.5.1.3 Scan Time

As the technology in this field has increased, the scan time has decreased. It wasn't until multislice CT that the scan time was short enough to image the heart within a single breath hold. An effect of this technology on scan time is that a 4 multislice CT took ~40

seconds to scan a heart and a 64 multislice CT can scan the same heart in 12 seconds. Mollet et al reports a breath hold of 20 seconds is tolerable for most patients [65]. One of the contradictions for coronary CT angiography is the inability to hold one's breath for 15 seconds [47].

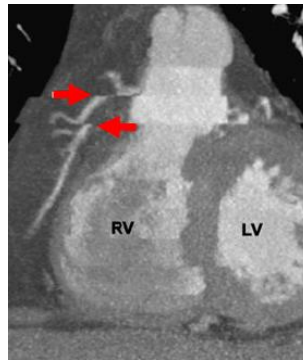


Figure 42 – CT scan motion artifact [47]

4.5.1.4 Synchronization with Cardiac Cycle

Multislice CT scans are subject to severe motion artifacts due to the contraction of the heart. Thus, retrospective electrocardiography (ECG) is used to only obtain data from the diastolic phase of the heart cycle. This phase is during the rest and recovery phase when the heart's motion is minimized. To utilize retrospective ECG, an ECG trace monitors the entire scan and during reconstruction after the scan, the optimal data can be chosen to ensure the least amount of motion artifact [65]. Restrospective ECG requires a high radiation exposure, but it allows the technician the ability to minimize artifacts with optimal reconstruction segments [65]. Restrospective ECG is shown below in Figure 43; a volume model is created by combining segments 1-4 during the reconstruction process.

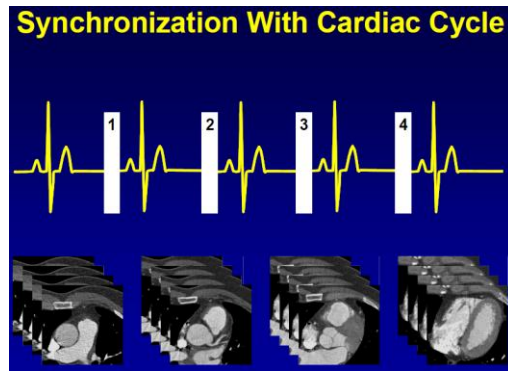


Figure 43 – Retrospective ECG [65]

4.5.1.5 Proper Contrast Gating

As previously described, one of the steps required to obtain a CT scan is to determine when the contrast media will arrive at the anatomical region of interest. This final requirement was added by this author when doing the work of manipulating CT data for reconstruction of ASDs. This is critical and requires tracking of the bolus through both atriums to ensure proper gating of contrast media, therefore, providing sufficient contrast in both the right atrium and the left atrium simultaneously. According to the Hounsfield scale, blood has a HU range of +30 to +45 where as muscle is near +40 [3]. In the area of the atrial septal wall, the muscular structure is extremely thin and thus the difference between blood and tissue is extremely hard to determine. However, the addition of contrast, which is +130 HU, makes the difference between blood and muscle very easy to see the difference [3].

4.5.2 Image Processing

The second component, when creating a more anatomically accurate 3D model, is to reconstruct the CT images. For this, commercially available software, Mimics from Materialize, was used courtesy of SJM.

4.5.2.1 Mimics Description

At the time of this research, Mimics consisted of two base modules, the main program and the import module, and 5 additional modules that could be added: RP slice, STL+, simulation, MedCAD, and FEA. Below is a brief description and evaluation of each of these modules.

4.5.2.1.1 *Mimics Main Program*

The Mimics program interactively reads CT/MRI data in the Digital Imaging and Communications in Medicine (DICOM) format. Segmentation and editing tools enable the user to manipulate the data to select bone, soft tissue, skin, etc. Once an area of interest is separated, it can be visualized in 3D. After this visualization, a file can be made to interface with STL+ or MedCAD module. CAD data, imported as STL files, can be visualized in 2D and 3D for design validation based on the anatomical geometry.

4.5.2.1.2 *Import Module*

The Import module imports CT and MRI data from a wide variety of scanner formats. The data can be accessed from CD, optical disk, DAT tapes, 4 mm tapes, etc.

4.5.2.1.3 RP Slice Module

RP Slice module provides an interface to Rapid Prototyping systems via sliced files with patented support structure generation. The perforated support structures are generated in no time and use less material. This module has no real value because St. Jude's rapid prototyping machine has a program called 'Lightyear', which is a 3D file preparation software used to prepare STL files for part building on the stereolithography (SLA) system. Also, local rapid prototyping companies have similar programs.

4.5.2.1.4 STL+ Module

STL+ module provides interface options via triangulated formats. This module is the main interface with rapid prototyping. Also, the anatomy data can be exported to CAD through the use of small enough STL files.

4.5.2.1.5 MedCAD Module

MedCAD module provides a direct interface to CAD systems via surfaces, curves, and objects exported as IGES files. This module allows the user to build basic shapes (points, lines, cylinders, spheres, splines, etc.). These shapes can then be exported as IGES files. The anatomy data cannot be exported to a CAD system because not all of the data can be converted to the CAD system due to limitations placed on the CAD software.

4.5.2.1.6 *Simulation Module*

The Simulation module is an open platform for surgical simulations. The user can perform a detailed analysis of the data using the anthropometric analysis, plan osteotomies, and distraction surgeries or simulate and explain a surgical procedure for an implant design [9]. This module also allows the user to slice the 3D data set in a view not based on the 3 standard planes (axial {top-down}, sagittal {left-right}, and coronal {front-back}). This tool is extremely useful allowing the user to cut away features of the anatomy not crucial to their design.

4.5.2.1.7 *FEA Module*

The FEA module provides an interfacing to FEA (Finite Element Analysis) and CFD (Computational Fluid Dynamics). This module allows the user to reduce, smooth, and fix the mesh of the anatomy. Through reduction, smoothing, and fixing operations, the triangulated mesh can be exported with the STL+ module to CAD. When imported into CAD as a STL file, the mesh needs to be fewer than 20,000 triangles to be converted into a solid body and under 100,000 to be converted into a surface. If more than 100,000 triangles exist, the object will be treated as a graphic (a picture).

Dr. Erdman's team along with SJM evaluated these modules and determined the STL+, Simulation, and FEA modules would be added to the base modules for the purpose of reconstructing 3D anatomical heart models. With the ultimate goal to create a more accurate 3D anatomical model, each of these modules served a distinct purpose that will be described in more depth below.

4.5.2.2 Importing DICOM Images

As previously mentioned, the Mimics Import module is utilized to import DICOM images. This was accomplished by using the Automatic Import wizard, which in most cases recognized the file type and allowed for conversion. Almost always, the orientations needed to be changed or added to orient the DICOM slices correctly.

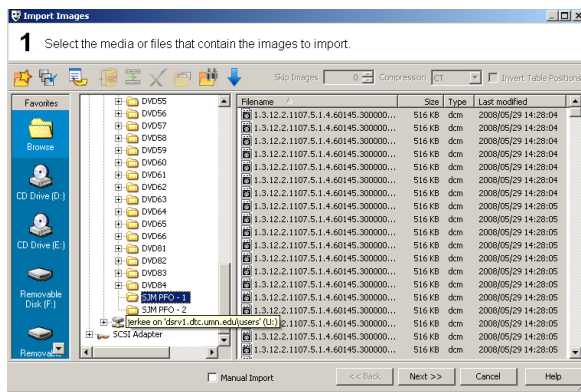


Figure 44 – Mimics Automatic Import Wizard

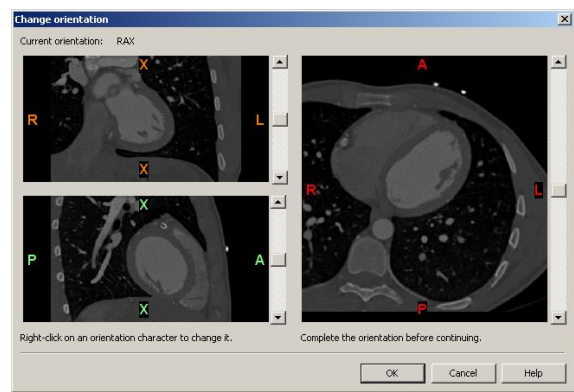


Figure 45 – Mimics orienting DICOM data

As described previously, obtaining quality DICOM data can be difficult. In the event that part of the data set is either missing or of poor quality, it was decided to exclude these images as seen in the example below, Figure 46. Besides filtering out images of poor quality, additional images were filtered out when the data set contains more anatomical structures than interested in.

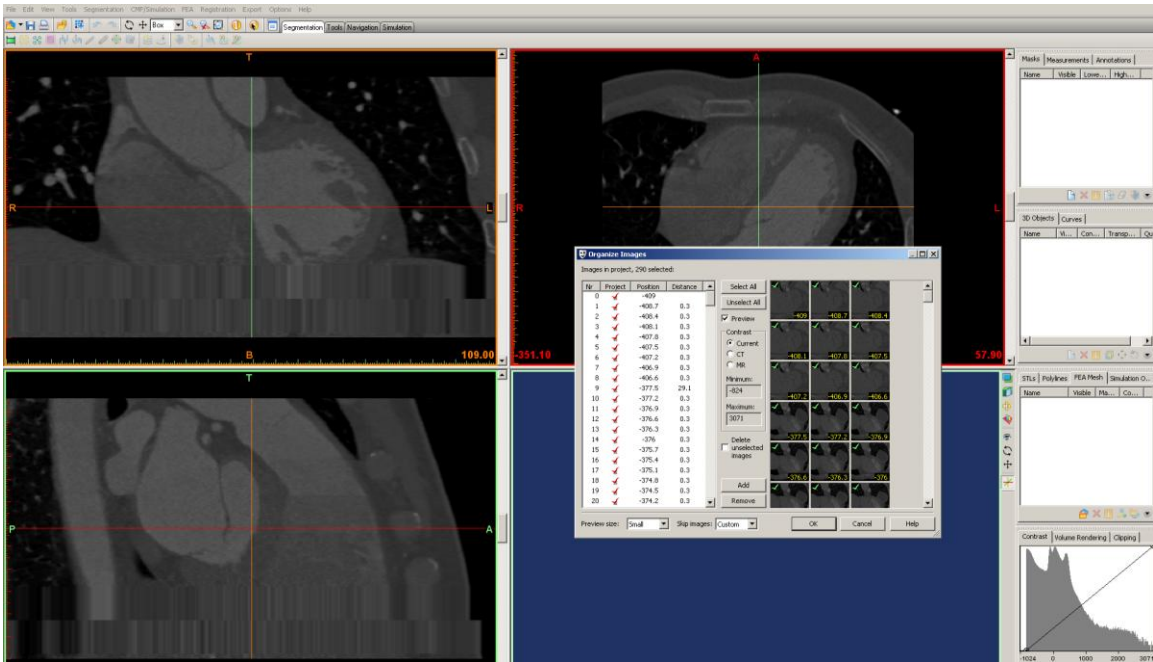


Figure 46 – Mimics CT scan with image distortion

4.5.2.3 Segmentation

Effective use of the Mimics segmentation tools allowed the ability to isolate the desired anatomy; however, there is no replacement for quality CT scans. If a CT scan has a high deviation of features based on gray scale values, mimics will have a much easier time selecting the region of data. For example, bone shows up well on CT images because of the high differential gray scale values that distinguish it from muscle tissue. However, as previously mentioned, muscle tissue and blood fall into the same general region of the gray scale. This is why it is important to have proper gating and use of contrast media with the capture of the CT scan. Similarly, the resolution and speed of the scan is important to minimize artifacts. No matter what manipulation is done, if the scan is unclear and anatomic features are not able to be distinguished, there will be poor results. Manual manipulation was done to create good models, but it was tedious and the data

was subjectively edited in an artistic way instead of objectively edited based on actual anatomical features.

The goal of this segmentation is to create a mask that highlights the anatomical structure of interest. This mask did not highlight blood and any other anatomical structure of non-interest. There is no right or wrong way to create a mask, but there are steps that were followed. The main tools used to create a mask of a heart scan are described below.

4.5.2.3.1 *Windowing*

Windowing was used to "see" the data more clearly. It highlights or maximizes the difference between certain anatomic features. This was used to distinguish anatomy and to determine if the generated masks accurately highlighted the desired region. The black line, in the figure below, was manipulated from showing the entire gray scale (-824, 3071) to a window (-150, 350) that amplified the clarity or contrast of the images. However, this didn't change the actual data; it merely amplified a certain gray scale range.

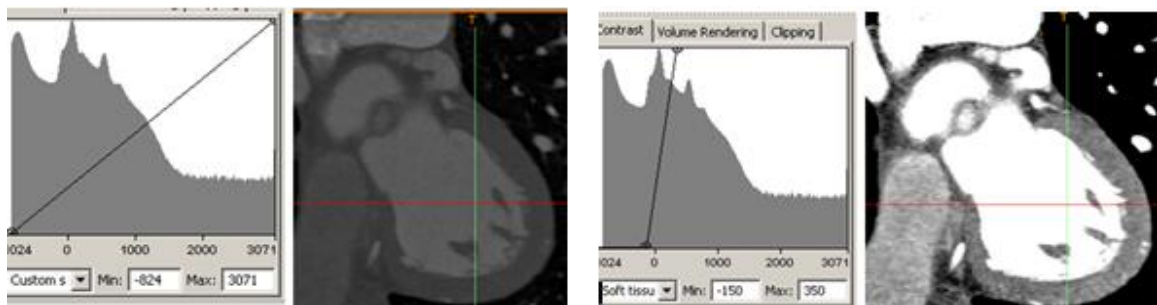


Figure 47 – Mimics windowing of imported CT scan. (Left) Standard window. (Right) Adjusted window

4.5.2.3.2 *Thresholding*

Thresholding means that the segmentation object (visualized by a colored mask) will contain only those pixels of the image with a value higher than or equal to the threshold value. Sometimes an upper and lower threshold is needed; the segmentation mask contains all pixels between these two values. There are a few tips for selecting an adequate threshold value: use a predefined threshold set such as soft tissue (CT) defined by Mimics, manually by looking through the different images and adjusting the values until the desired anatomy is showing, or draw a profile line.

Drawing a profile line in the main window across the atrial septal wall, for example, generated an intensity profile. Figure 48 is a representation of the profile line across the atrial septal border in the axial view. The straight horizontal line is the current threshold value. Lowering of the maximum threshold value from 225 to ~170 will result in deletion of most of the right atrium noise (blood that shows up as tissue). Due to the quality of the scan, lowering this value placed holes the atrial septal wall, which were filled in manually.

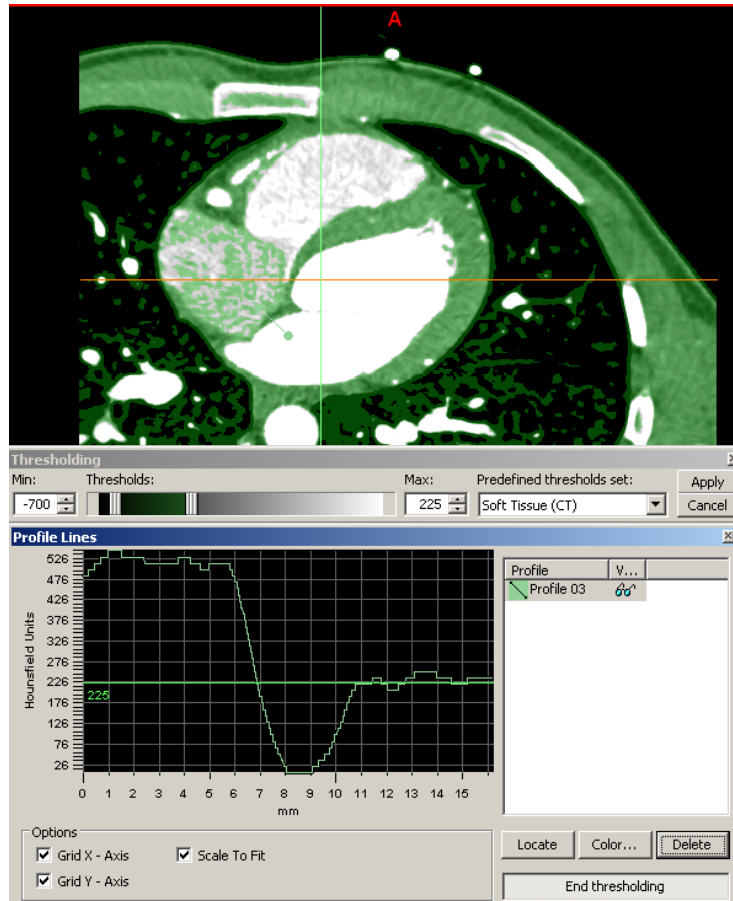


Figure 48 – Mimics profile line

4.5.2.3.3 Region Growing

The region growing tool made it possible to split the segmentation created by thresholding into several objects and to remove floating pixels. Region growing is one of the most powerful functions in the program. After any edits, region growing was always used on the current mask to eliminate floating pixels. Floating pixels are impossible to build using a rapid prototyping machine and thus need to be removed.

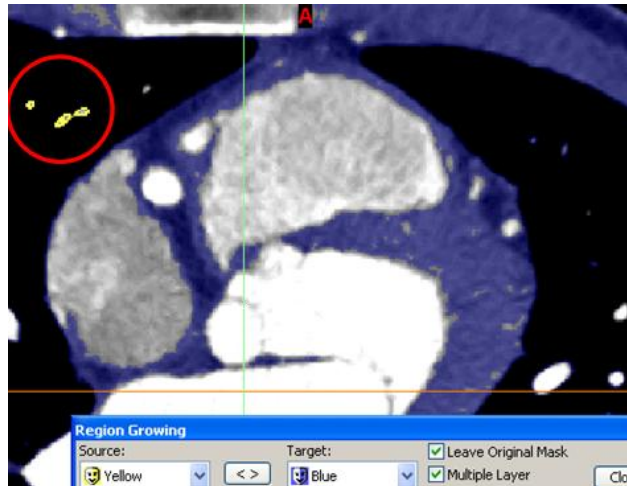


Figure 49 – Mimics effect of region growing will eliminate floating pixels

4.5.2.3.4 *Cropping*

Usually, a CT scan of the heart represents more than just the heart. Since the ribs, spine, and lungs were of little interest, cropping out these unwanted features of the current mask saved time when attempting to segment. The crop feature worked to manually shrink the potential masks border. The crop feature was changed in at least two of the views because the CT dataset is a cube. However, only four of the six borders are seen in the one view and the other two borders were selected in another view. Also, it was important to scroll through different slices to confirm deletion of unwanted anatomical features without deleting desired features.

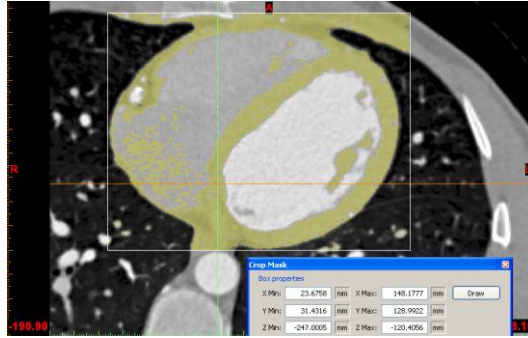


Figure 50 – Mimics image cropping

4.5.2.3.5 *Advanced Segmentation*

A few other segmentation tools that were used to add characteristics are presently not included in the current mask. Each of these tools allowed this author to overcome some of the quality issues of the original data set. Each one was used slightly differently to achieve the best results. These tools are:

- Dynamic Region Growing
- Edit Masks
- Multiple Slice Edit Mode
- Boolean Operations
- Morphology Operations

Dynamic Region Growing

The dynamic region growing tool was used to segment an object based on the connectivity of gray values in a certain gray value range. It allowed an easy segmentation of blood vessels, nerves, etc. in CT images.

The dynamic region growing tool is the only operation that doesn't require a threshold value. The minimum and maximum threshold values are set automatically. The creation of this new mask starts when a pixel is selected. Mimics compares the selected pixels

gray value with the gray values of its neighboring pixels. The pixels with gray values that obey the following rule: $|\hat{i} - i| < d$, are added to the new mask. Where \hat{i} is the average gray value, i is the new gray value, and d is the deviation.

Edit Masks

The edit masks tool was used to manually manipulate the active pixels through draw, erase, and threshold commands. All manual editing functions were performed on the active mask. In edit mask mode, an edit is only placed on the active slice. This was very time consuming and very subjective in determining what was artifact and what was real. Messmer et al confirmed that the automated threshold outcomes frequently require manual edits by experienced designers [64].

Multiple Slice Edit Mode

The multiple slice edit tool was great to remove scatter easily. It took the manual editing that was done on one slice and applied it to other slices. The multiple slice edit tool created a temporary mask for editing. The active voxels of the temporary mask were then added or removed from the original mask or a local threshold was done on the original mask at the active voxels.

Pixels were added and subtracted from the temporary mask through drawing and subtracting operations. This temporary mask was then copied to other slices. The intersecting parts of the temporary and active masks were colored in a third color. It was beneficial to create a new profile line in the area of interest when using local thresholding. In the figure below, the active mask has a threshold value of -134 to 162.

This threshold value falls below the values shown in the profile line. However, the aortic valve showed a contrast difference compared to the surrounding blood, thus, creating an ideal local threshold. With the area selected, a minimum threshold of -134 and a maximum threshold of 420 helped fill in the beginning of this valve. Additional steps and some manual edits were needed to finish reconstructing the aortic root. Then, this temporary mask was copied to additional slices and edited to follow the curvature of the aortic root.

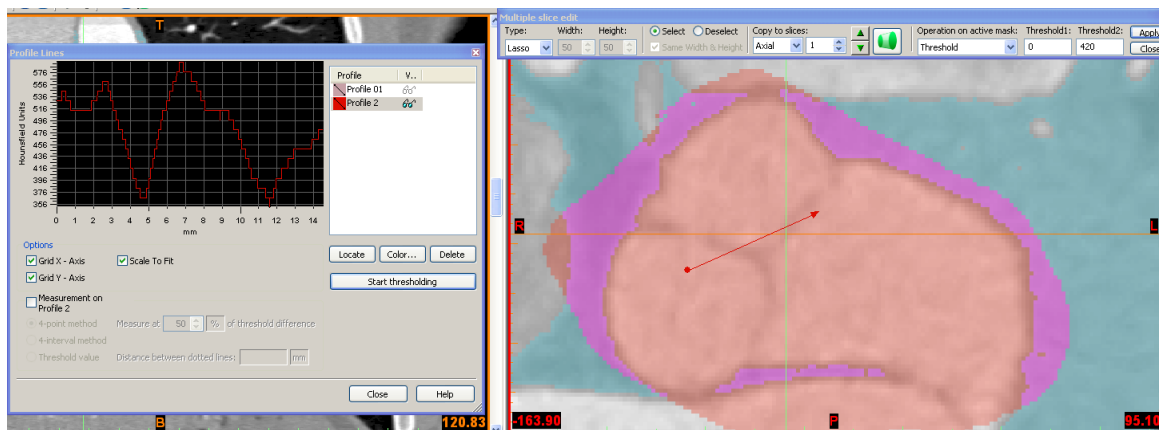


Figure 51 – Mimics local segmentation use of profile line

Boolean Operations

The boolean operation was used to make all different kinds of combinations by adding, subtracting, and intersecting two masks. Dynamic region growing tool was used to perform local thresholding. This threshold mask was combined with the original mask to create a new mask using boolean operations. .

Morphology Operations

The morphology operations tool was not utilized very much during segmentation, but was utilized with the FEA module. This tool will either add or take away pixels from the source mask. The morphology operations are:

- Erode: will take pixels from the edges. When followed by region growing separated parts.
- Dilate: will add pixels to the edges. This was used to restore the effect of the erosion.
- Open: will first apply erosion, followed by dilation. Small edges were removed or opened.
- Close: will first apply dilation, followed by erosion. Small cavities were closed.

4.5.3 3D Reconstruction

In the creation of a 3D anatomical model, the final step was to reconstruct the processed images into a 3D object. Mimics made this step simple, but it was also iterative with the image processing step. The 3D reconstruction process was accomplished by selecting the mask or masks required to build the 3D object.

With the 3D object created, the model was sliced into separate parts to view interior structures. The Simulation module previously mentioned was utilized to accomplish this step. There are three different methods to slice the 3D object: Cut with Cutting Plane, Freeform Cut with Curve, and Cut Orthogonal to Screen. Out of these three methods, using Cut Orthogonal to Screen was the easiest and quickest to use. This feature was used by creating points representing the cutting line that cuts the 3D object orthogonal to the screen. When the 3D object was cut, both of the new 3D objects created are placed on different masks.

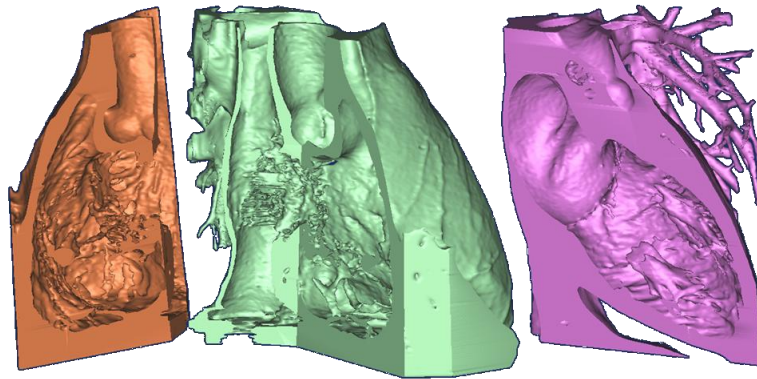


Figure 52 – Mimics slicing of the 3D reconstructed object

Slicing into the 3D object has other advantages besides simply selecting the anatomic region desired. It was used to find holes in the data that should be filled in, artifact data or noise, or missing data such as valves. Since the 3D object was created from 2D planes, by clicking the 3D object on the spot where the data should or should not be, this adjusted the corresponding 2D planes to the location of the mouse click.

4.5.4 Comparing 3D Object to Cadaver

Most of the anatomical positions of the 3D object were able to be verified when comparing to cadaver specimens at the University of Minnesota's Anatomy Laboratory and journal images as seen in Figure 53 and in Figure 54. The purpose of creating this comparison was to make sure all the anatomical structures were displayed with the exception of a PFO. While the fossa ovalis did show up in the form of an extremely thin section by the CT scan, a PFO was not able to be recognized.

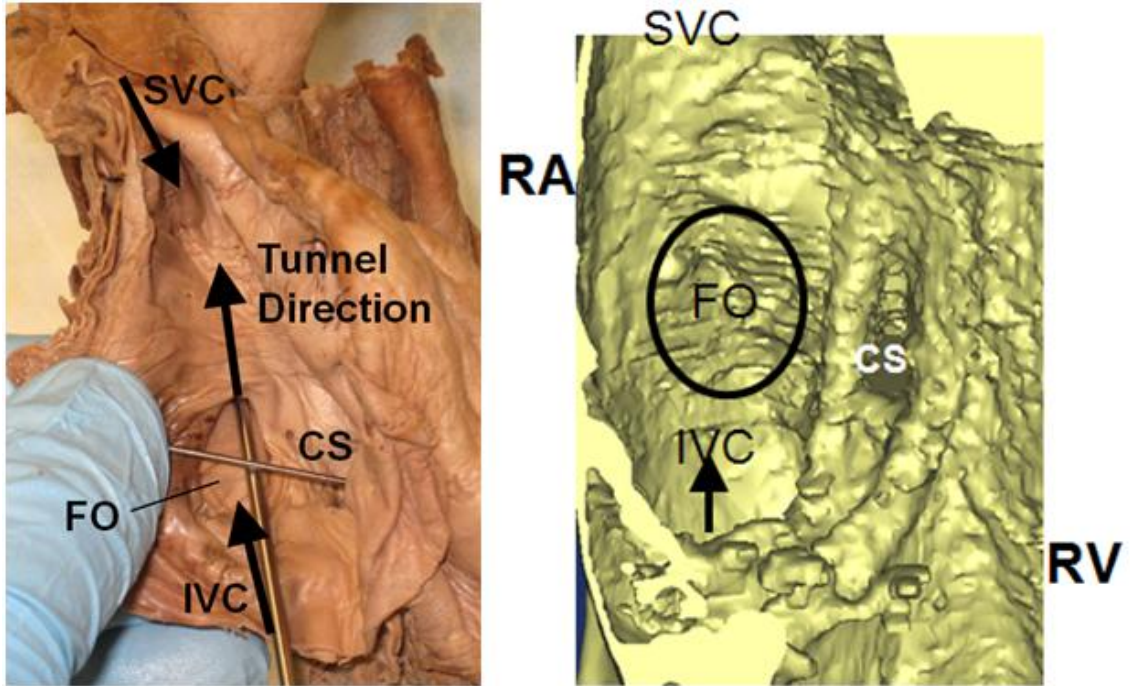


Figure 53 – Mimics right atrium comparison to cadaver

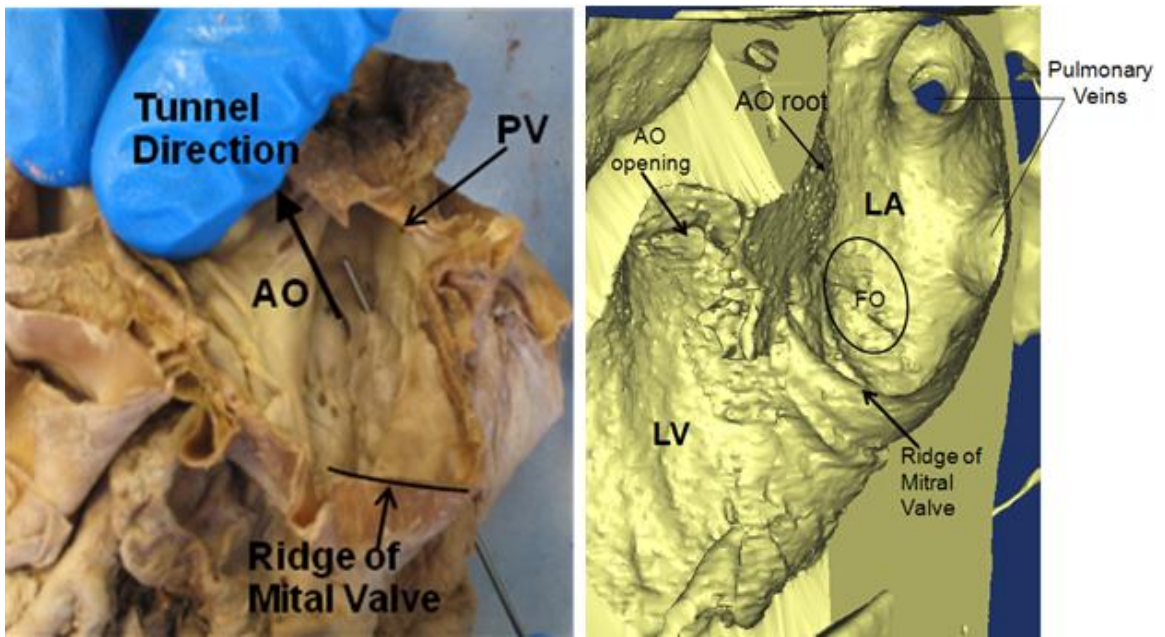


Figure 54 – Mimics left atrium comparison to cadaver

4.6 Anatomical CAD and Bench Top Model Creation

The ability to create bench top models of patient-specific anatomical structures helps in the design and development of next generation medical devices by providing engineers and physicians with an accurate assessment of spatial relationships within the heart [71]. Noecker et al described how his research team created a plastic SLA model of the heart and then created a flexible mold of the exterior structure for the design and development of next generation medical devices. Noecker went on to say that flexible models possess characteristics similar to human heart tissue that are particularly useful in the preclinical development and evaluation of new medical devices [71]. Messmer et al determined that more important than concluding what was considered an average bone was to create the potential deviations or variations from normalcy [64].

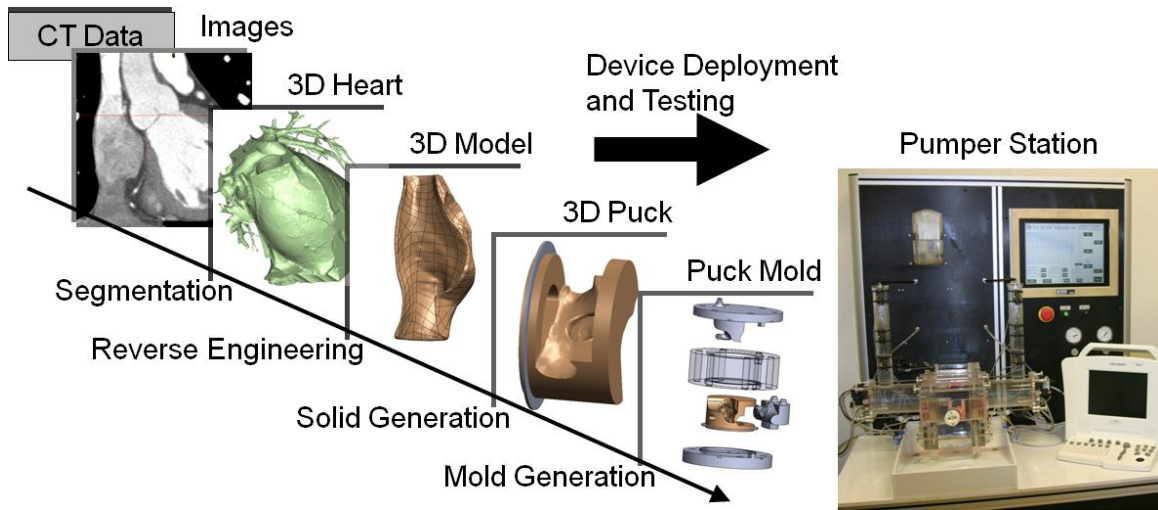


Figure 55 – Bench Top Model Creation Process

At this point, a 3D reconstructed object has been created. In this section, the next steps of converting the 3D object into a 3D CAD model, manipulating this model to conform to

the Heart Beat Pumper Station (3D puck shown in Figure 55), and creating a mold of this 3D puck will be described.

4.6.1 Converting the 3D Object into a 3D CAD Model

For an engineer to have the ability to look at human or animal data in the form of a 3D model is a very powerful tool. To then take this data and convert it into a form compatible with a 3D solid modeling program is even more powerful. The various methods explored to convert the 3D reconstructed object into a CAD model will be discussed below.

4.6.1.1 Direct Import Method

There were three basic methods for directly importing into CAD software explored by this author. The first utilized the Mimics FEA module to reduce the triangle count to a number that the CAD programs (SolidWorks and Pro-E) would allow to import. The second was ScanTo3D [24], a SolidWorks program that converts the triangles into mathematical smooth surfaces. The last was another Mimics module called MedCAD, which was briefly explained earlier, but it provides a direct interface to CAD systems via surfaces, curves, and objects exported as IGES files.

4.6.1.1.1 *Mimics FEA Module*

The FEA module was a method used to reduce, smooth, and fix the mesh of the anatomy. When segmentation is complete and the model is sliced to the engineer's specifications, it

may be desired to export this model directly into a CAD package as a solid model. For this export to occur correctly, the model will most likely need to be reduced in size as popular CAD packages like SolidWorks can only convert <20,000 faces into solid bodies. However, the heart is extremely complex with an entire heart consisting of more than 2,000,000 surfaces in some of the models this author created. Reduction of surfaces can occur without the FEA module, but the current surface count is not known and therefore there is no knowledge as to how much more reduction is needed. Also, through reductions, faulty faces occur and the FEA module was used to fix these faulty faces.

Another primary use of the FEA module was to raise the quality of the triangles so that the preprocessor of an FEA package can build a tetrahedron mesh from the triangles. Prior to opening the FEA Remesher, a couple of steps were followed to assure a smooth remeshing procedure. A shell reduction operation with a value of 1 was used when calculating a 3D object, as many holes as possible were filled in, and the morphology operation was used to smooth out small surface details.

Typically, the entire heart model is not required for the development of next generation medical devices, so the desired input into the CAD system would be only the reduced 3D object of the desired anatomical region. In this case, the 3D object was scaled down to just the atrial septal wall as well as the IVC, SVC, AO root, ridge of the mitral valve, and the entrances of the pulmonary veins. These reductions plus the use of the FEA module made it possible to create an anatomical model under 20,000 triangles.

Figure 56 was a successful attempt to convert the 3D object into SolidWorks. There were many prior attempts that resulted in faulty faces that needed to be corrected in order to have a useable model. The best way to fix these faulty faces was to use some of the features and tools in the FEA module.

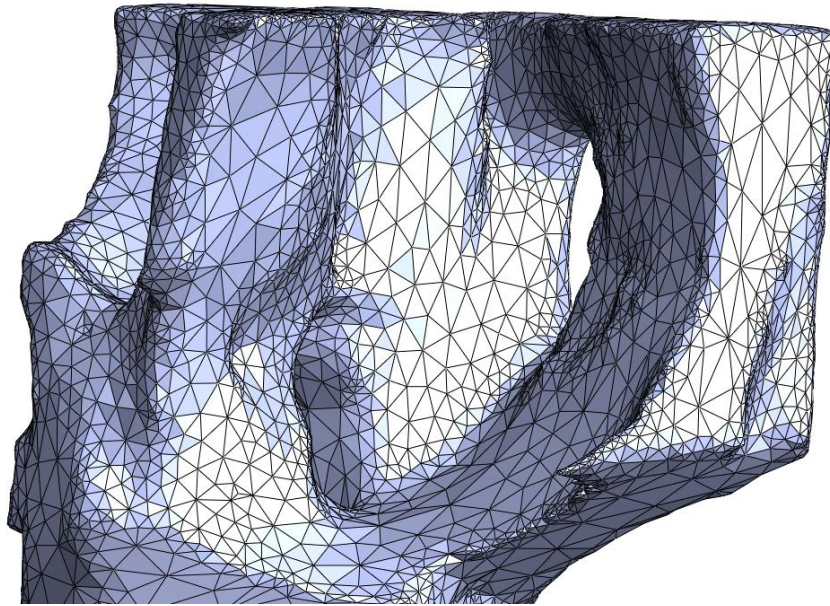


Figure 56 – Mimics direct import

- Smoothing: The smoothing operation decreased the noise in the mesh by adjusting the positions of each triangle's vertices. Generally, the more uniform the triangles prior to smoothing, the better the results.
- Triangle Reduction: The triangle reduction operation allowed for the number of triangles in an STL or 3D object file to be reduced. This reduction can occur on the entire part or just one surface.
- Adjust Inspection Page: Adjust inspection page used a histogram to set the quality threshold for the remesher.

- Fix Wizard: The fix wizard tool provided an interface and advice on how to fix the mesh. The fix wizard helped fix overlapping, intersecting, bad triangles, etc.

4.6.1.1.2 *ScanTo3D*

Solid modeling programs, like SolidWorks, use mathematical expressions, non-uniform rational B-spline (NURBS), to represent curves and surfaces [21]. Currently, there are a variety of existing programs that can create NURBS surfaces when starting with point cloud data or STL data. At the time of this research, SJM used SolidWorks 2008 and it offered an add-on feature called ScanTo3D which attempts to auto construct NURBS surfaces. However, a NURBS surface is made for each triangle. An initial limitation is to get a file under 20,000 triangles just to be able to import the file and then ScanTo3D will convert one triangle to one NURBS surface. Thus, the Mimics FEA module is needed to reduce the triangle count to below 20,000 prior to using this method.

Following this approach would result in an extensive amount of data that is too cumbersome for SolidWorks to process quickly enough to be valuable. Rather, models with 20-100 surfaces are favorable. Therefore, it was decided not to purchase the SolidWorks add-on as these limitations outweighed the benefits.

4.6.1.1.3 *Mimics MedCAD Module*

As mentioned, the MedCAD module was a simplified version of a CAD system, which connected CT data to CAD software. This module was used to build basic shapes (points,

lines, cylinders, and spheres), as well as, modeling of freeform shapes using B-spline surfaces. Figure 57 shows the process used by Starly et al to model the femur bone [81]. These shapes can then be exported as IGES files. However, this module has a severe limitation that not all anatomy data can be exported to a CAD system due to the complexity of the anatomical model. In Starley's research, often surface models would be generated representing the need to close the model to obtain a solid model in CAD [81]. The heart models created are extremely complex and therefore these limitations ruled out the purchase of this module.

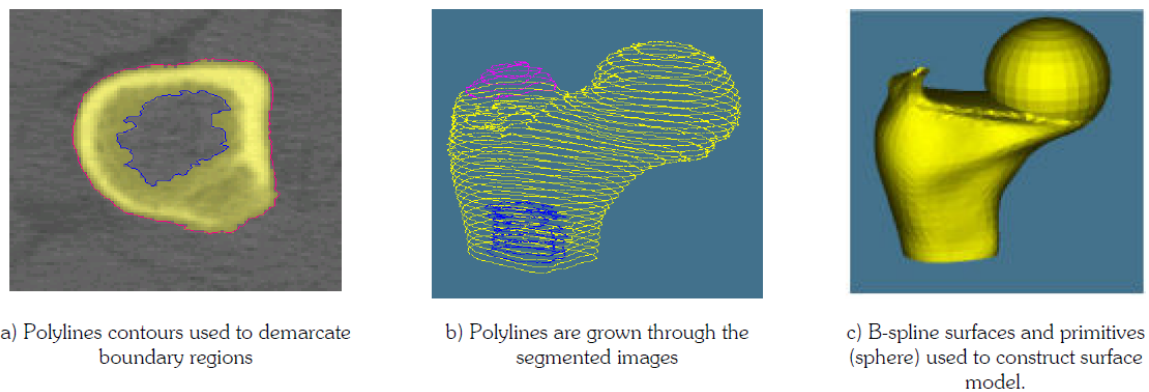


Figure 57 – Mimics MedCAD surface model reconstruction [81]

4.6.1.1.4 Direct Import Method Conclusions

The potential speed by which a patient CT scan could be converted to a useable 3D CAD model would have benefits in certain situations. For example, a simpler anatomic model, such as a bone, with fewer surfaces would be easily converted and readily usable in CAD. However, for the purpose of this research, it is this writer's opinion that none of the direct import options were very useful due to the large number of surfaces created.

4.6.1.2 Reduced Mesh Method

The reduced mesh method takes a Mimics 3D reconstructed model and utilizes commercial reverse engineering packages like GeoMagics or Maya. These programs require the 3D reconstructed model to be imported in as point cloud data or stl data. These points or triangles are then converted into NURBS surfaces. This conversion method from CT to CAD, as shown below in Figure 58, results in IGES files that are commonly 20 to 30 times smaller than corresponding STL files [64].

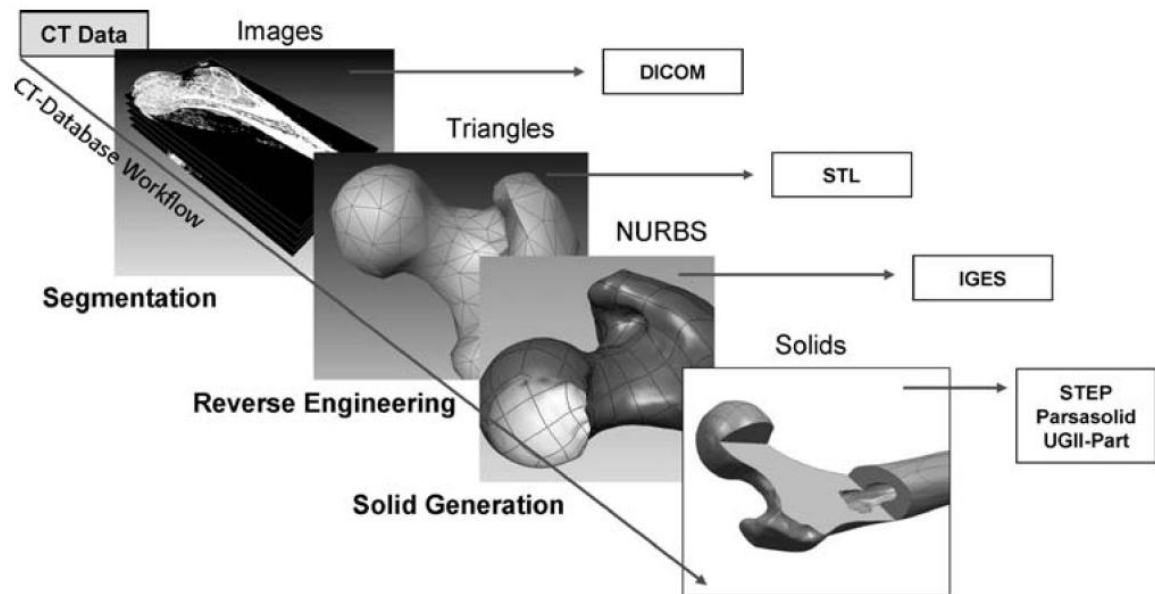


Figure 58 – Conversion process from CT to CAD [64]

4.6.1.2.1 *GeoMagics Studio (Raindrop Inc)*

The Mimics FEA module provided the ability to triangulate, creating a faceted model that can be cleaned up and exported as an STL. Rather than starting at this stage, it is preferred to begin at the most basic level by exporting a point cloud data set to input into GeoMagics. Once the points are in GeoMagics, the decimation of points may be required

as well as a cleaning up of noise. The points are then triangulated forming a model that is similar to STL models. Additional refining and smoothing can eliminate unwanted features and reduce the file size. Finally, NURBS surfaces are created from freeform surfaces. This process as described is shown below in Figure 59.

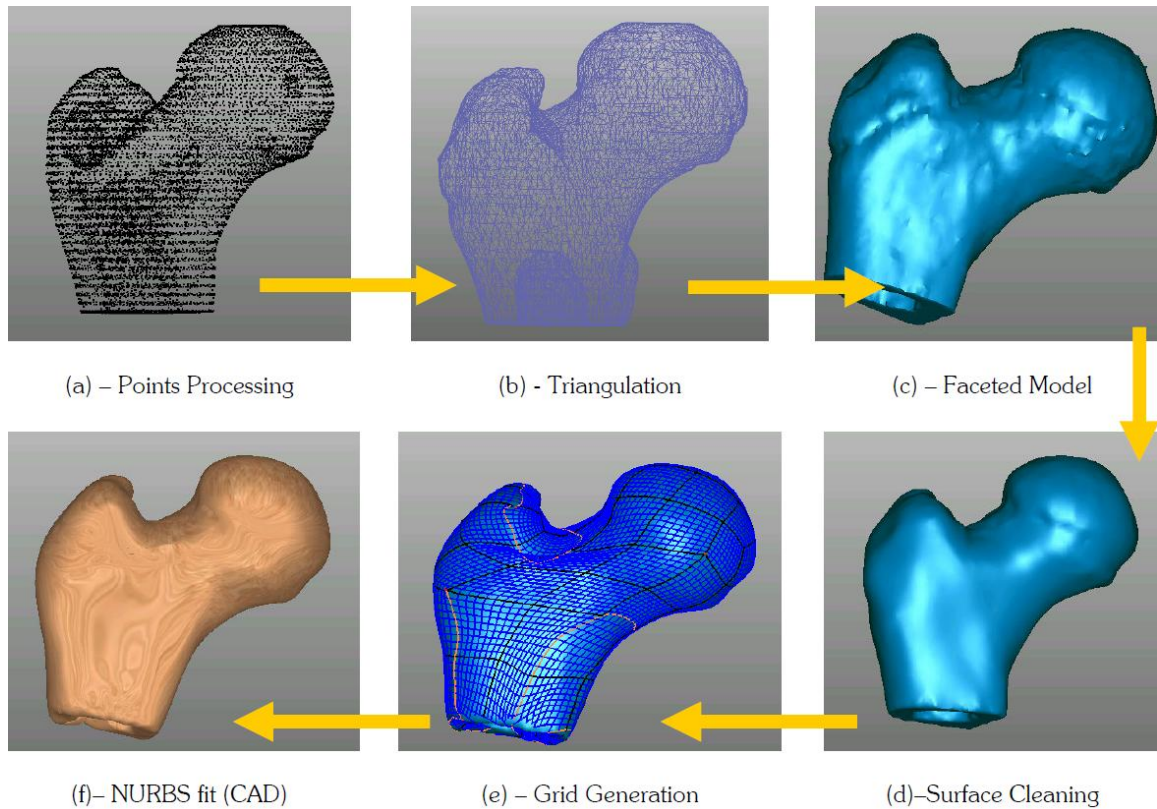


Figure 59 – Conversion process from Mimics to CAD using GeoMagics [81]

4.6.1.2.2 *Reduced Mesh Method Conclusions*

The creation of a 3D CAD model from the 3D reconstructed object utilizing reverse engineering packages creates the most desirable results as the process starts from the simplest form, i.e. points, and can create the mathematical surfaces without error. This process is much longer than the direct import methods, but the file size and usability are superior. Besides these advantages, as most medical devices are routinely analyzed using

FEA and CFD packages, obtaining models in this form are less error prone when transferring files to these analysis packages [81].

4.6.1.3 Work Performed to Convert to a CAD Model

First, the work performed to convert CT data to a CAD model involved the exploration of over 1500 human patient CT scans to find the data sets that were most promising to convert. After finally selecting a data set, the heart anatomy was imported into Mimics to be manipulated and reduced. This was then followed by 3D model reconstruction until only the defined region of interest was remaining as can be seen in Figure 60. The next step in the process, according to Figure 58, was to create NURBS surfaces by using a reduced mesh program like GeoMagics. However, neither SJM nor the University of Minnesota was willing to purchase this program for such short term usage thus the decision was made to outsource the GeoMagics model creation to First Article Inc.

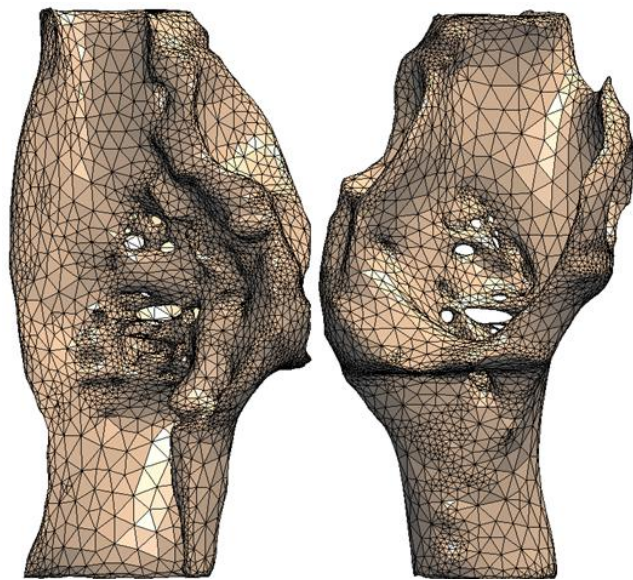


Figure 60 – Mimics 3D reconstructed Model

A couple of additional steps were added in between due to both the quality of the CT scan and the limited knowledge when first beginning this research with the Mimic's program. First, an STL file of the Mimics 3D reconstructed model was created that was built by a rapid prototype into a SLA model. The next step was to smooth out the SLA model by sanding and polishing the model. Then any holes were filled in with molding putty. These additional steps are not normally needed, but at the time this research was conducted the smoothing algorithms and other more advanced image processing techniques in Mimics were not fully realized. Due to the poor contrast difference between the right atrium and the atrial septal wall, molding putty was required to fill in the holes that existed in the current 3D reconstructed model.

After the SLA model was finalized, this model was given to First Article, Inc., where it was laser scanned, then brought into GeoMagics, where it was stitched together by selecting similar points in each scan. Next, NURBS surfaces were created and then the model was saved as an IGES model. The IGES model is shown below in Figure 61 with the reduction in file size from 49.1 MB to 2.7 MB or ~95%. This reduction is critical as designing features into the larger file creates numerous system problems.

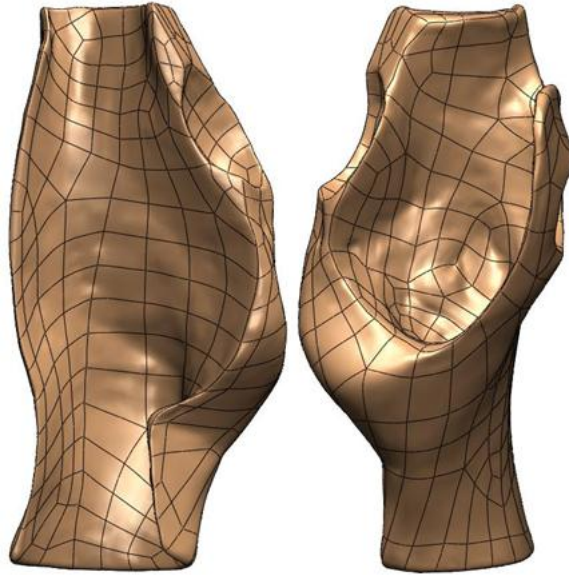


Figure 61 – Anatomical model converted to IGES

4.6.2 3D CAD Model Development

After the CT scan had been converted into an IGES model, normal solid modeling tools were used to add the missing anatomical features previously discussed. Specifically, the fossa ovalis and PFO, which were not recognizable on the CT scan. Besides adding these features, the model was modified to work with the beating heart pumper station.

4.6.2.1 Adding Anatomical Features

The current IGES model, which was smoothed, was missing the fossa ovalis and PFO. In order to add the necessary features, certain modeling techniques were employed. The first was to create an offset surface and then extrude a cut to this offset surface. This offset surface represented the thickness of the septum primum and this thickness was determined to be .02” based on molding capabilities, which will be discussed later. Also,

this thickness fell within the range measured by SJM team members when measuring cadaveric human hearts at the Jesse Edwards Laboratory. The size or diameter of the extruded cut was chosen to be 18mm, which is approximately the average of the three values given in Table 1. The next step was to create the PFO tunnel. This was done by using the loft function with multiple sketches and guide curves to define the trajectory and shape as shown in Figure 62. Through the use of the shell command the lofted item went from a solid extruded body to the tunnel represented in Figure 63. The direction of the guide curves, which determines the direction of the tunnel, was desired to be as close to inline with the IVC as possible. Typically, the tunnel would curve toward the aortic root [82]. However, the guide curves had to lie on intersection points that already existed on the current IGES model (Figure 61).

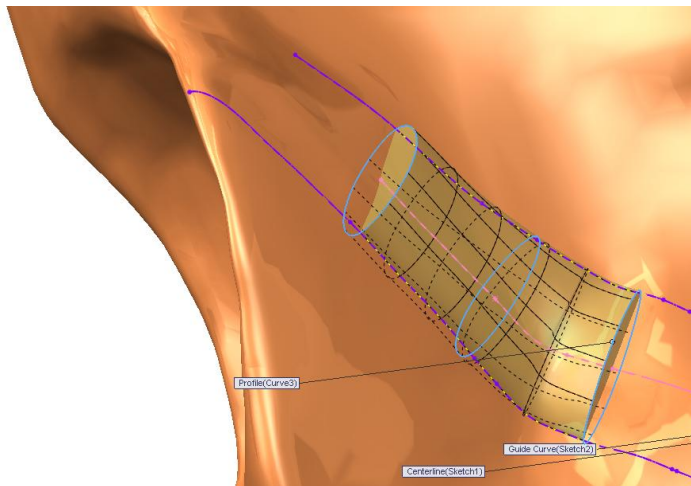


Figure 62 – SolidWorks PFO creation

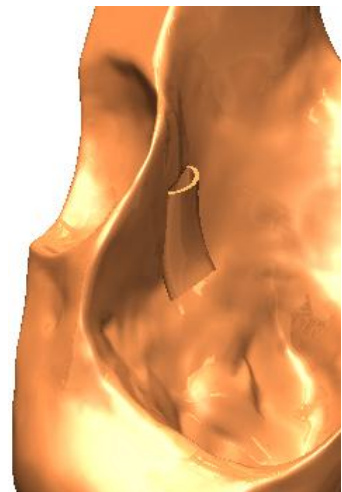


Figure 63 – SolidWorks PFO

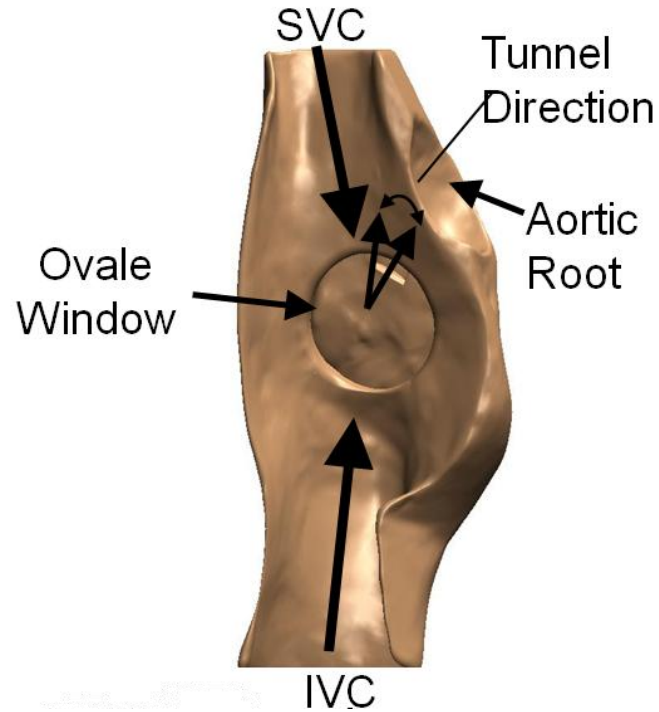


Figure 64 – SolidWorks right atrium view of anatomical features

4.6.2.2 1st Generation CAD Bench Top Model

To achieve the goal of creating a physical bench top model, the CAD model needed to be modified to allow it to interface with the heart beat pumper station. Also, the orientation of the CAD model in relation to the heart beat pumper station was determined based on the patient CT scans where the patient was lying on their back. This relationship correlates to the vantage point of the physician, mimicking the clinical environment.

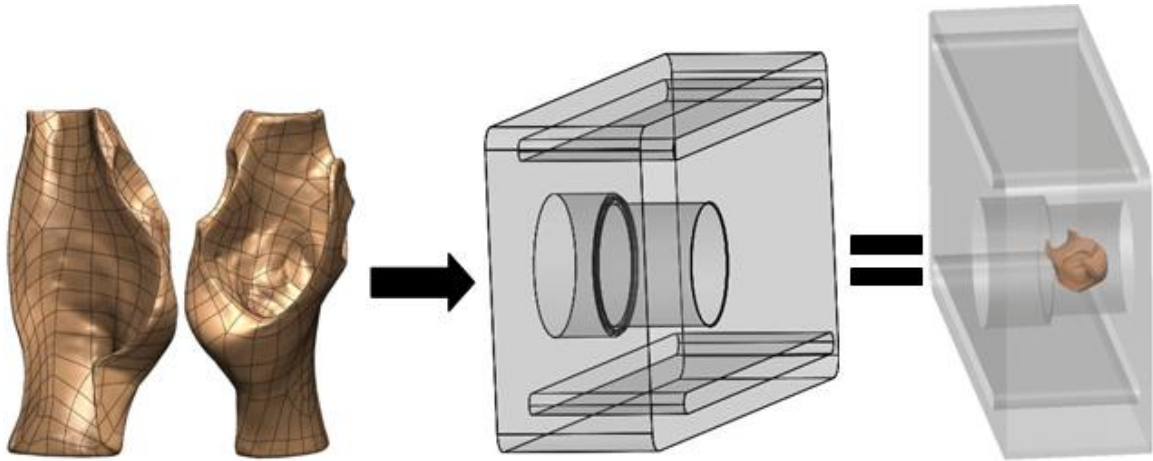


Figure 65 – CAD to functional bench top prototype

The next step was to add enough support material to create a pressure seal between the two chambers, which represents the left and right atriums. The PFO is supposed to be the only passageway between the two. However, whatever material was added couldn't interfere with device placement and it still had to be moldable. To add this extra material, first the original geometry was translated onto an offset sketching plane and then extruded back to the original body as shown below in Figure 66.

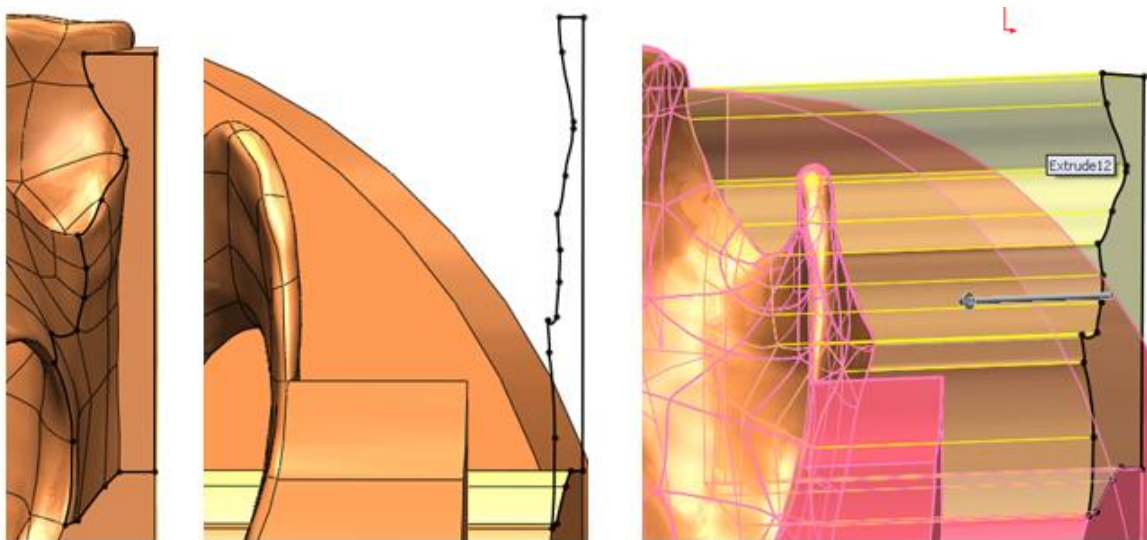


Figure 66 – SolidWorks offset convert entity sketch

Considering the intention to make a mold out of a flexible material, the original model contained too many thin sections to mold. Thus, all thin sections were bulked up, and support material needed to be added. The solution for support material was two customized plastic brackets as shown in Figure 67. This also helped form a pressure seal between the two chambers.

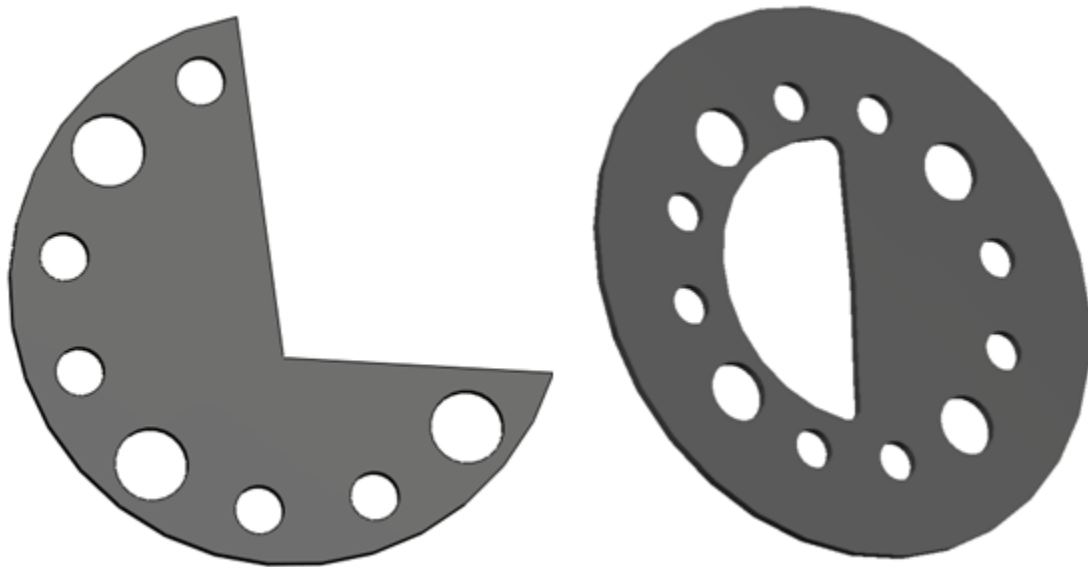


Figure 67 – Brackets added to provide support and pressure seal

During this model development it was decided to eliminate the PFO tunnel feature to prove out the ability to mold the rest of the anatomical structure. This decision was made based on previous experience of SJM team members, who expressed concern about getting the mold material into this region. Therefore the final result for the 1st generation CAD bench top model is shown below in Figure 68.

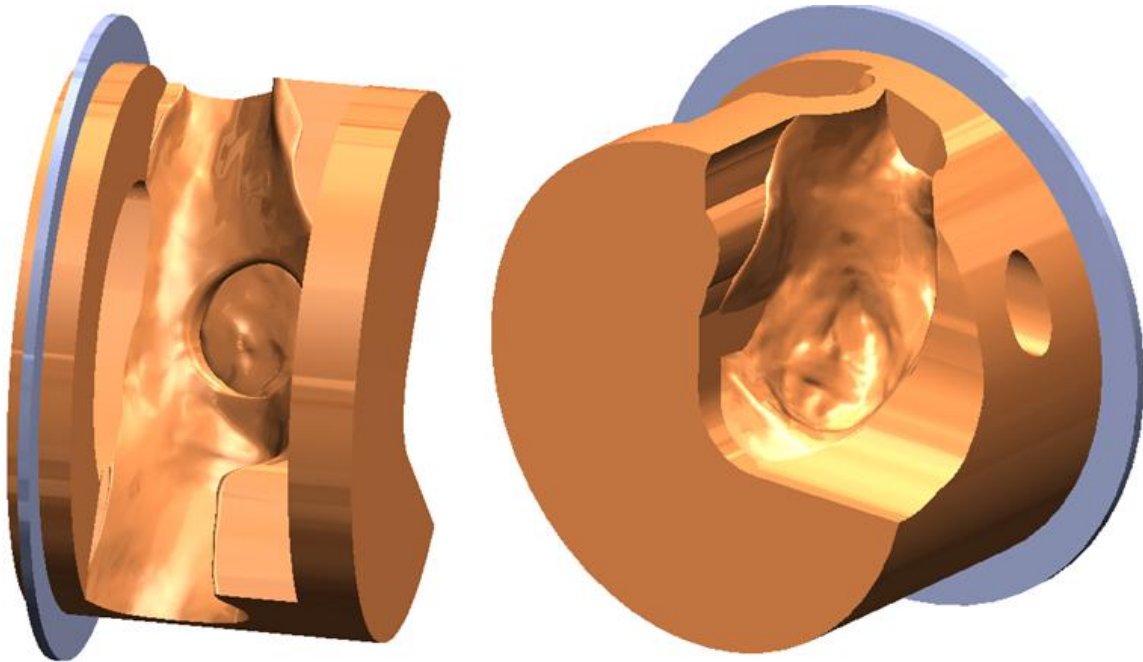


Figure 68 – SolidWorks 1st generation CAD bench top model

4.6.3 Mold Creation

After finalizing the 1st generation CAD bench top model a mold needed to be developed that could be assembled, disassembled, allowed alignment of all pieces, correctly sealed to prevent any leakage, and permitted injection of the mold material into all crevices.

The 1st generation CAD bench top mold was created by making a cylinder and then using the Boolean subtraction function with the CAD bench top model. This resulted in a mirror image of the original model. The mold was decided to be broken into 4 pieces, where the right atrium's insert piece would be separately attached onto the end plate, the left atrium piece was incorporated with the other end plate and finally a middle cylinder. The Boolean subtraction operation was performed for every piece of the mold.

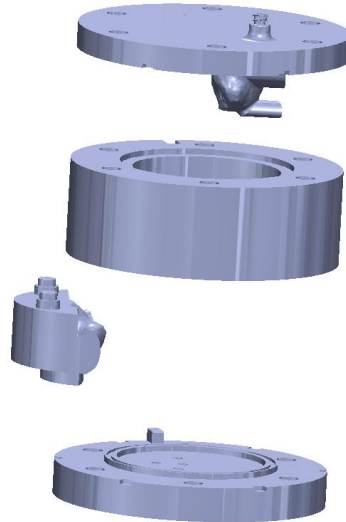


Figure 69 – SolidWorks 1st generation bench top mold pieces

Several features were added to the mold including a groove for o-rings to prevent leakage, small cut-outs in each of the end plates to assist in removal, and two vent holes to aid in getting rid of air during the molding process. Additional features were added to assist in alignment. One, a keying feature was added which incorporated two cutouts in the center cylinder and a protrusion on each end plate as shown in Figure 70. Another alignment feature was to keep the $\frac{3}{4}$ bracket in place. This feature, as can be seen in Figure 71, included two protrusions on the right atrium piece as well as two mating cutouts in the left atrium's end plate.

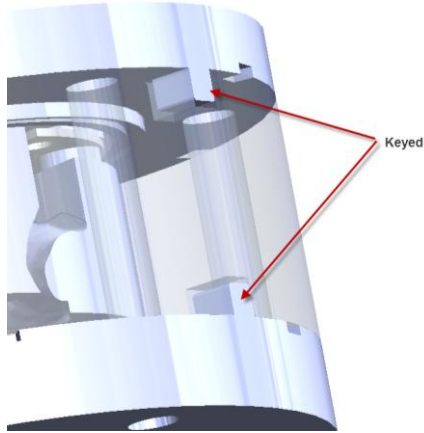


Figure 70 – SolidWorks 1st generation bench top mold keying feature

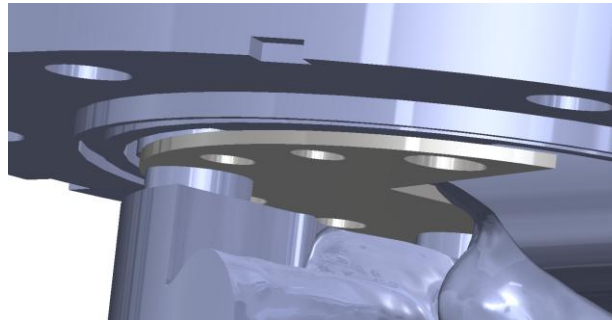


Figure 71 – SolidWorks alignment of 3/4 bracket in 1st generation mold

4.6.3.1 1st Generation CAD Bench Top Mold Assembly Method

Below are the steps to assemble the mold prior to molding:

1. Starting with the right end plate lying flat, an o-ring would be laid in the groove prior to the full bracket being positioned.
2. The right atrium's insert piece is added and screwed into position.
3. Place center cylinder onto the end plate
4. Separately, with the left end plate lying down, place the o-ring and 3/4 bracket.
5. Carefully, holding the cylinder and right end plate tight, turn these upside down and place them on the left end plate aligning the keying notches.

6. Bolt together

4.6.3.2 1st Generation CAD Bench Top Mold Removal Method

Below are the steps to remove the mold after molding:

1. Remove bolts and right end plate screws
2. Starting with the right end plate facing down, pry loose the left end plate, then remove the left end plate rotating and tilting to allow the pulmonary vein hole location to come free.
3. Remove the right end plate
4. Push the mold and right atrium's insert piece through the center cylinder
5. Carefully, remove the right atrium's insert piece by lifting the $\frac{3}{4}$ bracket from the alignment protrusions and then pulling it out at an angle

4.6.3.3 1st Generation Bench Top Molding

The materials and methods of the molding process are considered a trade secret by SJM and will not be discussed in this thesis. After the mold was created, a small hole was cut through the top of the fossa ovalis to represent a short PFO tunnel. The figure below shows the SJM Premere device deployed in the molded model.



Figure 72 – 1st generation mold with SJM Premere device deployed

4.6.4 2nd Generation 3D CAD Model Development

Once the molding technique was proved out for the 1st generation CAD bench top model, work was performed to create a 2nd generation CAD bench top model that included an atrial septal aneurism (ASA) that is prevalent in about 1/3 of all diagnosed PFOs. The diameter of the fossa ovalis was increased from 18mm to 19.5mm. This size is close to the top end of the size range for this feature according to Table 1.

4.6.4.1 2nd Generation CAD Bench Top Model

The modeling steps were basically the same compared to the 1st generation with the exception of the ASA. The ASA represents the dome shape as seen in Figure 73. This particular feature was very difficult to add because SolidWorks, or any solid modeling software, has difficulties handling the complex nature of multiple surfaces coming together. After many failed attempts, finally the ASA was created by using the loft command based on 12 unevenly spaced cross sections and a 3D-sketched guide curve as can be seen in Figure 73. The cross sections are shown in blue and correspond to half of a

hollow sphere. The guide curve is shown in black at the intersection between the dome and the anatomical valley. The number of cross sections and their location was done based on trial and error as well as based on how complex the guide curve was in a particular area. In this particular example, more cross sections were added on the bottom half and less for the top half. This was mainly due to change in angle that occurred at this junction point.

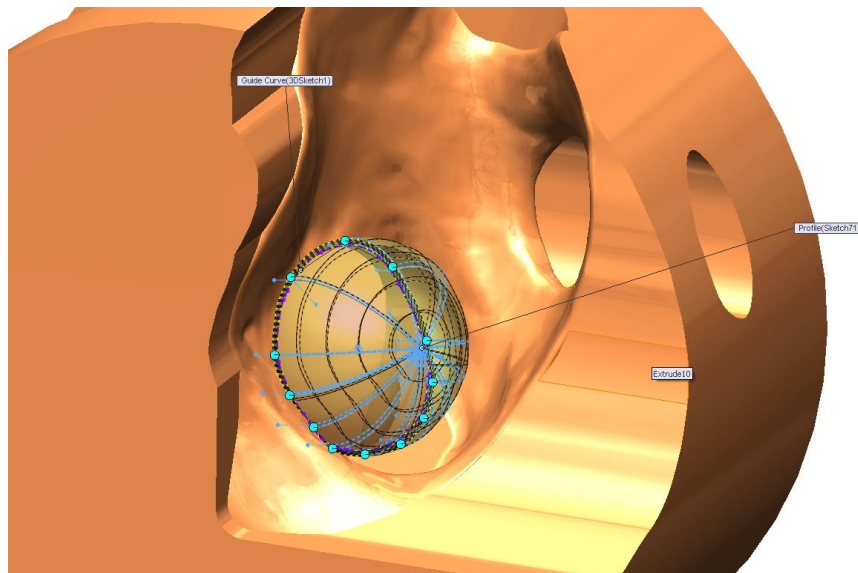


Figure 73 – SolidWorks ASA defect creation

Again, during this model development it was decided to leave the PFO tunnel feature out to prove out the ability to mold the rest of the anatomical structure. Therefore the final result for the 2nd generation CAD bench top model is shown below in Figure 74.

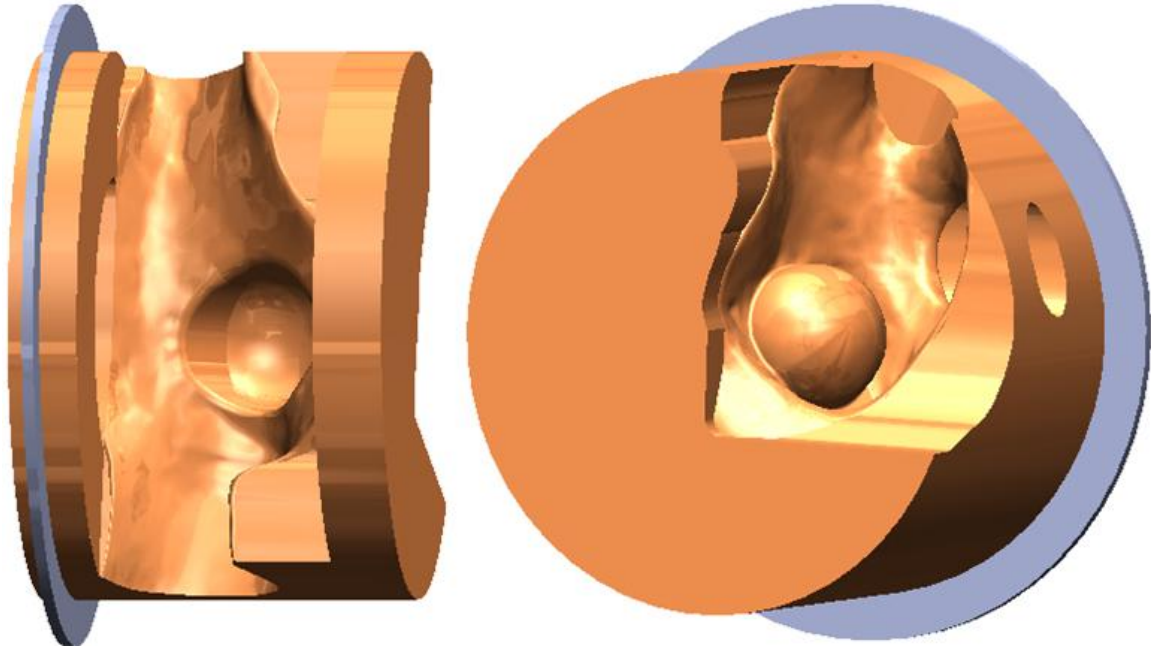


Figure 74 – SolidWorks 2nd generation CAD bench top model

4.6.5 2nd Generation Mold Creation

When creating the 2nd generation CAD bench top mold model, changes to remedy deficiencies noticed in the 1st generation were included in the new design. One of the deficiencies was noticed during step 5 of the assembly process. It was difficult to both hold together and align all of the pieces correctly. Two deficiencies were noticed during the removal process. One was the first step, which was to remove the left atrium's end plate by rotating and tilting. This step proved to be difficult because the newly cured silicone mold prevented the end plate from being removed easily. This often resulted in tearing of the septum primum. The second was the removal of the right atrium piece. This step involved separating the right atrium's piece from the silicone mold in two directions and one of those directions was from the septum primum which was thin and very prone to tearing.

To overcome these challenges, the 2nd generation CAD bench top mold was broken into 6 pieces. The most noticeable change was to split the center cylinder into two unequal halves. An additional change was the removal of one of the vent holes because it proved unnecessary. Thus, the new model featured only one vent hole in the opposite corner as the inlet.

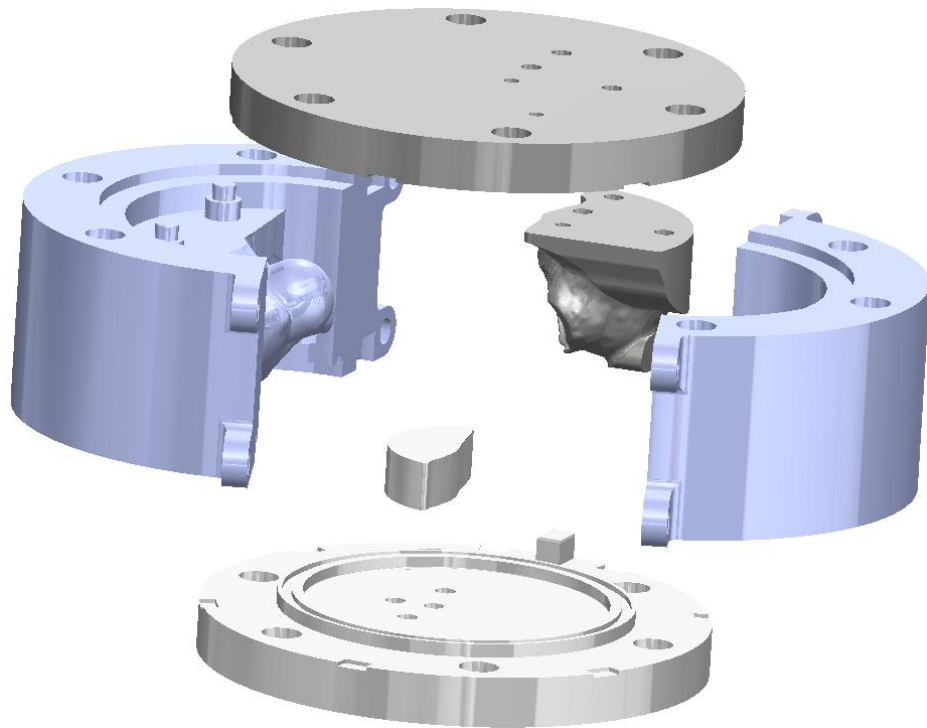


Figure 75 – SolidWorks 2nd generation CAD bench top mold

4.6.5.1 2nd Generation CAD Bench Top Mold Assembly Method

Below are the steps to assemble the mold prior to molding:

1. Attach the left atrium piece to the left end plate
2. Place the o-ring and $\frac{3}{4}$ bracket on the left end plate
3. Place the right half cylinder/atrium

4. Place the left half cylinder
5. Place the full bracket attempting to align the window with the right end plate's middle piece
6. Place o-ring on full bracket in the approximate position
7. Attach the right middle piece to the right end plate
8. Place the right end cap with middle piece paying attention to the location of the o-ring
9. Attach all remaining hardware

4.6.5.2 2nd Generation CAD Bench Top Mold Removal Method

See Figure 76 as well as the steps below to remove the mold after molding:

1. Remove all hardware (2)
2. Remove right end cap, once the mold releases, this part comes off easily (3)
3. Remove left end cap (4)
4. Remove left cylinder side (5)
5. Cut out flash material around the left atrium's inserted piece
6. Remove left atrium, needs to be done carefully to prevent rupture of the septum primum (6)
7. Remove the right cylinder half/atrium by lifting the $\frac{3}{4}$ bracket while separating this piece, needs to be done carefully to prevent rupture of the septum primum (7)
8. Remove the right end cap middle piece. Cut out any flash material. (8)

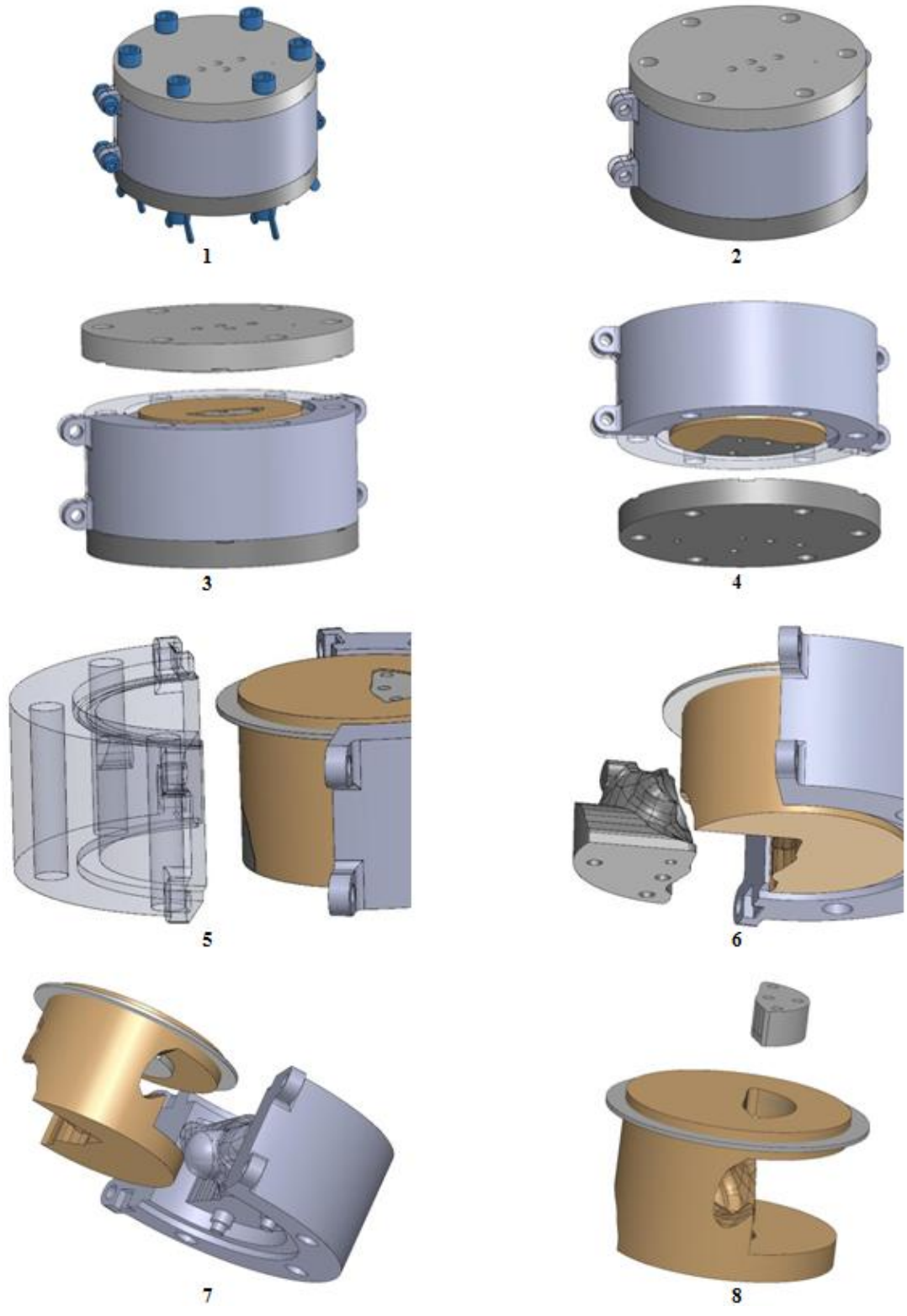


Figure 76 – SolidWorks 2nd generation bench top mold removal

4.6.5.3 2nd Generation Bench Top Model Molding

As mentioned earlier, the materials and methods of the molding process are considered a trade secret by SJM and will not be discussed in this thesis. After the mold was created, a small hole was cut through the top of the fossa ovalis to represent a long PFO tunnel. The figure below illustrates the SJM Premere device deployed in the molded model.



Figure 77 – 2nd generation mold with SJM Premere device deployed

4.7 Mold Validation and Verification

The intended purpose of creating the mold was to create anatomically accurate bench top models for device deployment and testing. Validation of the mold was performed by using the pumper station, which allowed device deployment to be validated while simulating the beating heart beat. Also, during device deployment, the intracardiac echocardiography (ICE) probe was used to verify anatomical structures and defect sizing and compare their accuracy to patient data.

4.7.1 The Pumper Station

Previously, in section 4.2.1, the concept of creating the pumper station was introduced. The pumper station was not finished until the very end of the project. The pressure and

vacuum controlled pumper station was designed to simulate a beating heart beat. The entire setup can be seen in Figure 78 and included an access portal drilled to line up with the IVC when the patient is lying on the back or in the supine position. This access portal allowed both the device to be delivered and deployed as well as the ICE probe to be accurately positioned.



Figure 78 – SJM pumper station [17]

This setup included a flat panel touch screen that allowed for complete control and customization of the pressure/vacuum, heart rate, phase, and temperature settings. All deployments occurred in an isothermal saline solution bath, held at a controlled temperature of 37° C or 98.6° F, which provided a corrosive environment for the specimens. The testing temperature has a large impact on the deployment of the SJM Premere device due to the shape memory characteristics of its Nitinol components. The

isothermal bath was kept at body temperature and ensured consistent environment conditions.

4.7.2 ICE Background

During a PFO closure procedure, echocardiography along with fluoroscopy allows for positioning of the catheter and guidewire through the PFO as well as deployment of the closure device [67]. The initial method of imaging transcatheter closure of ASDs, including PFOs, was TEE. However, at the time of this research, ICE was becoming more popular and the preferred method of imaging for device closure was up for debate [53] & [55].

The advantages of ICE were well documented by Koenig et al and Bartel et al where they concluded less patient stress, continuous guidance without the need for general anesthesia, easier scheduling logistics (echocardiographer, anesthesiologist, and cardiac catheterization time), shortened fluoroscopy time, and improved imaging of the interatrial septum [22], [53], [54], & [55].

The main disadvantages of ICE include the cost of the catheter, an additional large-bore venous sheath, and the catheter is not wire-guided [22] & [67]. Koenig et al disregarded the cost disadvantage due to TEE requiring the addition of an anesthesiologist and echocardiographer [53].

Based on the advantages of ICE over TEE, the ICE imaging modality was chosen for validation of device placement, as well as verification of the bench top mold's accuracy. Thus, it is important to understand the views needed by the ICE catheter for diagnosis and to guide device deployment. SJM had a significant number of patient data sets all based on TEE images and only the long axis view of TEE was a relevant view when comparing this imaging modality to ICE. The representative fluoroscopic and ICE views, as well as an illustration of the relative view of the ICE probe are shown in the figures below.

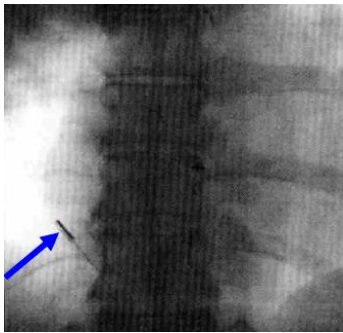


Figure 79 – Representative fluoroscopic view [55]



Figure 80 – Relative ICE position [54]

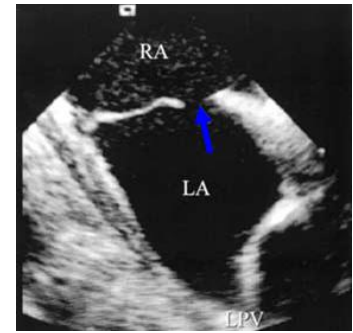


Figure 81 – Representative ICE view [54]

4.7.3 Mold Validation and Verification using ICE

Validation of both the 1st and 2nd generation molds was accomplished by simulating a surgical procedure for detection of a PFO through deployment of the SJM device with only the guidance of ICE. The following figures show contrast being introduced in the right atrium, the contrast crossing the atrial septal wall, and finally the deployed device closing the defect and preventing future shunting.

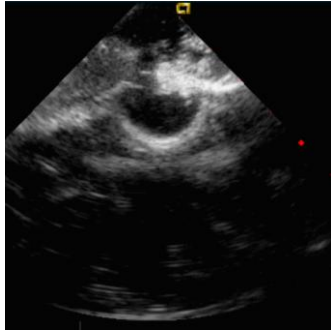


Figure 82 – Introducing Contrast

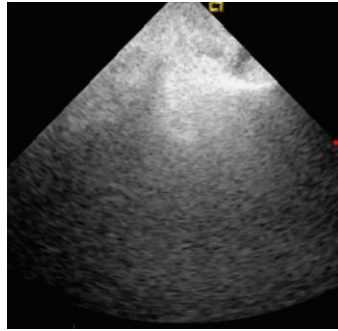


Figure 83 – PFO Detection



Figure 84 – Device Placement

Verification of the mold was accomplished by taking corresponding measurements of the anatomical defects and comparing them to measurements taken of patient defects using TEE. TEE and ICE images of anatomical features are flipped due to the positions of the TEE probe compared to the ICE probe. A comparison image of these two views is shown in Figure 85.

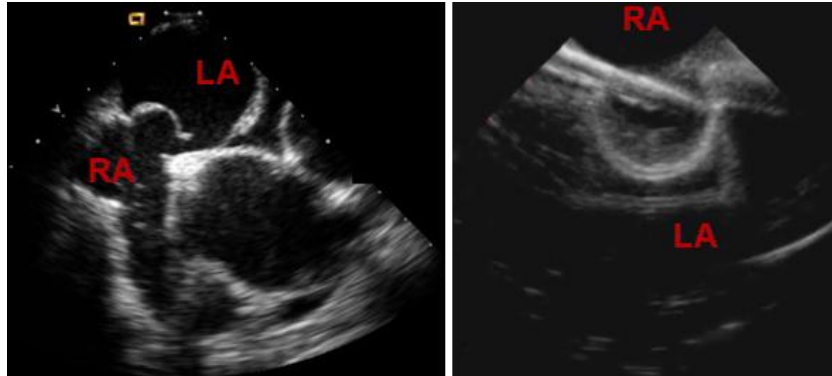


Figure 85 – Representative echocardiograms. (Left) TEE (Right) ICE [17]

The ICE probe was delivered via the access portal that was drilled to lineup with the IVC when a patient lying in the supine position. The probe was then angled away from the PFO, as shown in Figure 86, to increase the field of view of the anatomical structures.

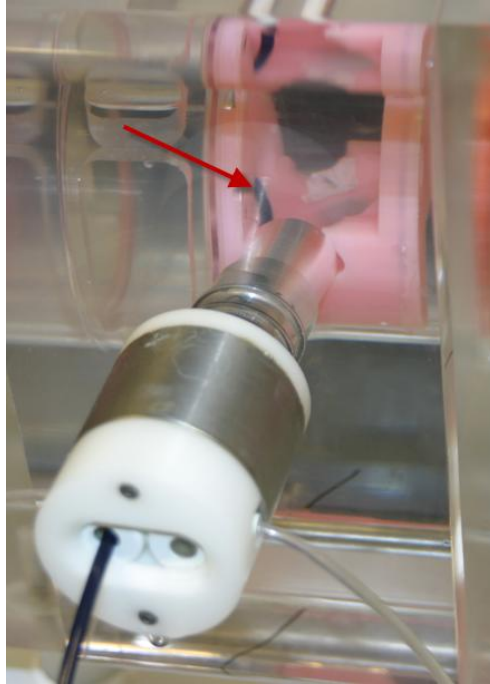


Figure 86 – ICE probe in Pumper station

Using an ICE probe allows for detection of a PFO, but doesn't lend itself to measuring the size of a PFO. This meant the 1st generation mold was unable to be verified with an ICE probe, however, the 2nd generation mold included an ASA and this was verified by comparing to a patient ASA. When looking at the left mobility of the ASA, the patient's fossa ovalis was measured at 16.3mm and the aneurism was measured at 16.6mm. This compared to the mold's fossa ovalis measurement of 19.6mm and aneurism measurement of 12.4mm as shown in Figure 87. Similarly, the right mobility of the ASA was compared with the patient's fossa ovalis and aneurism measuring 18.34mm and 4.94mm, respectively, and the mold's fossa ovalis and aneurism measuring 20.02mm and 4.54mm, respectively, as shown in Figure 88.

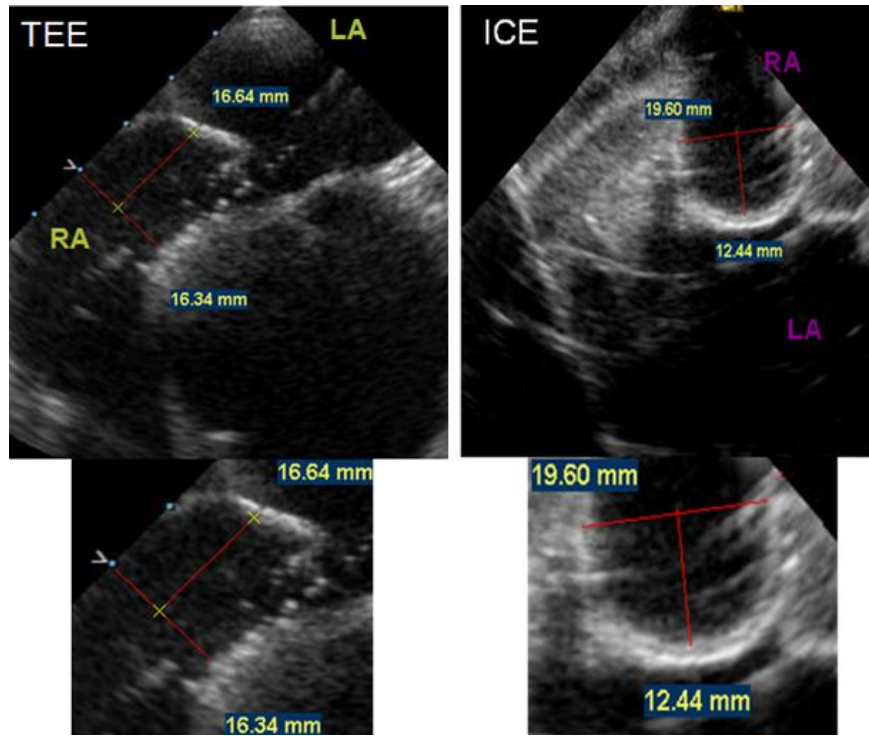


Figure 87 – ASA left mobility verification of 2nd generation bench top mold versus patient data. (Left) Patient TEE image of the ASA. (Right) 2nd generation bench top mold ICE image of the ASA. [17]

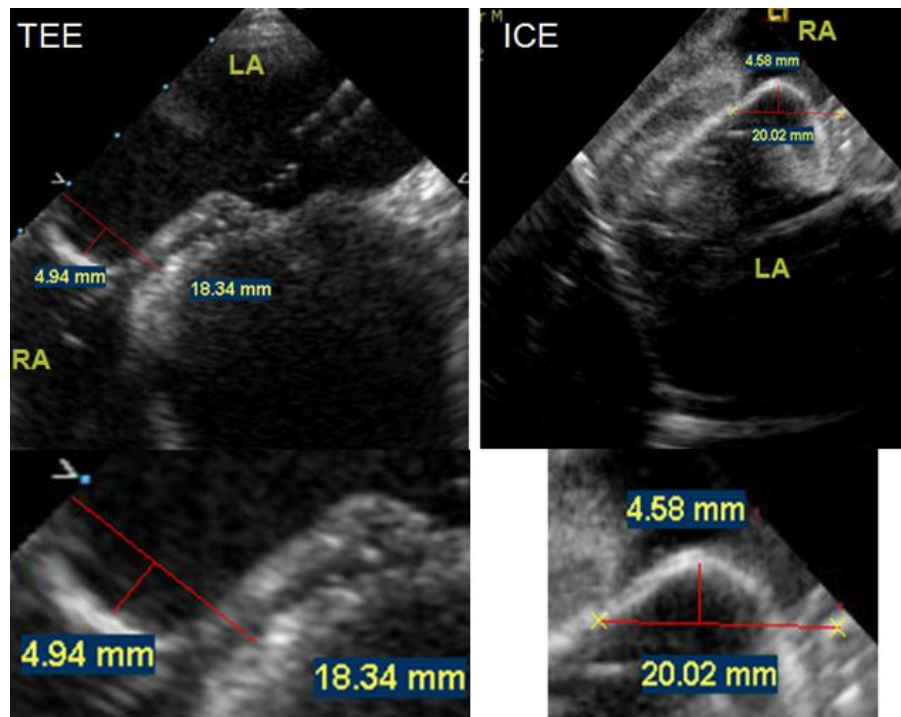


Figure 88 – ASA right mobility verification of 2nd gen bench top mold versus patient data. (Left) Patient TEE image of the ASA. (Right) 2nd gen bench top mold ICE image of the ASA. [17]

The bench top prototype is not a perfect simulation of the real anatomical structure, but the comparisons made show similarity in both function and in feature size when compared to real patient data. The developed bench top models allowed SJM to analyze the strengths and weaknesses of the Premere closure device as well as aiding in the development of the next generation PFO closure device.

5. Conclusion

When research began on creating a VR based medical device design system, the primary objective was a novel integration of CAD software with 3D anatomical and surgical modeling programs in a single software VR environment. The team laid out three steps that needed to be completed for the system to be successful. The first was to merge CAD, anatomic modeling, and analytical software into a single virtual environment that will allow for the technologies to interact. Initially, this seemed relatively easy to combine the different pieces into the VR environment, but several limitations were noted during this process. The most prominent was the file type that the VR software required from CAD and anatomic modeling programs. VR software companies typically only support one mathematical surface representation, which is a triangular mesh. Converting CAD models from their mathematical representations to this simple triangular surface element limits the model's use for manipulation in the second step.

The second step was the ability to make changes in one or more design features and export the changes directly back to the CAD software. During this exploration, several challenges and limitations were discovered. One solution was to create a partnership with a CAD software company. The team worked with MSC software, the creator of the ADAMS CAD package to overcome the integration of CAD in VR. This future partnership would allow the team access into key software parameters hopefully allowing for changes made in the VR environment to be directly imported back into the CAD software. With the use of Mimics, the anatomic modeling steps and techniques were thoroughly explained throughout this paper. Lastly, the team discovered the availability

of VE Suite, an open-source analytical modeling VR software that could be customized to work for the team's needs.

The final step was to combine all of this in a visualization system with other haptic tools to enhance the user's design ability in the virtual environment. The team's hope was to utilize an already existing VR system and the ImmersaDesk system stood out as a possible system that could be utilized for a first generation design.

In order to further the team's research, a partnership was formed with St Jude Medical as they desired to better understand the geometric morphology of a PFO as well as the ability to test their devices on a more anatomically correct bench top model. This partnership would allow the team access to specific modeling packages as well as patient specific CT scans. A PFO is formed between the left and right atrium in the heart when fusion doesn't occur upon birth by the overlap of the thick and muscular septum secundum and the thin and compliant septum primum (Figure 20) [60]. It has been reported up to 33% of all children retain some communication between the right and left atriums through the PFO [25] When designing transcatheter closure devices, one must consider the device placement and anatomic structures for the ultimate goal of closing the defect. In general, for device design, the engineer must consider the average anatomy that will affect the device, but almost more importantly, they must consider variations to the norm. Some of the variations that need to be considered for device deployment are the location, size, rim dimensions, and tissue quality of a PFO [51].

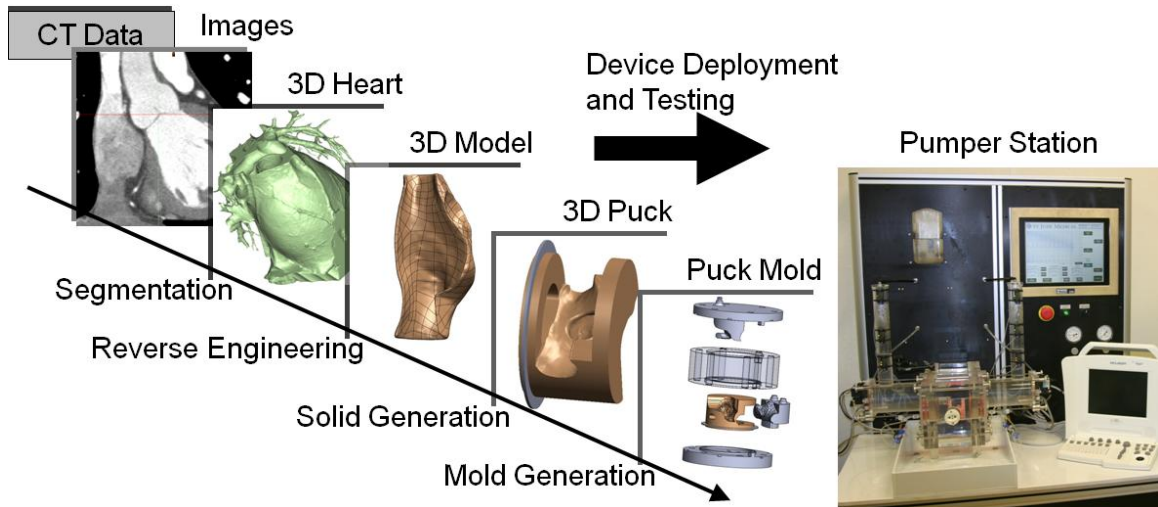


Figure 89 – Modeling techniques

Figure 89 shows the overall process followed when creating a more accurate anatomic bench top model for device deployment. The first step was to obtain a patient CT data set. A good CT data set should have a scan size of less than $.04 \text{ mm}^3$ voxels, have a scan time of less than 15 seconds, utilize data from only the diastolic heart phase, utilize single segment image reconstruction with a heart rate less than 65 beats per minute, and have proper contrast gating to provide contrast in both the right and left atriums simultaneously.

The next step was to process the CT data to create a 3D heart model of the PFO anatomy. This step was accomplished with the use of Mimics and the specific tools described in depth in this paper. Once proper segmentation of the data was performed, a 3D volume model was created and rapid prototyped. This rapid prototype was then modified and reverse engineered using GeMagics into an IGES model that was brought into Solidworks. Reverse engineering is critical as it reduced the file size ~95% allowing for faster processing times.

With the anatomic structure now in CAD, the model was manipulated to work with the heart beat pumper station. The first generation model was setup to be near the norm of population and allowed this author to better understand how to model the device successfully to be molded as well as how to create the subsequent molding device. The model included support brackets to help reinforce the structural rigidity preventing unwanted shunting around the device. The 2nd generation model furthered this knowledge by adding a deviation from the norm, an ASA, that affects device closure of a nearly 1/3 of all PFO closure patients. In addition, the molding device was improved from the first generation making molding much easier and preventing waste of damaged molds during the process.

The more accurate bench top models were then validated for device placement and verified against actual patient data in the heart beat pumper station with the use of an ICE probe. These models were not a perfect simulation of the real anatomical structure, but the comparisons made showed similarity in both function and in feature size when compared to real patient data. The developed bench top models allowed SJM to analyze the strengths and weaknesses of the Premere closure device as well as aiding in the development of the next generation PFO closure device.

In coordination with St. Jude Medical's more accurate bench top model creation, the 3D volume models of the heart were rapid prototyped and exported to the VR environment. The VR and rapid prototyped models were used to enhance visualization for the purpose

of medical device design. A virtual 3D model and a fly-through of the VR model were created using EnSight software [6]. Viewing anatomy in an immersive environment helped to improve the understanding of anatomic structures in the heart. The fly-through using VR instead of a 2D rendering helped to distinguish cardiac structures as well as give a sense of relationships between structures based on depth and orientation.

The ultimate goal of any design system is to merge together all the data gathered in order to make better engineering decisions and to develop products that provide improved patient outcomes. This ultimate goal was the vision that the team started with during the initial stages of VR research. The team furthered the vision by creating partnerships with various groups at the University of Minnesota, industry, leading academic institutions, and with experts in the field. Through the partnerships, several grants were applied for and awarded, which are the basis for ongoing research. Beyond research and grants, the team created virtual heart models from CT data that were imported into a VR environment.

With the completion of a validated pumper station, the group at SJM's CTG facility can now add Nathan Handel's classification project to create models utilizing the modeling techniques described in this research (Figure 89). These new models will represent the future of bench top testing for SJM. These bench top models should provide SJM with the tools needed to create a new closure device.

At the completion of this author's portion of research it was apparent VR is a valuable tool to enhance visualization of the anatomy as well as understand how a device may interact with the anatomy, allowing engineers to modify devices in a radical new way. However, further advancements in technology are required for VR to be used for medical device model creation. Unfortunately, the team's vision of a VR based medical device design system was not realized in this research due to the several major barriers which were encountered.

5.1 Future Work

This classification system and validated bench top setup marks the beginning step that is needed in order to create virtual models to be used in a virtual testing setup. Some of the additional steps needed are:

- To perform a material verification of the bench top model
- To input all material characteristics into the 3D model for FEA analysis
- VR creation of the heart anatomy for simulation of the device deployment
- Linking the FEA results into VR

Each of these steps is extensive and requires further research. Also, this demonstrates the complexity that is associated with each implantable medical device development.

Works Cited

- [1] Patent Foramen Ovale. Available at:
<http://www.clevelandclinic.org/heartcenter/pub/guide/disease/congenital/pfo.htm>. Accessed 2/6, 2008.
- [2] Available at:
<http://www.3dscanco.com/3DScanningProducts/3dscanningsoftware.cfm>.
Accessed 8/7, 2007.
- [3] Hounsfield scale. Available at: http://en.wikipedia.org/wiki/hounsfield_scale.
Accessed 07/11, 2011.
- [4] Virtual reality and CAD - complementary or competing? CSA Newsletter
[serial online]. ;XII, No. 3:1/2008. Available from:
<http://csanet.org/newsletter/winter00/nlw0010.html>.
- [5] Electronic Visualization Laboratory. Available at:
<http://www.evl.uic.edu/core.php?mod-2&type=1&cat=1>. Accessed 7/5,
2011.
- [6] EnSight. Available at: <http://www.ensight.com/>. Accessed 7/5, 2011.
- [7] The Geowall Consortium. Available at: <http://www.geowall.org>. Accessed 7/5,
2011.
- [8] HITLab. Available at: <http://www.hitl.washington.edu/home/>. Accessed 7/5,
2011.
- [9] Mimics. Available at: <http://www.materialise.com/mimics>. Accessed 7/5,
2011.

- [10] Minnesota Supercomputing Institute for Advanced Computational Research.
Available at: <https://www.msi.umn.edu/>. Accessed 7/5, 2011.
- [11] PowerWall. Available at:
<http://www.lcse.umn.edu/research/powerwall/powerwall.html>. Accessed
7/5, 2011.
- [12] Virtual Reality Applications Center. Available at: <http://www.vrac.iastate.com>.
Accessed 7/5, 2011.
- [13] CREST. Available at: <http://www.crest.umn.edu/about.htm>. Accessed 7/6,
2011.
- [14] Cave Automatic Virtual Environment. Available at:
http://en.wikipedia.org/wiki/Cave_Automatic_Virtual_Environment.
Accessed 7/6, 2011.
- [15] Adams for Multibody Dynamics. Available at:
<http://www.mscsoftware.com/Products/CAD-Tools/Adams.aspx>.
Accessed 7/7, 2011.
- [16] ImmersaDesk. Available at:
http://www.polhemus.com/?page=motion_case_studies_fakespace.
Accessed 7/6, 2011.
- [17] St. jude medical.
- [18] Abdulla R. The three-dimensional heart. *Pediatr Cardiol*. 2000;21:409-409.
- [19] Anderson RH, Ho SY. The Anatomy of the Atrioventricular Node. Available
at:

http://www.hrsonline.org/Education/SelfStudy/Articles/anderson_hol.cfm.
Accessed 6/11, 2008.

- [20] Atkins DL, Clark EB, Marvin WJ, Jr. Foramen ovale/atrial septum area ratio: A marker of transatrial blood flow. *Circulation*. 1982;66:281-283.
- [21] Banerjee P. Data interface software for windows PC-compatible virtual reality scene graphs. *Journal of computing and information science in engineering*. 2002;2:72.
- [22] Bartel T, Konorza T, Arjumand J, et al. Intracardiac echocardiography is superior to conventional monitoring for guiding device closure of interatrial communications. *Circulation*. 2003;107:795-797.
- [23] Berta J. Integrating VR and CAD. *IEEE Comput Graphics Appl*. 1999;19:14.
- [24] Biasotti M. ScanTo3D introduction.
- [25] Boucek M. Patent foramen ovale closure: Role of the pediatric cardiologist. *Cardiol Clin*. 2005;23:35-45.
- [26] Brooks FP, Jr. What's real about virtual reality? *Computer Graphics and Applications, IEEE*. 1999;19:16-27.
- [27] Carroll J, Dodge S, Groves B. Percutaneous patent foramen ovale closure. *Cardiol Clin*. 2005;23:13-33.
- [28] Corseuil ETL, et al. ENVIRON–Visualization of CAD models in a virtual reality environment. *Eurographics Symposium on Virtual Environments*. 2004.

- [29] Crick SJ, Sheppard MN, Ho SY, Gebstein L, Anderson RH. Anatomy of the pig heart: Comparisons with normal human cardiac structure. *J Anat.* 1998;193 (Pt 1):105-119.
- [30] Czernuszenko M, Pape D, Sandin D, DeFanti T, Dawe GL, Brown MD. The ImmersaDesk and infinity wall projection-based virtual reality displays. *ACM SIGGRAPH Computer Graphics.* 1997;31:46-49.
- [31] De Castro S, Cartoni D, Fiorelli M, et al. Morphological and functional characteristics of patent foramen ovale and their embolic implications. *Stroke.* 2000;31:2407-2413.
- [32] DeFanti TA, Dawe G, Sandin DJ. ImmersaDesk. Available at: <http://www.evl.uic.edu/core.php?mod=4&type=1&indi=163>. Accessed 7/5, 2011.
- [33] Dewey M, Teige F, Schnapauff D, et al. Noninvasive detection of coronary artery stenoses with multislice computed tomography or magnetic resonance imaging. *Ann Intern Med.* 2006;145:407-415.
- [34] Drighil A, El Mosalami H, Elbadaoui N, Chraibi S, Bennis A. Patent foramen ovale: A new disease? *Int J Cardiol.* 2007;122:1-9.
- [35] D'Urso PS, Thompson RG, Atkinson RL, et al. Cerebrovascular biomodelling: A technical note. *Surg Neurol.* 1999;52:490-500.
- [36] Evans B. The next 30 years. *MDDI [serial online].* 2009;June:7/5/2011. Available from: <http://www.mddionline.com/article/next-30-years>.

- [37] Feigal DW. CDRH Science Review: Center Perspectives. Available at:
http://www.fda.gov/ohrms/dockets/ac/01/slides/3799s1_11_Feigal/sld001.htm. Accessed 7/5, 2011.
- [38] Glanville MJ. Making data 'real' with VE-suite. VE-Suite. 2007;Spring.
- [39] Greenland P. Who is a candidate for noninvasive coronary angiography? *Ann Intern Med.* 2006;145:466-467.
- [40] Hagen PT, Scholz DG, Edwards WD. Incidence and size of patent foramen ovale during the first 10 decades of life: An autopsy study of 965 normal hearts. *Mayo Clin Proc.* 1984;59:17-20.
- [41] Hara H, Virmani R, Ladich E, et al. Patent foramen ovale: Current pathology, pathophysiology, and clinical status. *J Am Coll Cardiol.* 2005;46:1768-1776.
- [42] Hara H, Virmani R, Ladich E, et al. Patent foramen ovale: Standards for a preclinical model of prevalence, structure, and histopathologic comparability to human hearts. *Catheter Cardiovasc Interv.* 2007;69:266-273.
- [43] Harms V, Reisman M, Fuller CJ, et al. Outcomes after transcatheter closure of patent foramen ovale in patients with paradoxical embolism. *Am J Cardiol.* 2007;99:1312-1315.
- [44] Heim M. *Metaphysics of Virtual Reality*. New York: Oxford University Press; 1993.

- [45] Ho SY, Anderson RH, Sanchez-Quintana D. Gross structure of the atriums: More than an anatomic curiosity? *Pacing Clin Electrophysiol.* 2002;25:342-350.
- [46] Ho SY, McCarthy KP, Rigby ML. Morphological features pertinent to interventional closure of patent oval foramen. *J Interv Cardiol.* 2003;16:33-38.
- [47] Hoffmann U, Ferencik M, Cury RC, Pena AJ. Coronary CT angiography. *J Nucl Med.* 2006;47:797-806.
- [48] Jezernik A, Hren G. A solution to integrate computer-aided design (CAD) and virtual reality (VR) databases in design and manufacturing processes. *The International Journal of Advanced Manufacturing Technology.* 2003;22:768-774.
- [49] Kim MS, Hansgen AR, Wink O, Quaife RA, Carroll JD. Rapid prototyping. *Circulation.* 2008;117:2388-2394.
- [50] Kim SR, Weissmann D. Middleware-based integration of multiple CAD and PDM systems into virtual reality environment. *Computer-Aided Design & Applications.* 2006;3:547-556.
- [51] Kim MS, Klein AJ, Carroll JD. Transcatheter closure of intracardiac defects in adults. *J Interv Cardiol.* 2007;20:524-545.
- [52] Kircher BJ, Himelman RB, Schiller NB. Noninvasive estimation of right atrial pressure from the inspiratory collapse of the inferior vena cava. *Am J Cardiol.* 1990;66:493-496.

- [53] Koenig P, Cao QL. Echocardiographic guidance of transcatheter closure of atrial septal defects: Is intracardiac echocardiography better than transesophageal echocardiography? *Pediatr Cardiol.* 2005;26:135-139.
- [54] Koenig P, Cao QL, Heitschmidt M, Waight DJ, Hijazi ZM. Role of intracardiac echocardiographic guidance in transcatheter closure of atrial septal defects and patent foramen ovale using the amplatzer device. *J Interv Cardiol.* 2003;16:51-62.
- [55] Koenig PR, Abdulla RI, Cao QL, Hijazi ZM. Use of intracardiac echocardiography to guide catheter closure of atrial communications. *Echocardiography.* 2003;20:781-787.
- [56] Krafczyk M, Cerrolaza M, Schulz M, Rank E. Analysis of 3D transient blood flow passing through an artificial aortic valve by lattice-boltzmann methods. *J Biomech.* 1998;31:453-462.
- [57] Kuypers FA. Red cell membrane damage. *J Heart Valve Dis.* 1998;7:387-395.
- [58] Leigh J. Interview by Eric Jerke and Nathan Handel. University of Illinois at Chicago: ; June 2007.
- [59] Luciano C, Banerjee P, Florea L, Dawe G. Design of the ImmersiveTouch™: A high-performance haptic augmented virtual reality system. 2005.
- [60] Marshall AC, Lock JE. Structural and compliant anatomy of the patent foramen ovale in patients undergoing transcatheter closure. *Am Heart J.* 2000;140:303-307.
- [61] Meier B. Closure of patent foramen ovale: Technique, pitfalls, complications, and follow up. *Heart.* 2005;91:444-448.

- [62] Menzel A, Himpel G, Kuhl E, Steinmann P. Anisotropic remodelling of biological tissues. *Mechanics of Biological Tissue*. 2006;91–104.
- [63] Messe SR, Silverman IE, Kizer JR, et al. Practice parameter: Recurrent stroke with patent foramen ovale and atrial septal aneurysm: Report of the quality standards subcommittee of the american academy of neurology. *Neurology*. 2004;62:1042-1050.
- [64] Messmer P, Matthews F, Jacob AL, Kikinis R, Regazzoni P, Noser H. A CT database for research, development and education: Concept and potential. *J Digit Imaging*. 2007;20:17-22.
- [65] Mollet NR, Cademartiri F, de Feyter PJ. Non-invasive multislice CT coronary imaging. *Heart*. 2005;91:401-407.
- [66] Mori S, Endo M, Nishizawa K, Murase K, Fujiwara H, Tanada S. Comparison of patient doses in 256-slice CT and 16-slice CT scanners. *Br J Radiol*. 2006;79:56-61.
- [67] Muench A, Boccalandro F, Ellis K, Smalling R. Approaches to correct device malposition in percutaneous PFO closure: Anatomical and technical implications. *Catheterization and cardiovascular interventions*. 2005;64:338-344.
- [68] Natanzon A, Goldman ME. Patent foramen ovale: Anatomy versus pathophysiology--which determines stroke risk? *J Am Soc Echocardiogr*. 2003;16:71-76.

- [69] Natanzon A, Goldman ME. Patent foramen ovale: Anatomy versus pathophysiology--which determines stroke risk? *J Am Soc Echocardiogr.* 2003;16:71-76.
- [70] Ngan EM, Rebeyka IM, Ross DB, et al. The rapid prototyping of anatomic models in pulmonary atresia. *J Thorac Cardiovasc Surg.* 2006;132:264-269.
- [71] Noecker AM, Chen JF, Zhou Q, et al. Development of patient-specific three-dimensional pediatric cardiac models. *ASAIO J.* 2006;52:349-353.
- [72] Patten B. The closure of the foramen ovale. *American Journal of Anatomy.* 1931;48:19-44.
- [73] Pearson AC, Nagelhout D, Castello R, Gomez CR, Labovitz AJ. Atrial septal aneurysm and stroke: A transesophageal echocardiographic study. *J Am Coll Cardiol.* 1991;18:1223-1229.
- [74] Rabatje R. Integration of basic CAD functions into a VR environment. *IEEE;* :238-241.
- [75] Raposo A, Corseuil ETL, Wagner GN, dos Santos IHF, Gattass M. Towards the use of cad models in VR applications. *ACM;* 2006:67-74.
- [76] Riva G. Applications of virtual environments in medicine. *Methods Inf Med.* 2003;42:524-534.
- [77] Schilling A, Kim S, Weissmann D, Tang Z, Choi S. CAD-VR geometry and meta data synchronization for design review applications. *Journal of Zhejiang University-Science A.* 2006;7:1482-1491.

- [78] Schuijf JD, Bax JJ, Shaw LJ, et al. Meta-analysis of comparative diagnostic performance of magnetic resonance imaging and multislice computed tomography for noninvasive coronary angiography. *Am Heart J.* 2006;151:404-411.
- [79] Seymour N, Røtnes J. Challenges to the development of complex virtual reality surgical simulations. *Surg Endosc.* 2006;20:1774-1777.
- [80] Sommer RJ. Patent foramen ovale: A primer for headache physicians. *Headache Currents.* 2006;3:23-36.
- [81] Starly B, Fang Z, Sun W, Shokoufandeh A, Regli W. Three-dimensional reconstruction for medical-CAD modeling. *Computer-Aided Design & Applications.* 2005;2:431-438.
- [82] Sweeney LJ, Rosenquist GC. The normal anatomy of the atrial septum in the human heart. *Am Heart J.* 1979;98:194-199.
- [83] Warriner RK, Haddad M, Hendry PJ, Mussivand T. Virtual anatomical three-dimensional fit trial for intra-thoracically implanted medical devices. *ASAIO J.* 2004;50:354-359.
- [84] Weidlich D, Cser L, Polzin T, Cristiano D, Zickner H. Virtual reality approaches for immersive design. *International Journal on Interactive Design and Manufacturing.* 2009;3:103-108.
- [85] Williamson EE, Kirsch J, Araoz PA, et al. ECG-gated cardiac CT angiography using 64-MDCT for detection of patent foramen ovale. *AJR Am J Roentgenol.* 2008;190:929-933.